

Peer Review File

Manuscript Title: A type 2 cytokine Fc-IL-4 revitalises exhausted CD8+ T cells against cancer

Reviewer Comments & Author Rebuttals

Reviewer Reports on the Initial Version:

Referees' comments:

Referee #1 (Remarks to the Author):

Feng et al have submitted a very impressive study, revealing a novel role for IL-4 in activating CD8 T cells with an exhausted phenotype (PD-1+Tim-3+) in the tumor microenvironment. They have generated an Fc-IL-4 fusion protein and find that this protein enhances the anti-tumor cytotoxicity of different types of CD8 T cells. The majority of the studies are very well performed and bring a significant discovery to the cancer immunotherapy field.

That being said, the term “reinvigorate” in the title and “reprogram” in the subtitles are not suitable. The term “re-” invigorate or “re-” program suggests that Fc-IL-4 alters the T cell phenotype. One point interest in this study is that “exhausted” Fc-IL-4-stimulated T cells continue to express markers of exhaustion but exhibit higher functionality. As regards a “re-programming,” the authors show higher glycolysis but the signaling pathways resulting in these changes were not fully evaluated (see point 5 below). Additionally, while it wouldn't take away from the excitement of this study, the authors have not directly shown that the anti-cytotoxic effects are not dependent (or partially dependent on endogenous T cells; see point 2 below).

Specific comments:

1. The authors indicate that they are performing ex vivo and in vivo experiments in the presence of 20ng/ml and 20ug/ml of Fc-IL-4, respectively. How does this translate to units of IL-4 (the authors state that they have compared bioactivity with commercial IL-4 (Lines 4-5, p21). As the half-life of Fc-IL-4 in animals is 6.3h but the animals are injected every 48h, does this suggest that an on-off IL-4 stimulation has a different impact as compared to a continuous IL-4 stimulation? Does IL-4 have a similar effect to Fc-IL-4?

2. In figure 3, the authors show that Fc-IL-4 has a significant impact on the anti-tumor activity of endogenous T cells, with higher anti-tumor activity than PBS for B16F10 and MC38-HER2; indeed, for MC38, Fc-IL-4 alone results in much higher cytotoxicity than HER2-CART (equivalent to HER2-CART+Fc-IL4). Surprisingly, this result is not discussed. These data strongly suggest an impact of Fc-IL-4 on endogenous T cells which are unlikely to be TTE. This comes back to the point regarding the title and conclusions, indicating an impact on non-TTE cells. In this regard, it would be interesting to know

whether Fc-IL-4 would impact the activity of adoptively transplanted HER2-CART or activated PMEL into tumor-bearing mice in a Rag or NSG background.

Another reason why this point is raised is because IL- IL-4-Fc treatment increased the number of PD-1+TIM3+ endogenous TILs. Do these cells exhibit antigen-specific TCR responses or do they proliferate in an antigen-independent manner? In panels 1e/1f, it is not clear whether the granzymeB_and IFNg+/TNF1+ TIL represent PMEL T cells or endogenous T cells or both. From the numbers (1d), it appears that endogenous PD-1+TIM3+ cells account for >30% of TILs. It will therefore be important to assess this point.

Many of the presented experiments are based on the utilization of in-vitro activated PMEL T cells. However, the authors do not appear to show the phenotype of these cells. Furthermore, while the authors show the IFNg/IL-4 and T-bet/GATA3 plots of pre-transfer T cells, evaluation of Th2 polarization after IL-4-Fc treatment is critical (Figure 1, extended Figure 1).

3. The Tcf7 staining, as assessed using the GFP reporter, is not convincing (Extended Figure 5, Figure 4). The authors can either stain with Tcf7 directly or counterstain with Slamf6/ Tim-3 to identify exhausted progenitor cells and exhausted cells (Please also see LaFleur et al. 2019).

4. How is Fc-IL-4 upregulating glycolytic activity (Fig. 5)? Are the Fc-IL-4-upregulated pathways (i.e. Stat6, PI3K, Akt, mTOR) also upregulated following IL-4 treatment? It is well known that the differential contribution of two types of mTOR complexes, mTORC1 and mTORC2, are important for Th2 skewing (Delgoffe et al. Nat Immunol, 2011). Is there a differential activation of mTORC1/mTORC2 following Fc-IL-4 stimulation?

5. While potentially outside the realm of the present study, the data presented here suggest that modification of CART cells with either IL-4-Fc or tethered IL-4 on the cell surface with the TRUCK CAR system would promote CART activity.

Minor points:

1. NBDG staining (assessed in Fig 5a) was used as a proxy of glucose uptake but this method has been shown to be problematic (Sinclair LV, Barthelemy C, Cantrell DA. 2020 Aug 17;2(4):e200029. doi: 10.20900/immunometab20200029). Additionally, the authors measured Glut-1 MFI but the antibody used appears to be against an intracellular domain. It is also surprising that maximal OCR is lower than basal OCR. Please provide more detail.

2. The grammar used in the manuscript is often incorrect and may hamper the ability of the reader to understand the context. The manuscript should be reviewed in detail, possibly by a language editorial service.

3. The term “anticancer” is unusual. Please use “anti-tumor”. Please check other specific terms to fit the manuscript for the cancer immunotherapy paper.

Referee #2 (Remarks to the Author):

Feng and colleagues have presented a captivating report focusing on the use of type 2 cytokines to enhance the effectiveness of terminally exhausted CD8 T cells (TE CD8) against tumors. Their approach involved fusing the Fc domain to IL4, resulting in an improved half-life compared to recombinant IL4. They demonstrated that this modification led to enhanced accumulation of TE CD8 cells in a syngeneic tumor model. Notably, this accumulation correlated with improved effector functions, such as increased production of granzyme B and IFN γ . These enhancements translated into remarkable antitumor activity across various tumor models when employing adoptive transfer of tumor-specific T cells and CAR T cells. Importantly, these improved antitumor effects were observed without the need for pre-conditioning, which has the potential to advance the field of adoptive cell therapy (ACT). Through the utilization of various cell depletion methods, the authors revealed that the enhancement of antitumor activity by Fc-IL4 specifically depended on CD8 T cells, which was surprising considering the previous belief that this cytokine primarily modulates Macs, DCs, B cells, and CD4 T cells. Using elegant models, the authors demonstrated that Fc-IL4 improves TE CD8 T cells, independently of Tpex, by enhancing glycolysis mediated by lactate dehydrogenase A (LDHA).

In summary, this study exhibits high technical and experimental quality. The experiments conducted, along with the implementation of numerous syngeneic models, provide substantial support for the authors' claims and mechanistic interpretations. This discovery is poised to have a profound impact on the field of immunotherapy.

Comments:

- 1) In figure 3, during the rechallenge experiment. Were the tumors controlled by endogenous T cells or ACT T cells? Data from multiple figures suggest that Fc-IL4 mostly impact TE-CD8 T cells. After tumor clearance, are these cells persisting or Fc-IL4 also generated a pool of memory T cells that can respond to the rechallenge?
- 2) It is intriguing that Fc-IL-4 treatment only affects ECAR and not OCR. Further investigation is necessary to determine whether LDHA is the primary factor responsible for these observations. Can overexpression of LDHA alone enhance T cell antitumor immunity?
- 3) The study did not assess the role of endogenous IL-4. While the authors demonstrated that Fc-IL-4 enhances antitumor immunity, this prompts the question of whether blocking the production of endogenous IL-4 impairs antitumor immunity. Furthermore, it remains unclear which cells are responsible for producing IL-4 in normal tumor responses.
- 4) In figure 3, it is unclear from the methods and legends if the CAR T cells were composed of CD8 T cells only or a mix of CD4 and CD8 as used in patients. CD4 CAR T cells are known to be cytotoxic and when tested individually are better than CAR CD8 T cells alone. The authors should precise the composition of the CAR T cell used in figure 3.

Referee #3 (Remarks to the Author):

Feng et al. show that IL-4Fc fusion protein strongly promotes anti-tumor activity by both endogenous CD8 T cells and adoptively transferred ex vivo activated T cells. Although the described effects are very interesting, there are several points that slightly limit my enthusiasm for the present manuscript. These include the lack of mechanistic evidence how the IL4 impact occurs and how this alters the function of cells.

Major points:

There are many reports praising new strategies for their anti-tumor efficacy that later turn out to be less impressive. For me, it is therefore very important to see how a new effect compares to existing strategies. My question is therefore how effective is the IL-4Fc approach compared to anti-PD1 blockade or combined anti-PD1/anti-CTLA4 treatment. Are there synergistic effects between anti-PD-1 and IL-4 FC in this context?

What I find less convincing are the metabolic studies included into the manuscript. The authors argue that IL-4 induced metabolic reprogramming and that this is critical for the re-activation of cells. However, the authors present only correlative evidence and it remains unclear what is the driving event. T cell activation goes typically along with metabolic changes. It is therefore equally likely that IL-4 somehow activates the cells which then translates into metabolic changes.

A similar problem arises with the conclusions drawn from the LDHA studies. In my opinion, it is an essential enzyme at the end of the glycolysis pathways. We know that glycolysis is required for effector T cell function. Is this enzyme dispensable under other conditions where effector cells are formed? I suspect that it is not, but then the proposed mechanism would have nothing to do specifically with IL-4-induced activation but rather with T-cell activity in general.

Thus, a shortcoming of the manuscript are the limited mechanistic insights how IL-4 enhances the anti-tumor activity of CD8 T cells. In particular, this relates to how IL-4 promotes recruitment and why it increases the expression of cytokines and granzymes in tumors. Does IL-4Fc cause a different signal quality or just a stronger signal because the lifespan is extended by the use of a fusion construct?

The authors conclude that progenitor cells are not required for the IL-4-induced effects. However, the authors write in the methods section that the cells were activated for 2-3 days. I am not sure how many progenitor cells are present after this short culture, but long-term cultures usually do not contain T_{pex}. Therefore, could the authors provide evidence that T_{pex} were transferred? If such cells are not present, then the depletion approach provides no evidence. Moreover, the absence of T_{pex} would even leave unanswered the question of whether there is a possible effect on T_{pex}?

Ex vivo cultures with IL-2 tend to raise nonexhausted T cells, implying that IL-4 treatment of previously ex vivo activated cells enhances the response of nonexhausted cells. Now, one could argue that endogenous T cells also respond to IL-4 treatment and that IL-4 treatment alone (without cell transfer)

has significant antitumor effects in the B16 and MC38 models. Nevertheless, the question remains whether depleted or nonexhausted cells respond under these conditions. Therefore, clear evidence that nonexhausted cells can be reactivated would be crucial to support the message put forward by the authors.

Minor points:

Perhaps the authors can find other wording in the abstract for "a type 2 cytokine that acts directly on CD8+ T cells via the IL-4 receptor and specifically enriches functional, nonexhausted CD8+ T cells (CD8+ TTE) in the tumor independently of the exhausted progenitor CD8+ T cells. resulting in dramatically increased antitumor efficacy and durable cure in multiple solid tumor models when combined with adoptive T cell transfer therapies targeting type 1 immunity. " The length of the sentence and the terminology are very confusing to a broader audience, especially when referring to "functional, terminally exhausted" cells that have superior antitumor function.

As for the list of author contributions, it is surprising to read that a senior scientist (i.e., W.H.) performed experiments without analyzing them.

"CD8+ TTE cells have higher cytotoxicity than nonexhausted progenitor CD8+ T cells and therefore contribute directly to the elimination of cancer cells." I do not think it is useful to specifically highlight that differentiated cells have higher cytotoxic potential than their progenitor cells, which are related to memory cells.

Referee #4 (Remarks to the Author):

Type 2 cytokine Fc-IL-4 reinvigorates terminally exhausted CD8+ 1 T cells to potentiate anticancer immunotherapy

In this manuscript, Feng et al. show that treating tumor-responding T cells with IL-4 promotes an advanced exhaustion differentiation state (PD-1+, TIM-3+) that has increased functional capacities and tumor controlling ability. Upon administration of IL-4, there is a selective increase in the number of TIM-3+ CD8 T cells responding to tumor challenge and these cells also possess increased granzyme and cytokine producing capacity. This result is striking as these more differentiated cell types in the T cell exhaustion differentiation lineage are thought to relatively less plastic and less responsive to conventional ICB compared to the less-differentiated, progenitor differentiation state. The authors show that these more terminally exhausted T cells are the responders to the IL-4 treatment by utilizing a system that allows for selective depletion of the progenitor differentiation state. This experimental system showed that a lack of progenitors did not abrogate the IL-4 treatment phenotype (increased tumor control). The IL-4 treatment increased glycolytic capacity of the tumor-responding CD8 T cells, which is notable as glycolytic activity is known to be critical for both functional capacities of T cells (like IFN γ production) as well as their proliferative potential. In summary, this study claimed that IL-4

treatment increases TIL functionality and tumor-controlling capacity.

This study strengthens the notion that certain type-2 cytokines can be beneficial for reprogramming tumor-responding T cells and tumor control, however, the conceptual rationale for why this would be the case and how this could relate to human ICB responses is limited in this paper. The relevance is also not entirely clear given that the entire manuscript rests entirely on the treatment of murine models of subcutaneous implanted tumors and is lacking clinical correlates. Also, what are the clinical contexts wherein IL-4 would be associated with a good prognosis in tumors as there are decades of reports showing that this does not have a positive correlation with patient outcome. That doesn't mean that the IL-4 therapy couldn't have paradoxical effects on promoting anti-tumor immunity like IL-10, but it would require that the authors identify the physiological settings for when IL-4 would naturally be associated with promoting function and reversing exhaustion of CD8+ Tex cells. Furthermore, given the group recently showed similar effects of IL-10 on TILs it would be important to extend from this to understand how IL-4 and IL-10 operate independently or cooperatively of one another. Thus, at this stage, while an interesting and well done study, it lacks the overall physiological and clinical relevance needed to have a larger impact on the field, and would be more suited for a more specialized journal.

Major Comments:

- 1) Overall, the authors showed a very interesting effect of IL-4 on controlling both functional capacities of tumor-responsive T cells as well as the differentiation program they adopt. There has only been a small amount of work suggesting that the non-progenitor subsets of tumor-responding T cells could be "rejuvenated" to the degree that the authors show here and the effects of tumor controlling capacity by the IL-4 treatment are exciting. However, the novelty of this finding is dampened by the previous work done by Tang group showing that another Type-2 cytokine (IL-10) treatment increases tumor controlling capacity of T cells through a similar mechanism (increased functional TIM-3+ T cells). What would be the rationale for terminally exhausted cells become more responsive to type 2 cytokines if indeed they promote their anti-tumor activities? How does this differ from the conventional roles of IL-4-STAT-6 and IL-10-STAT3 in suppressing Type-I IFN γ -inducing immune responses? How STAT3 and STAT6 operate uniquely from one another or cooperatively in CD8 TILs would be important to understand.
- 2) Importantly, the authors suggest that IL-4 acts on the terminal exhausted subsets but there are some concerns with the TCF-DTR model (discussed below). As an alternative, and a potentially more convincing approach, the authors should study the effects of the individual subsets of T cells and their effects on tumor growth with IL-4 treatment, sorting the PD-1+ TIM-3- and PD-1+ TIM3+ subsets and transferring them into separate tumor-bearing recipients would be a strong assay for understanding the effects of the IL-4 treated PD-1+ TIM-3+ subset specifically.
- 3) The claimed mechanism from the authors by which IL-4 treatment is achieving increased T cell functionality and tumor-controlling capacity is through an induction of glycolytic flux. Work from Hashimoto et al. (Nature, 2022) and Mo et al. (Nature, 2021) show that IL-2 treatment can increase glycolytic flux (with certain engineered IL-2 variants increased glycolysis more than others) can also increase tumor controlling capacity of CD8 T cells. However, the mechanism by which this is achieved is through an enrichment and reinvigoration of progenitor-like cells, not terminally exhausted cells. So, if increased glycolysis is truly the mechanism driving the phenotypes seen here with IL-4 treatment, it is at

odds with the observations that IL-2 treatment (which also increases glycolysis) does not achieve the same differentiation effects. Can the authors deconvolute these different effects of IL4 and IL-2?

4) Though the authors have very convincing data showing that IL-4 controls tumor-responsive T cell differentiation, there are a few areas that could be strengthened. Given that there is an increase in function of the TIM-3+ CD8 T cell population with IL-4 treatment, further investigation into the mechanism by which this is occurring would be valuable. The work presented here relies heavily on the loss of LDHA to abrogate IL-4 treatment phenotypes. This may indicate that increased glycolysis is one component driving the IL-4 treatment phenotypes, however, loss of LDHA significantly compromises effector T cell expansion and function. This makes interpreting the mechanistic experiments done with LDHA knockout difficult to interpret as this would be the expected result of LDHA KO cells. Does a constitutively active STAT4 prevent exhaustion or rescue an LDHA KO? An orthogonal approach could be to see if IL-4r expression or downstream signaling is lost in LDHA knockout T cells. In that same idea, deeper analysis of the sequencing results on the TIM-3+ subset of CD8 T cells could reveal a novel transcriptional program allowing the restoration of function in these cells, which would be exciting and build a more complete understanding of the mechanism of IL-4 treatment.

5) It would also be important to know what cell types are naturally producing IL-4 in the TME in humans and mice.

Minor Points:

-In figure 2, panel C, it would be helpful to see stacked bar graphs in order to more easily see the relative contribution of each treatment group to each defined subset

-Regarding figure 4 and the DT treatment, it is difficult to see whether the DT treatment truly depleted the PD-1+ TIM-3- subset (presumably the TCF7 expressing cells), including a day 12 time point showing loss of this population is suggested. Also, the authors should demonstrate this is occurring directly in the tumors and draining lymph nodes. There are very few TCF7+ cells in the blood that is used as a proxy, and so it is not clear if all the progenitor TEX cells are truly depleted in the tissues and tumors where it matters more.

-Similarly, regarding the profiling of the TILs in figure 4, the T cell population analysis by PD-1 and TIM-3 should be included for the TCF7 DTR and IL-4r KO experiment

Author Rebuttals to Initial Comments:

(Reviewers' comments in bold and authors' response in blue)

Referee #1 (Remarks to the Author):

Feng et al have submitted a very impressive study, revealing a novel role for IL-4 in activating CD8 T cells with an exhausted phenotype (PD-1+Tim-3+) in the tumor microenvironment. They have generated an Fc-IL-4 fusion protein and find that this protein enhances the anti-tumor cytotoxicity of different types of CD8 T cells. The majority of the studies are very well performed and bring a significant discovery to the cancer immunotherapy field. That being said, the term "reinvigorate" in the title and "reprogram" in the subtitles are not suitable. The term "re-" invigorate or "re-" program suggests that Fc-IL-4 alters the T cell phenotype. One point interest in this study is that "exhausted" Fc-IL-4-stimulated T cells continue to express markers of exhaustion but exhibit higher functionality. As regards a "re-programming," the authors show higher glycolysis but the signaling pathways resulting in these changes were not fully evaluated (see point 5 below). Additionally, while it wouldn't take away from the excitement of this study, the authors have not directly shown that the anti-cytotoxic effects are not dependent (or partially dependent on endogenous T cells; see point 2 below).

We thank the reviewer for the favorable remarks. We have thoroughly addressed all the points as shown below in detail. To avoid any ambiguity, we have changed the title to "A type 2 cytokine Fc-IL-4 potentiates cancer immunotherapy by enriching functional terminally exhausted CD8⁺ T cells".

Specific comments:

1. The authors indicate that they are performing ex vivo and in vivo experiments in the presence of 20ng/ml and 20ug/ml of Fc-IL-4, respectively. How does this translate to units of IL-4 (the authors state that they have compared bioactivity with commercial IL-4 (Lines 4-5, p21). As the half-life of Fc-IL-4 in animals is 6.3h but the animals are injected every 48h, does this suggest that an on-off IL-4

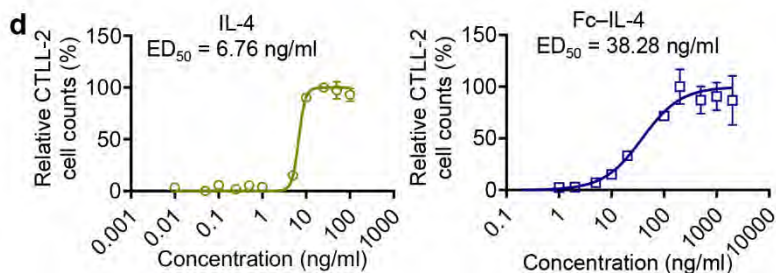
stimulation has a different impact as compared to a continuous IL-4 stimulation? Does IL-4 have a similar effect to Fc-IL-4?

We have determined the bioactivity of Fc-IL-4 by measuring the CTLL-2 cell proliferation induced by Fc-IL-4 in a dose-dependent manner, a widely adopted method to calculate the units of cytokines, in comparison with native IL-4. The median effective dose (ED₅₀) of commercial murine IL-4 is 6.76 ng/ml, corresponding to specific activity 1.47 × 10⁵ units/mg; the ED₅₀ of Fc-IL-4 is 38.28 ng/ml, corresponding to specific activity 0.26 × 10⁵ units/mg as shown below (**New Extended Data Fig. 1d**). The formula used to convert ED₅₀ (in ng/mL) to specific activity (in units/mg)¹ is:

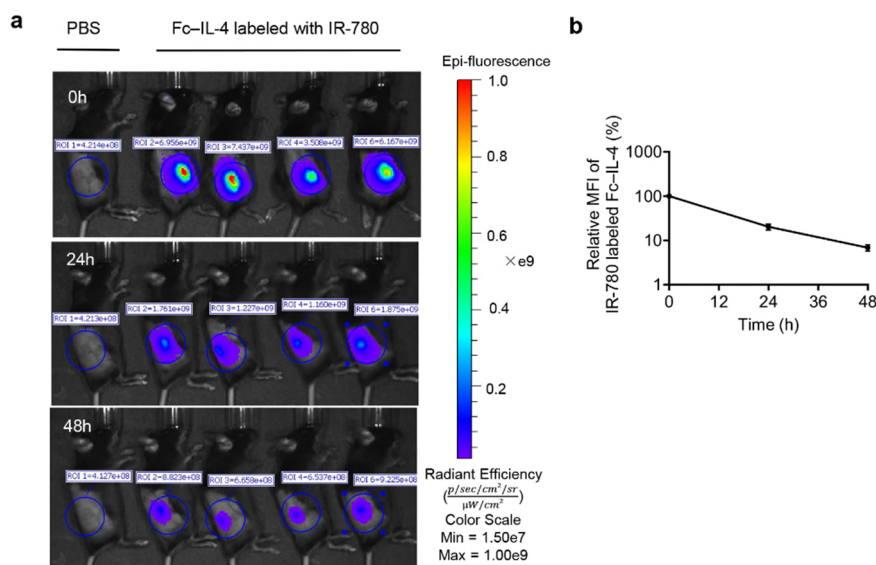
$$\frac{1 \times 10^6}{ED_{50} \text{ (ng/ml)}} = \text{specific activity (units/mg)}$$

The half-life of Fc-IL-4 (6.3 h) was determined upon systemic injection. However, in all the in vivo therapy and mechanistic studies, Fc-IL-4 was intratumorally injected in order to limit systemic distribution and increase tumor retention. In fact, we found that at least 10% of injected Fc-IL-4 (20 μg) sustained in the tumor 48 h post injection (**RL-only Fig. I**). With the designed dosage and schedule, the equivalent concentration of Fc-IL-4 in the tumor microenvironment was always much higher (~10³-10⁶ times higher) than that of the normal physiological level (~1 pg/ml in the serum, and ~5 pg/ml in the tumor tissues)^{2,3}. Therefore, our strategy resembles more of a “continuous stimulation” rather than an “on-off stimulation”.

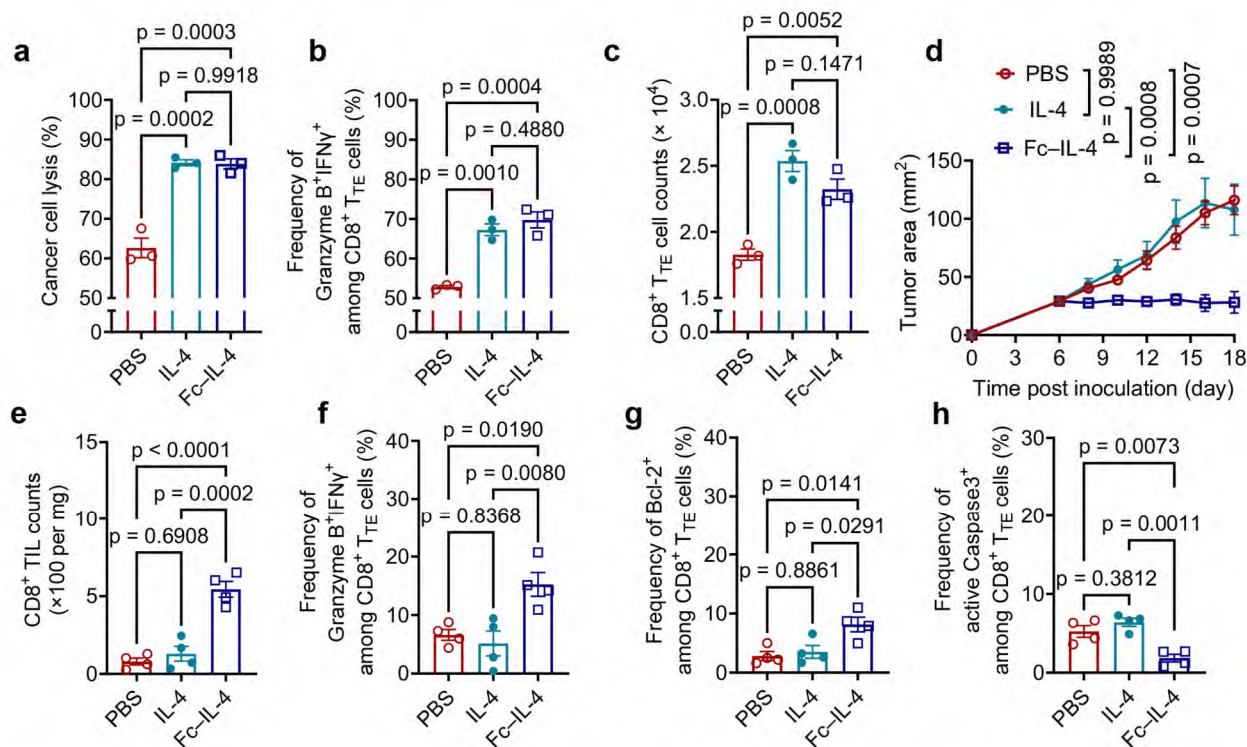
Native IL-4 has similar in vitro effects as Fc-IL-4 but is not suitable for in vivo applications, as the half-life is too short. We compared the effects of native IL-4 and Fc-IL-4 on ex-vivo-induced terminally exhausted CD8⁺ T cells and found that both of them can enhance the effector function and survival of CD8⁺ T cells. However, the administration of IL-4 in vivo with the same bioactivity dosage has negligible effects compared to Fc-IL-4 in terms of tumor progress control, enrichment of CD8⁺ TILs, or enhancement effector function (**RL-only Fig. II**). These results support the necessity of Fc fusion for in vivo application. These findings are not directly pertinent to the primary conclusions of the current manuscript, thus we have opted not to include them in the manuscript. (Response Letter (RL)-only).



New Extended Data Fig. 1d. Median effective dose (ED₅₀) of native IL-4 and Fc-IL-4 was determined using the CTLL-2 proliferation assay.



RL-only Fig. I. B16F10 tumor-bearing mice were intratumorally injected with Fc-IL-4 labeled with IR-780 dye for real-time monitoring of Fc-IL-4 retention in tumor for 2 days. Shown are the fluorescent images of tumor-bearing mice (a) and the dynamic change of the mean fluorescent intensity (MFI) (b) of IR-780 fluorescence.



RL-only Fig. II. Comparing the native IL-4 and Fc-IL-4. a-c, B16F10 tumor cells were co-cultured with ex-vivo-induced PMEL CD8⁺ T_{TE} cells for 2 days in the presence of IL-4 (3.6 ng/ml, corresponding to 0.53 units/ml) or Fc-IL-4 (20 ng/ml, corresponding to 0.52 units/ml). Shown are the percent of cancer cell lysis (a), frequency of Granzyme B⁺IFN γ ⁺CD8⁺ T_{TE} cells (b), and counts of CD8⁺ T_{TE} cells (c). d-h, MC38 tumor-bearing mice received the treatment of Fc-IL-4 (p.t. 20 μ g per injection, corresponding to 520 units per injection) or IL-4 (p.t. 3.6 μ g per injection, corresponding to 529 units per injection) every other day for 6 doses in total. Mice were sacrificed on day 18 and the tumor tissues were collected for analysis by flow cytometry. Shown are the tumor growth curves (d), the cell counts of CD8⁺ TILs (e), frequencies of Granzyme B⁺IFN γ ⁺ (f), Bcl-2⁺ (g), and active Caspase3⁺ (h) among CD8⁺ T_{TE} cells. All data represent mean \pm s.e.m. and are analyzed by One-way ANOVA and Tukey's test.

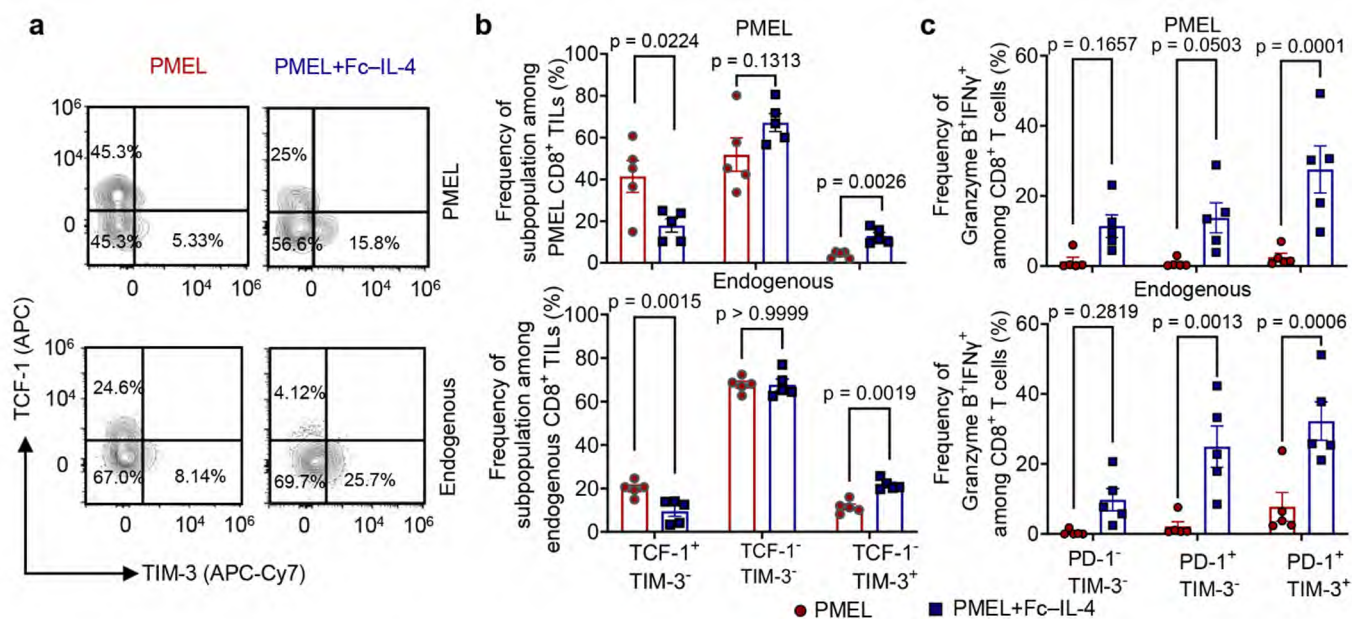
2. (a) In figure 3, the authors show that Fc-IL-4 has a significant impact on the anti-tumor activity of endogenous T cells, with higher anti-tumor activity than PBS for B16F10 and MC38-HER2; indeed, for MC38, Fc-IL-4 alone results in much higher cytotoxicity than HER2-CART (equivalent to HER2-CART+Fc-IL4). Surprisingly, this result is not discussed. These data strongly suggest an impact of Fc-IL-4 on endogenous T cells which are unlikely to be TTE. This comes back to the point regarding the title and conclusions, indicating an impact on non-TTE cells. In this regard, it would be interesting to know whether Fc-IL-4 would impact the activity of adoptively transplanted HER2-CART or activated PMEL into tumor-bearing mice in a Rag or NSG background.

Fc-IL-4 has impact on antigen-specific endogenous T cells. Indeed, we observed that the overall efficacy is partially dependent on endogenous T cells in the syngeneic models (competent immune system). We have added a discussion on the antitumor efficacy of Fc-IL-4 alone in the main text (*Notably, administration of Fc-IL-4 alone effectively inhibited tumor progression and cleared approximately 33% tumors (Fig. 2d and Extended Data Fig. 4f, g)*).

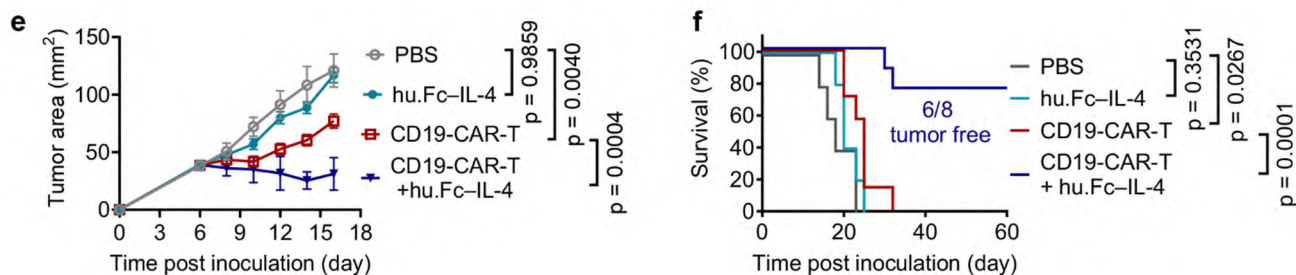
Similar to the transferred antigen-specific T cells, among the endogenous CD8⁺ T cells, there exist both progenitor exhausted CD8⁺ T cells and CD8⁺ T_{TE} cells ([New Extended Data Fig. 2a&b](#)). Fc-IL-4 indeed enriched the T_{TE} population and enhanced their effector function among both endogenous and transferred CD8⁺ T cells ([New Extended Data Fig. 2c](#)).

We have added the study in NSG mice (immune deficient) thanks to the suggestion. We assessed the

antitumor efficacy of combination therapy of human Fc-IL-4 and CD19-CAR-T in NSG mice bearing subcutaneous Raji solid tumor model, which lacks endogenous T cells. We found the antitumor efficacy of CD19-CAR-T was dramatically enhanced by human Fc-IL-4 in the absence of endogenous T cells. By contrast, the Fc-IL-4 treatment alone (without either endogenous or transferred T cells) showed negligible tumor control. These results again confirmed that antigen specific T cells are indispensable for Fc-IL-4 to exert antitumor effects ([New Fig. 3e&f](#)).



New Extended Data Fig. 2a-c. Experimental setting was described in [Fig. 1a](#). Shown are the representative flow cytometry plots ([a](#)) and the frequencies ([b](#)) of CD8⁺ T_{TE} cells (TCF1⁺TIM3⁺) among PMEL or endogenous CD8⁺ TILs, and frequencies of Granzyme B⁺IFNγ⁺ among different subpopulations of PMEL or endogenous CD8⁺ TILs ([c](#)). All data represent mean ± s.e.m. and are analyzed by Two-way ANOVA and Sidak multiple comparisons test.

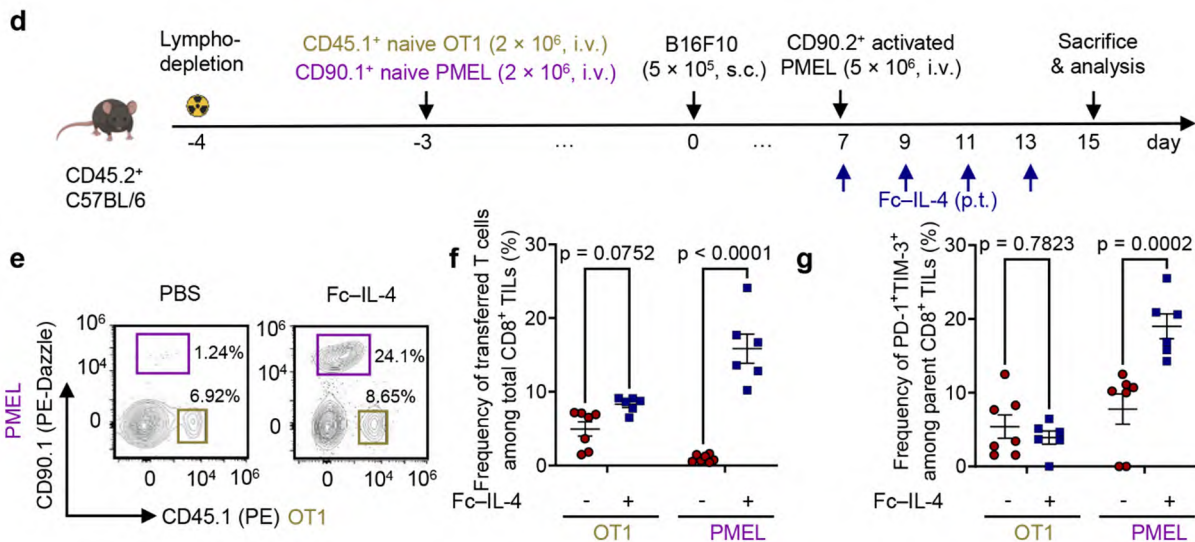


New Fig. 3e&f. NSG mice were inoculated with Raji lymphoma cells (2×10^6 , s.c.). Tumor-bearing mice received ACT of CD19-CAR-T (2×10^6 , i.v.) followed by administration of hu.Fc-IL-4 (20 μg, p.t.) or PBS every other day for 4 doses in total. Mice receiving injections of PBS only and hu.Fc-IL-4 (20 μg × 4, p.t.) only served as controls. Shown are the average tumor growth curves ([e](#)) and Kaplan-Meier survival curves ([f](#)) of mice. All data represent mean ± s.e.m. and are analyzed by one-way ANOVA and Tukey's test ([e](#)) or log-rank test for survival curves ([f](#)).

2(b) Another reason why this point is raised is because IL-4-Fc treatment increased the number of PD-1+TIM3+ endogenous TILs. Do these cells exhibit antigen-specific TCR responses or do they proliferate in an antigen-independent manner?

To study whether the endogenous CD8⁺ T_{TE} cells exhibit antigen-specific TCR response, we co-transferred naïve OT1 and PMEL T cells into C57BL/6 mice prior to tumor inoculation. The transferred OT1 and PMEL T cells therefore mimic “endogenous” T cells. OT1 T cells act as antigen non-specific cells, while PMEL T cells are antigen-specific. Subsequently, we inoculated the B16F10 tumor and compared the responses. We found that only PMEL T cells (for the total population and the PD1⁺TIM3⁺ subset) were significantly increased upon Fc-IL-4 treatment, while OT1 T cells showed negligible responses ([New Extended Data Fig. 2d-g](#)). These

results indicate that Fc-IL-4 enriches the endogenous CD8⁺ T_{TE} cells in an antigen-specific manner.



New Extended Data Fig. 2d-g. CD45.2⁺ C57BL/6 mice were sublethally lymphodepleted (day -4) and received adoptive co-transfer of CD45.1⁺ naive OT-I T cells (2 × 10⁶, i.v.) and CD90.1⁺ naive PMEL T cells (2 × 10⁶, i.v.) at (day -3). The mice were then inoculated with B16F10 tumor cells (day 0). On day 7, the mice were treated with ACT of activated CD90.2⁺ PMEL T cells (5 × 10⁶, i.v.) followed by administration of Fc-IL-4 (20 μg, p.t.) or PBS every other day for 4 doses in total. On day 15, mice were euthanized and tumor tissues were collected for flow cytometry analysis (n = 6 independent animals). Shown are the experimental timeline (**d**), representative flow cytometry plots (**e**), frequencies of transferred CD45.1⁺ OT1 and CD90.1⁺ PMEL T cells among total CD8⁺ TILs (**f**), and frequencies of PD-1⁺TIM3⁻³⁺ subpopulation among transferred CD45.1⁺ OT1 or CD90.1⁺ PMEL T cells (**g**). All data represent mean ± s.e.m. and are analyzed by unpaired two-sided Student's t-test.

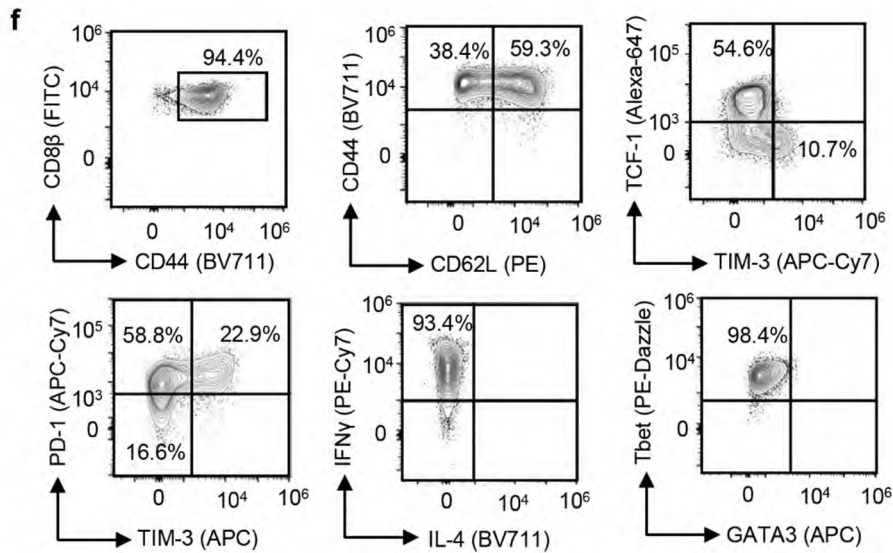
2(c) In panels 1e/1f, it is not clear whether the granzymeB₊ and IFNγ₊/TNF1₊ TIL represent PMEL T cells or endogenous T cells or both. From the numbers (1d), it appears that endogenous PD-1⁺TIM3⁻³⁺ cells account for >30% of TILs. It will therefore be important to assess this point.

As the cytotoxicity and effector function of both PMEL and endogenous CD8⁺ T_{TE} cells were enhanced upon Fc-IL-4 treatment, we showed the total CD8⁺ T cell responses in Fig. 1e&f. To make it clear, we now add the data of separate PMEL and endogenous CD8⁺ T_{TE} cells in the [New Extended Data Fig. 2c](#) (please see figure above, the response to question 2(a)).

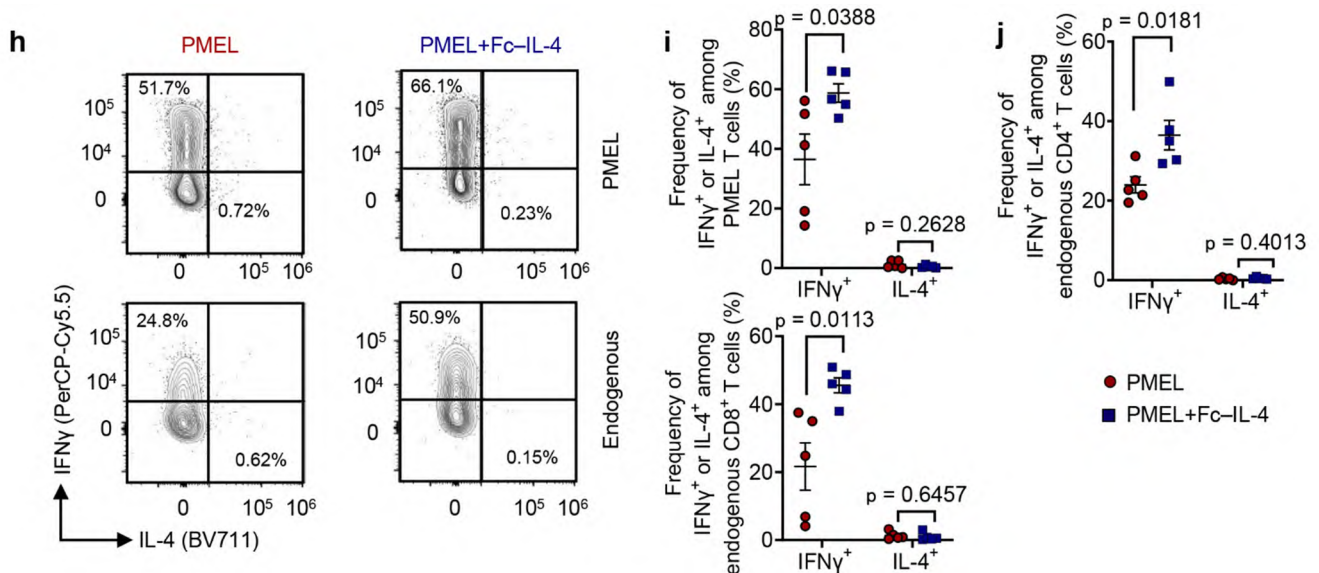
2(d) Many of the presented experiments are based on the utilization of in-vitro activated PMEL T cells. However, the authors do not appear to show the phenotype of these cells. Furthermore, while the authors show the IFNγ/IL-4 and T-bet/GATA3 plots of pre-transfer T cells, evaluation of Th2 polarization after IL-4-Fc treatment is critical (Figure 1, extended Figure 1).

The PMEL T cells were activated in a typical condition for type 1 T cell differentiation and displayed the Type 1 features. We now add the phenotyping results as suggested ([New Extended Data Fig. 1f](#)).

We evaluated the type 2 polarization post Fc-IL-4 treatment and found that both CD8⁺ T cells (including PMEL and endogenous CD8⁺ T cells) and CD4⁺ T cells did not show any type 2 features by measuring IL-4 secretion. Instead, upon Fc-IL-4 treatment, most T cells secreted IFNγ ([New Extended Data Fig. 2h-j](#)), which indicated that Fc-IL-4 treatment did not skew intratumoral T cells towards type 2 polarization.



New Extended Data Fig. 1f. The phenotype, cytokine profiles, and expression of transcription factors of activated PMEL T cells prior to transfer.

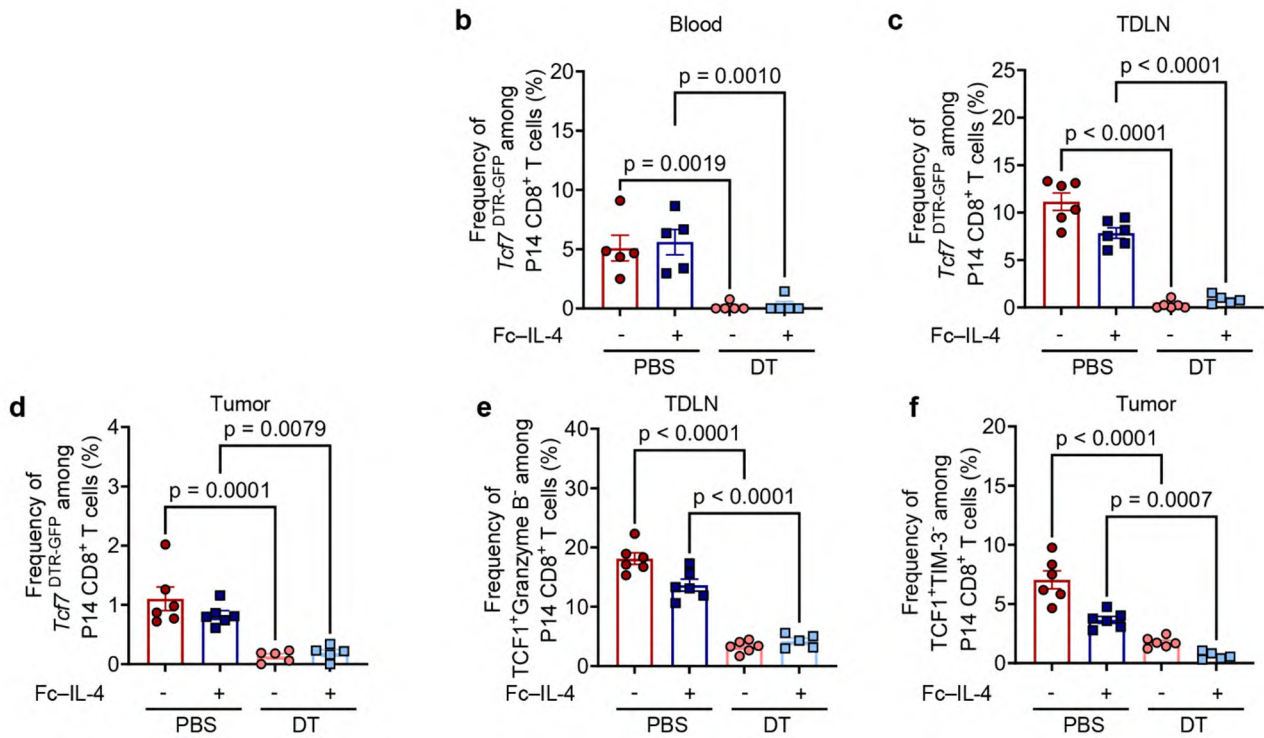


New Extended Data Fig. 2h-j. Experimental setting was described in **Fig. 1a**. Shown are representative flow cytometry plots (**h**) and frequencies of IFN γ ⁺ or IL-4⁺ among PMEL and endogenous CD8⁺ T cells (**i**), and frequencies of IFN γ ⁺ or IL-4⁺ among endogenous CD4⁺ T cells (**j**). All data represent mean \pm s.e.m. and are analyzed by unpaired two-sided Student's t-test.

3. The Tcf7 staining, as assessed using the GFP reporter, is not convincing (Extended Figure 5, Figure 4). The authors can either stain with Tcf7 directly or counterstain with Slamf6/ Tim-3 to identify exhausted progenitor cells and exhausted cells (Please also see LaFleur et al. 2019).

As suggested, we directly stained TCF1 and found the TCF1⁺ T cells were indeed efficiently depleted in the TDLN (**New Extended Data Fig. 7e**). The results are consistent with those based on the GFP reporter support (**New Extended Data Fig. 7b-d**), and therefore support that the GFP reporter is reliable in this model.

To further reinforce the conclusion, we used TCF1 and TIM-3 staining to identify the progenitor exhausted CD8⁺ T cells and terminally exhausted CD8⁺ T cells, and we found similar results (**New Extended Data Fig.7f**).



New Extended Data Fig. 7b-f. Experimental setting was similar as described in **Fig. 4a** except that mice were sacrificed on day 12 and the tumor-draining lymph node (TDLN), spleen, blood, and tumor tissues were collected for analysis by flow cytometry. Shown are the frequencies of $Tc77^{DTR-GFP+}$ progenitor exhausted T cells among transferred P14 T cells in the peripheral blood (**b**), TDLN (**c**), and tumor (**d**), and frequencies of $TCF1^{+}Granzyme B^{+}$ among transferred P14 T cells in the TDLN (**e**), and frequencies of $TCF1^{+}TIM3^{-}$ among transferred P14 T cells in the tumor (**f**). All data represent mean \pm s.e.m. and are analyzed by One-way ANOVA and Tukey's test.

4. How is Fc-IL-4 upregulating glycolytic activity (Fig. 5)? Are the Fc-IL-4-upregulated pathways (i.e. Stat6, PI3K, Akt, mTOR) also upregulated following IL-4 treatment? It is well known that the differential contribution of two types of mTOR complexes, mTORC1 and mTORC2, are important for Th2 skewing (Delgoffe et al. Nat Immunol, 2011). Is there a differential activation of mTORC1/mTORC2 following Fc-IL-4 stimulation?

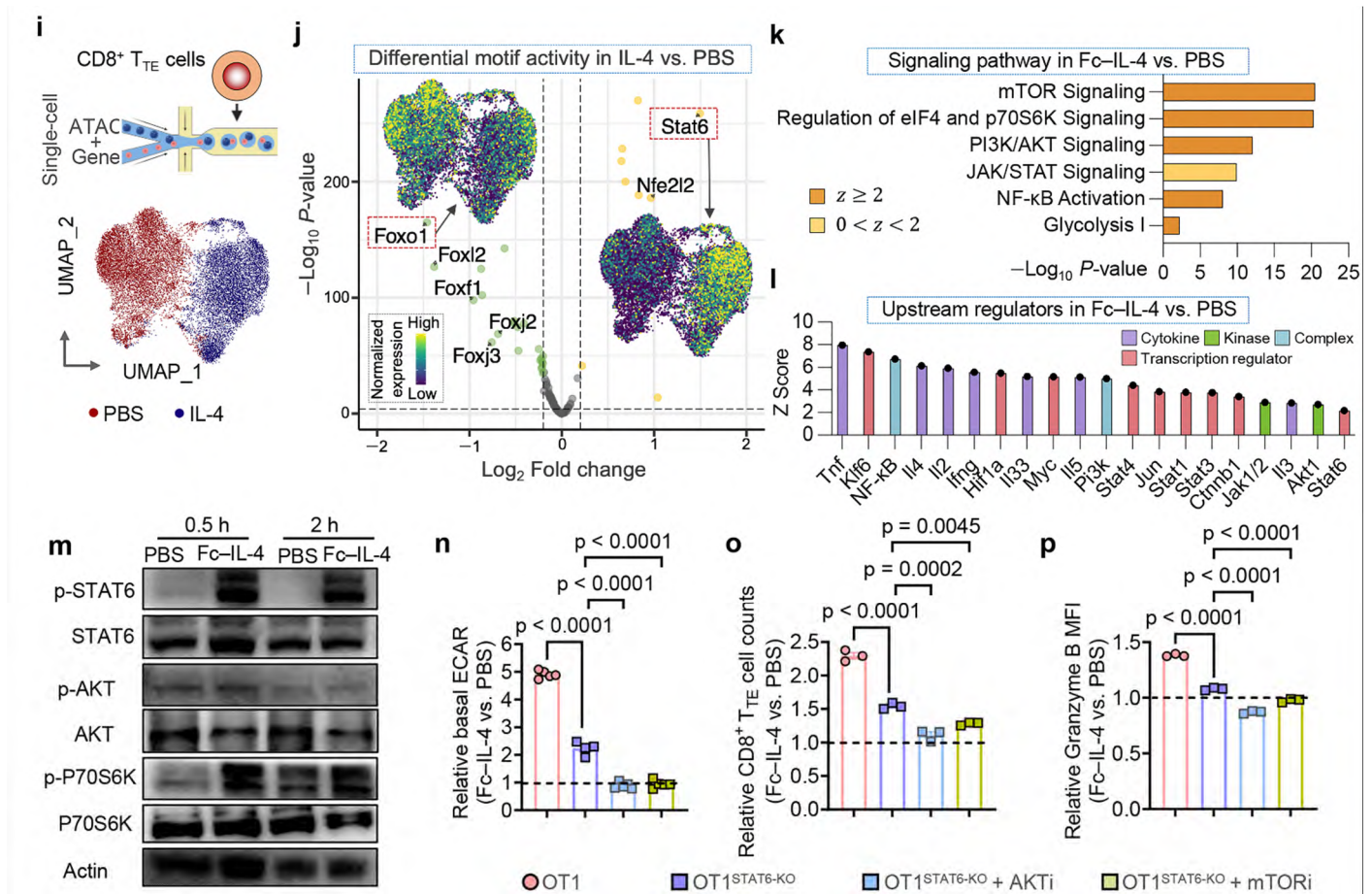
To elucidate the molecular mechanisms driving the heightened glycolysis induced by Fc-IL-4, we performed single-cell ATAC and transcriptome co-profiling of ex vivo-induced CD8⁺ T_{TE} cells (**New Fig. 5i**). The integrated UMAP analysis merging ATAC and transcriptome datasets revealed distinct molecular profiles in T_{TE} cells between the two conditions, suggesting an intrinsic regulatory impact on this specific cell type due to the inclusion of IL-4 (**New Fig. 5i**, bottom panel). We performed a differential motif analysis using ATAC data to identify potential transcription factor binding sites within open chromatin regions. In IL-4-treated CD8⁺ T_{TE} cells compared to the PBS condition, Stat6 emerged as the most significantly enhanced motif, while Foxo1, a canonical negative regulator of mTOR, exhibited the highest degree of reduction (**New Fig. 5j**). We also investigated the signaling pathways regulated by differentially expressed genes (DEGs) within CD8⁺ TILs obtained from B16F10 tumors in mice subjected to Fc-IL-4 combined ACT, in comparison to the PBS control. The analysis revealed a significant upregulation of mTOR signaling, eIF4 and p70S6 signaling, and PI3K/AKT signaling in Fc-IL-4 treated cells, along with the upregulation of JAK/STAT signaling, NF- κ B activation and glycolysis (**New Fig. 5k**). Upstream regulator analysis based on the DEGs identified multiple functional molecules predicted to be upregulated in the Fc-IL-4 group, particularly NF- κ B, Myc, Pi3K, Akt1, and Stat6 (**New Fig. 5l**).

These findings prompted us to delve deeper into the role of the PI3K-AKT-mTOR axis and STAT6 in the heightened glycolytic activities observed following Fc-IL-4 treatment. Through flow cytometry and western blot analysis, we confirmed an elevation in the phosphorylation levels of AKT, P70S6K, and STAT6 following Fc-IL-4 treatment (**New Fig. 5m** and **New Extended Data Fig. 12a-c**). In an ex vivo stimulation assay, the partial attenuation of Fc-IL-4 treatment benefits, including glycolysis level, T cell counts, enhanced effector

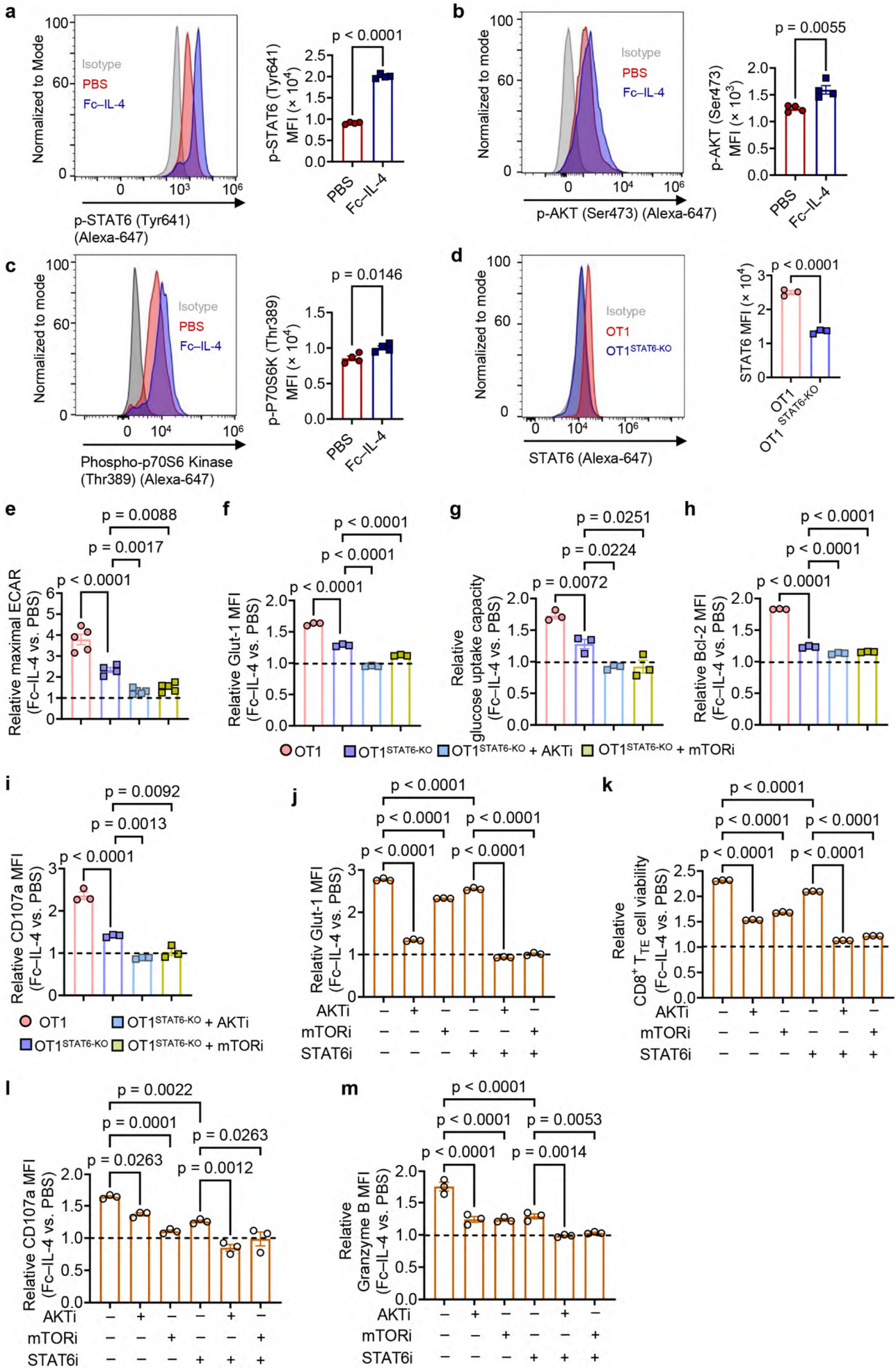
function, increased Glut-1 expression, glucose uptake capacity, and upregulation of Bcl-2 and CD107a, was observed in STAT6 knockout OT1 cells (OT1 STAT6-KO). However, the complete abrogation of Fc-IL-4 benefits occurred exclusively when AKT or mTOR signaling was concurrently blocked (**New Fig. 5n-p** and **New Extended Data Fig. 12d-i**). Additionally, co-inhibition of STAT6 along with either AKT or mTOR signaling using chemical inhibitors yielded similar outcomes (**New Extended Data Fig. 12j-m**).

Altogether, these results indicate that Fc-IL-4 enhances glycolysis, survival, and effector function of CD8⁺ T_{TE} cells through STAT6 signaling and PI3K-AKT-mTOR axis.

In investigating the potential differential activation of mTORC1/mTORC2 following Fc-IL-4 stimulation, we observed notable activation of P70S6K (a readout of mTORC1), whereas AKT phosphorylated at Ser473 (a readout of mTORC2) showed only slightly increased (**New Fig. 5m**). These results suggest that Fc-IL-4 primarily activates mTORC1 in the terminally exhausted CD8⁺ T cells.



New Fig. 5i-p. **i, j**, Schematic illustration of single-cell ATAC and gene co-profiling of ex vivo-induced CD8⁺ T_{TE} cells in the presence or absence of IL-4. Shown is a joint ATAC-gene UMAP of all the single cells, with cells color-coded by their respective conditions (**i**), and volcano plot showing differentially active motifs between IL-4 vs. PBS-treated T_{TE} cells (**j**). The expression intensity for the top upregulated and downregulated motifs was displayed. **k, l**, Experimental setting was described in **Fig. 1g**. Shown are signaling pathways regulated by DEGs in Fc-IL-4 vs. PBS-treated PMEL CD8⁺ TILs. Pathway terms are ranked by $-\log_{10}$ (p-value) (**k**), and top 20 ranked upstream regulators predicted from DEGs in Fc-IL-4 vs. PBS-treated PMEL CD8⁺ TILs, categorized by molecule type (**l**). In **k** and **l**, z score is computed and used to reflect the predicted activation level ($z > 0$, activated/upregulated; $z < 0$, inhibited/downregulated; $z \geq 2$ or $z \leq -2$ can be considered significant). **m**, Ex vivo-induced CD8⁺ T_{TE} cells were re-stimulated by dimeric anti-CD3 antibody ($0.1 \mu\text{g ml}^{-1}$) in the presence or absence of Fc-IL-4 ($n = 4$ biological replicates) for 0.5 h or 2 h. Shown are the WB images of phosphorylated STAT6, AKT (Ser473), and p-P70S6K (Thr389). **n-p**, Ex vivo-induced OT1 and OT1^{STAT6-KO} CD8⁺ T_{TE} cells were re-stimulated by dimeric anti-CD3 antibody ($0.5 \mu\text{g ml}^{-1}$), and treated with AKT inhibitor VIII (HY-10355, $1 \mu\text{M}$) or mTOR inhibitor (Rapamycin, 100 nM) in the presence or absence of Fc-IL-4 for 24 h. Shown are the relative basal glycolysis (**n**), CD8⁺ T_{TE} cell counts (**o**), and Granzyme B MFI (**p**) in the Fc-IL-4 treatment group normalized by that in the PBS group. Data are one representative of three independent experiments with $n = 3-5$ biological replicates. All data represent mean \pm s.e.m. and are analyzed by one-way ANOVA and Tukey's test (**n, o, and p**).



New Extended Data Fig. 12 | Fc-IL-4 enhances the glycolytic metabolism of CD8⁺ T_{TE} cells through STAT6 signaling and PI3K-AKT-mTOR axis.

a-c, Ex vivo-induced PMEL CD8⁺ T_{TE} cells were re-stimulated by dimeric anti-CD3 antibody (0.1 µg ml⁻¹) in the presence or absence of Fc-IL-4 (n = 4 biological replicates) for 0.5 h. Shown are the representative flow cytometry plots and MFI of p-STAT6 (**a**), p-AKT (Ser473) (**b**), p-P70S6K (Thr389) (**c**). **d**, The STAT6 was knock-out in OT1 T cells using CRISPR-Cas9 gene editing. Shown are representative flow cytometry plots and MFI of STAT6. **e-i**, Experimental setting was described in **Fig. 4n**. Shown are relative maximal ECAR (**e**), relative expression of Glut-1 (**f**), relative glucose uptake capacity (**g**), and relative expression of Bcl-2 (**h**) and CD107a (**i**) in the Fc-IL-4 treatment group normalized by that in the PBS group. **j-m**, Ex vivo-induced PMEL CD8⁺ T_{TE} cells were re-stimulated by dimeric anti-CD3 antibody (0.5 µg ml⁻¹) and treated with AKT inhibitor VIII (HY-10355, 1 µM), mTOR inhibitor (Rapamycin, 100 nM), or STAT6 inhibitor (AS1517499, 50 nM) in the presence or absence of Fc-IL-4 for 24 h. Shown are relative expression of Glut-1 (**j**), relative T cell viability (**k**), and relative expression of CD107a (**l**) and Granzyme B (**m**) in the Fc-IL-4 treatment group normalized by that in the PBS group. Data are one representative of three independent experiments with n = 3-5 biological replicates. All data represent mean ± s.e.m. and are analyzed by unpaired two-sided Student's t-test (**a-d**), or by one-way ANOVA and Tukey's test (**e-m**).

5. While potentially outside the realm of the present study, the data presented here suggest that modification of CART cells with either IL-4-Fc or tethered IL-4 on the cell surface with the TRUCK CAR system would promote CART activity.

We appreciate the suggestion. We are very interested in exploring the possibility of incorporating IL-4 or IL-4-Fc in CAR-T cell therapy based on the discovery reported in this manuscript. However, as pointed out by the reviewer, it is beyond the scope of the current study.

Minor points:

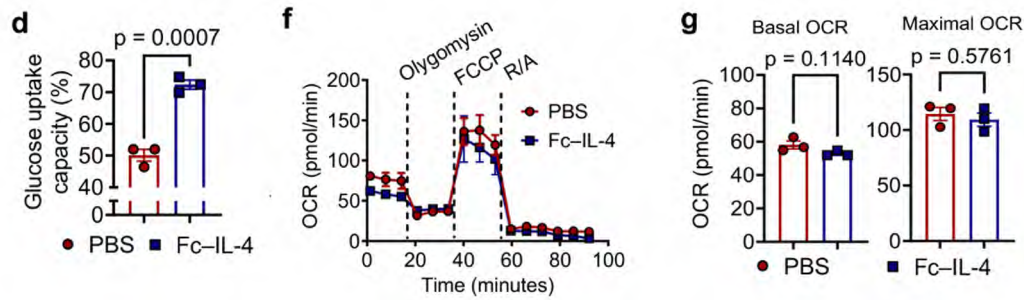
1. NBDG staining (assessed in Fig 5a) was used as a proxy of glucose uptake but this method has been shown to be problematic (Sinclair LV, Barthelemy C, Cantrell DA. 2020 Aug 17;2(4):e200029. doi: 10.20900/immunometab20200029). Additionally, the authors measured Glut-1 MFI but the antibody used appears to be against an intracellular domain. It is also surprising that maximal OCR is lower than basal OCR. Please provide more detail.

The mentioned literature (doi: 10.20900/immunometab20200029) showed that in the thymus, there was a poor correlation between 2-NBDG labeling and glucose transport capacity for thymocytes. However, they also showed that 2-NBDG labeling data correlated well with the relative levels of expression of glucose transporters and glucose uptake capacity in the activated CD8⁺ T cells. Moreover, higher MFI of 2-NBDG staining often correlates with higher glycolytic metabolic activity in activated CD8⁺ T cells, which has been confirmed by different studies in vivo and in vitro^{4,5}. To reinforce the conclusion, we also utilized the Glucose Colorimetric Assay Kit (Invitrogen™) to directly detect the level of glucose in the supernatant of T cell culture and found that Fc-IL-4 could dramatically increase the glucose uptake capacity of CD8⁺ T cells (**New Extended Data Fig. 9d**).

We used this anti-Glut-1 antibody (Cell signaling technology, mAb#12939) in a WB assay and cellular staining to measure the intracellular Glut1 expression instead of cell membrane staining.

The reason that maximal OCR was lower than basal OCR is due to the fact that the basal OCR level of activated T cells was already quite high. Therefore, the FCCP inhibition could not increase the OCR level sometimes, especially with the typical concentration (10 µM), which was reported to impair the function of mitochondria of over-activated T cells. These phenomena were also noted in other studies⁶.

We also repeated the seahorse experiment with a lower concentration of FCCP (1 µM) and obtained a typical Seahorse OCR curve showing similar findings that Fc-IL-4 did not affect the OCR levels of T cells (**New Extended Data Fig. 9f&g**). These results and the corresponding methods were updated in the revised version.



New Extended Data Fig. 9d, f, g. **d**, Glucose uptake capacity was calculated by measuring the left extracellular glucose level in the supernatant using the Glucose Colorimetric Detection Kit (Invitrogen™, EIAGLUC). **f**, Real-time OCR analysis of ex vivo-induced CD8⁺ T_{TE} cells re-stimulated by dimeric anti-CD3 antibody (0.5 μg ml⁻¹) for 48 h in the presence or absence of Fc-IL-4. **g**, Average basal and maximal OCR from (f). All data represent mean ± s.e.m. and are analyzed by unpaired two-sided Student's t-test.

2. The grammar used in the manuscript is often incorrect and may hamper the ability of the reader to understand the context. The manuscript should be reviewed in detail, possibly by a language editorial service.

We apologize for any grammar mistakes. We have thoroughly reviewed and refined the language in the revised manuscript.

3. The term “anticancer” is unusual. Please use “anti-tumor”. Please check other specific terms to fit the manuscript for the cancer immunotherapy paper.

We have replaced "anticancer" with "anti-tumor" throughout the manuscript and reviewed all other terms to ensure that the descriptions align with the context of a cancer immunotherapy paper.

Referee #2 (Remarks to the Author):

Feng and colleagues have presented a captivating report focusing on the use of type 2 cytokines to enhance the effectiveness of terminally exhausted CD8 T cells (TE CD8) against tumors. Their approach involved fusing the Fc domain to IL4, resulting in an improved half-life compared to recombinant IL4. They demonstrated that this modification led to enhanced accumulation of TE CD8 cells in a syngeneic tumor model. Notably, this accumulation correlated with improved effector functions, such as increased production of granzyme B and IFN γ . These enhancements translated into remarkable antitumor activity across various tumor models when employing adoptive transfer of tumor-specific T cells and CAR T cells. Importantly, these improved antitumor effects were observed without the need for pre-conditioning, which has the potential to advance the field of adoptive cell therapy (ACT). Through the utilization of various cell depletion methods, the authors revealed that the enhancement of antitumor activity by Fc-IL4 specifically depended on CD8 T cells, which was surprising considering the previous belief that this cytokine primarily modulates Macs, DCs, B cells, and CD4 T cells. Using elegant models, the authors demonstrated that Fc-IL4 improves TE CD8 T cells, independently of T_{pex}, by enhancing glycolysis mediated by lactate dehydrogenase A (LDHA).

In summary, this study exhibits high technical and experimental quality. The experiments conducted, along with the implementation of numerous syngeneic models, provide substantial support for the authors' claims and mechanistic interpretations. This discovery is poised to have a profound impact on the field of immunotherapy.

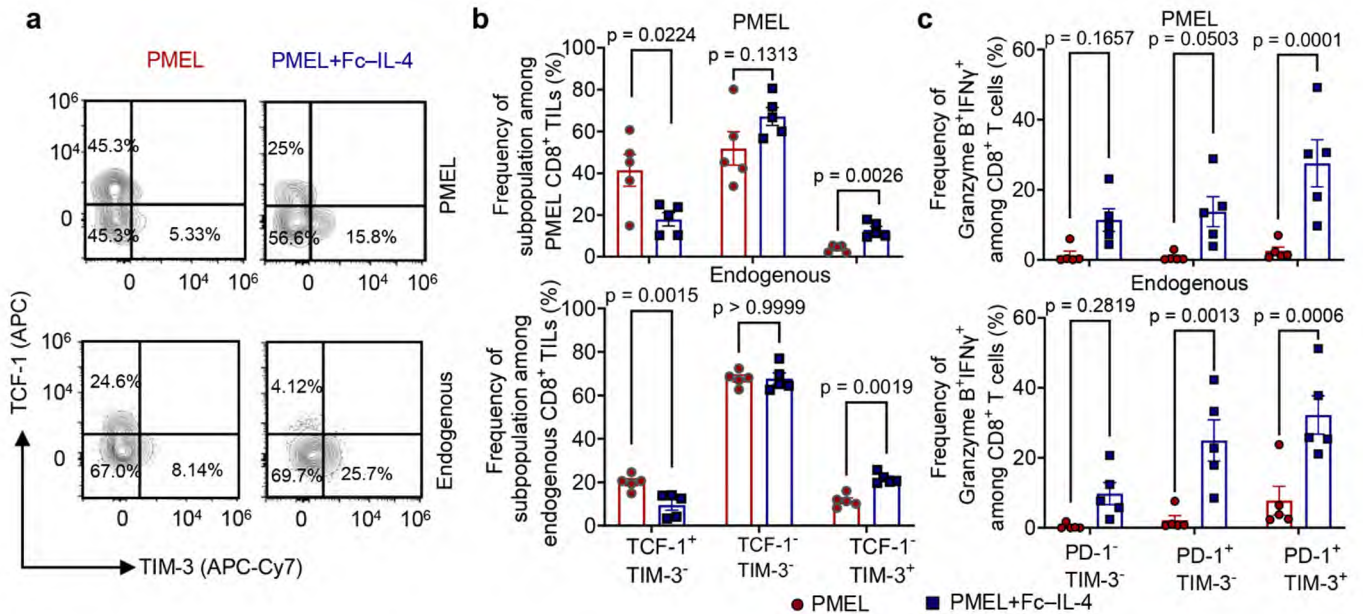
We appreciate the positive comments of the reviewer.

Comments:

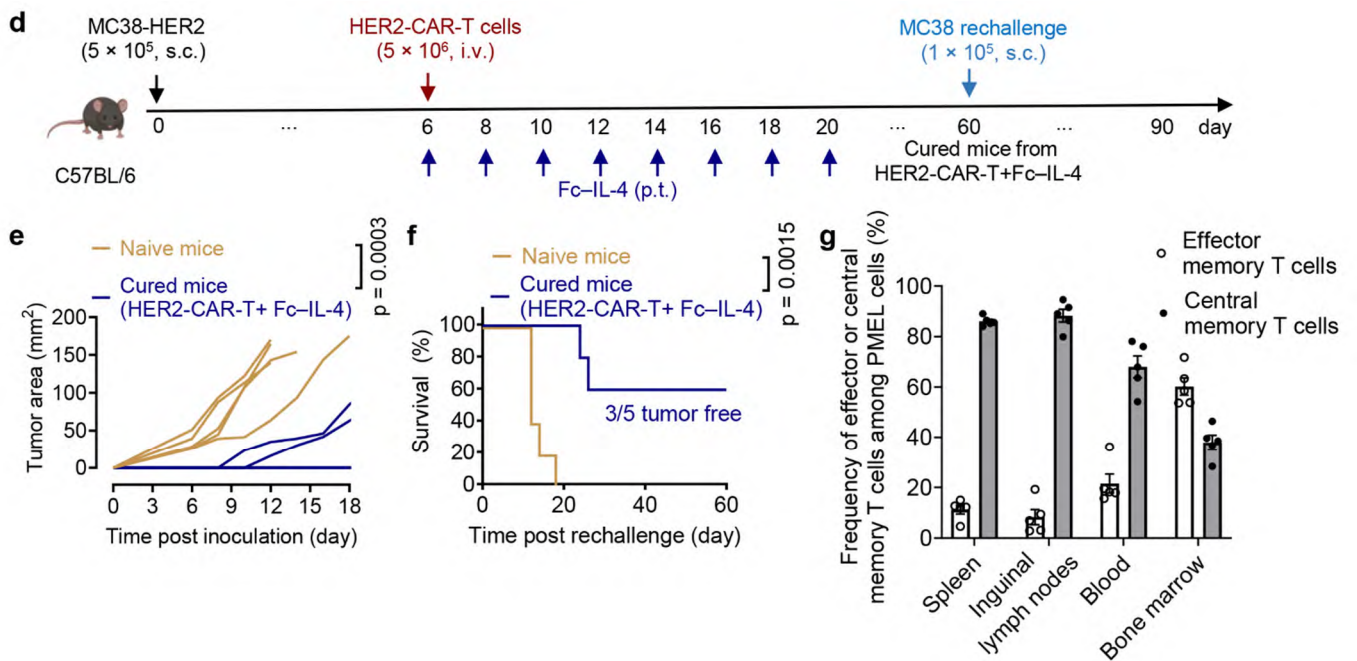
1) In figure 3, during the rechallenge experiment. Were the tumors controlled by endogenous T cells or ACT T cells? Data from multiple figures suggest that Fc-IL4 mostly impact TE-CD8 T cells. After tumor clearance, are these cells persisting or Fc-IL4 also generated a pool of memory T cells that can respond to the rechallenge?

Upon the treatment of Fc-IL-4, endogenous CD8⁺ T cells were also found reinvigorated in addition to transferred T cells (no lymphodepletion in all the therapeutic experiment models) (**Fig.1a-d** and **New Extended Data Fig. 2a-c**). Interestingly, we found that mice surviving from the combination therapy of HER2-CAR-T and Fc-IL-4 not only resisted the rechallenge of MC38-HER2 tumor cells (previous data, now moved to **Fig. 2g**), but also the parental MC38 tumor cell, which is HER2 negative (**New Extended Data Fig. 5d-f**). These results further indicated that both endogenous and ACT cells contributed to the rejection of tumor rechallenge.

We euthanized the survivor mice from the combination of PMEL and Fc-IL-4 treatment and could not find CD8⁺ T_{TE} cells existing in the major lymph organs, suggesting that CD8⁺ T_{TE} cells did not persist. By contrast, we found most transferred PMEL T cells became central memory T cell in various lymphoid organs (**New Extended Data Fig. 5g**). These results indicate that Fc-IL-4 induces a pool of memory T cells in these surviving mice and endows the mice with long-term antitumor immunity.



New Extended Data Fig. 2a-c. Experimental setting was described in **Fig. 1a**. Shown are the representative flow cytometry plots (**a**) and the frequencies (**b**) of CD8⁺ T_{TE} cells (TCF1⁺TIM-3⁺) among PMEL or endogenous CD8⁺ TILs, and frequencies of Granzyme B⁺IFNγ⁺ among different subpopulations of PMEL or endogenous CD8⁺ TILs (**c**). All data represent mean ± s.e.m. and are analyzed by Two-way ANOVA and Sidak multiple comparisons test.



New Extended Data Fig. 5d-g. **d-f**, Experimental setting was similar as that described in **Fig. 2a** except that the surviving mice were rechallenged with the parental cell line, MC38, which was HER2 negative. Shown are the experimental timeline (**d**), the tumor growth curves (**e**) and the survival curves (**f**) of the rechallenged mice (n = 5 mice). **g**, Experimental setting was described in **Fig. 2a**. Shown is the frequencies of effector memory (defined as CD44⁺CD62L⁻) and central memory (defined as CD44⁺CD62L⁺) T cells among PMEL T cells in different organs. All data represent mean ± s.e.m. and are analyzed by unpaired two-sided Student's t-test (**e**), or log-rank test for survival curves (**f**).

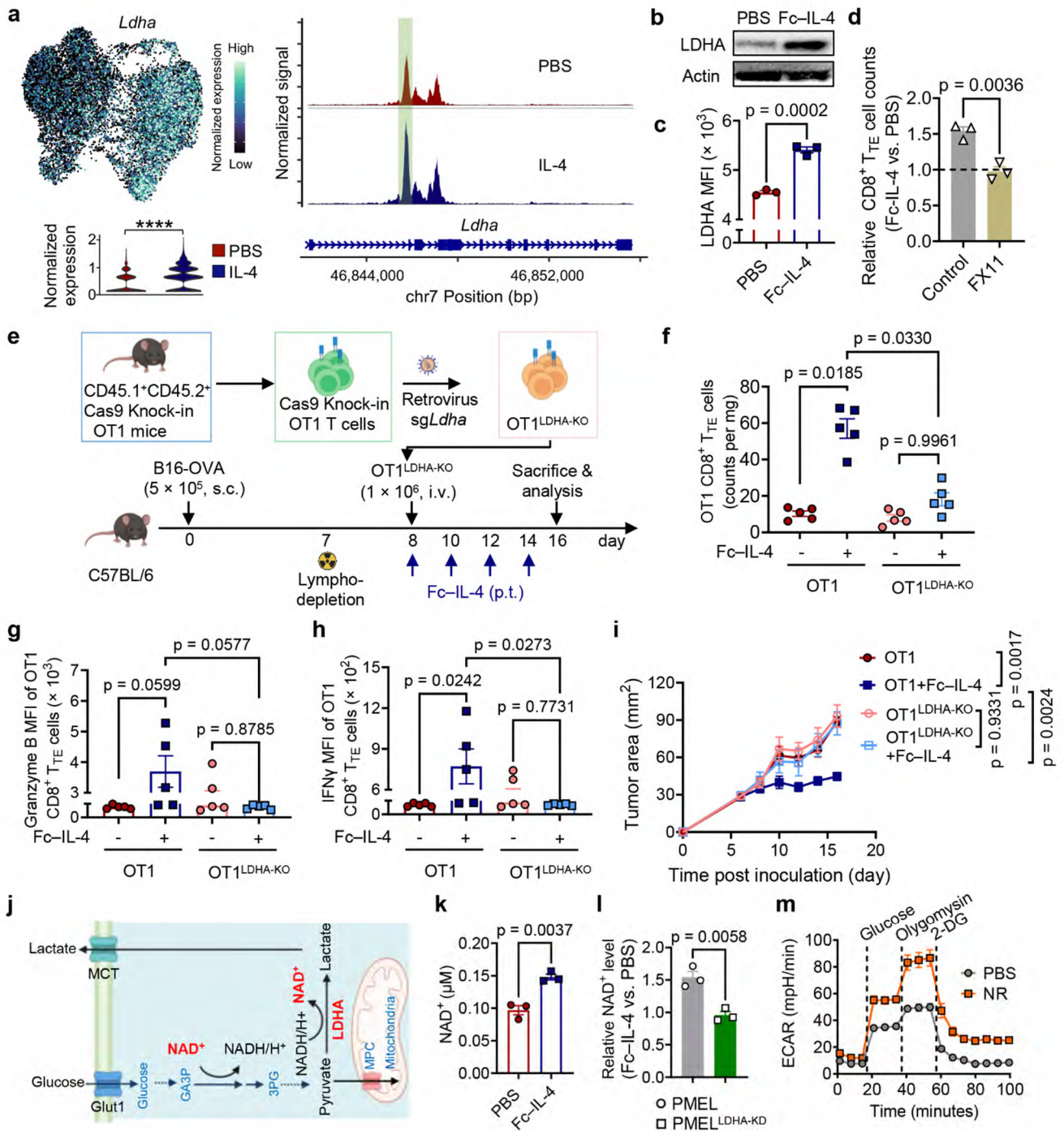
2) It is intriguing that Fc-IL-4 treatment only affects ECAR and not OCR. Further investigation is necessary to determine whether LDHA is the primary factor responsible for these observations. Can overexpression of LDHA alone enhance T cell antitumor immunity?

To assess the involvement of key enzymes in Fc-IL-4-induced glycolysis enhancement, we analyzed single-

cell ATAC and transcriptome co-profiling datasets, revealing alterations in chromatin accessibility associated with several glycolytic enzymes, among which *Ldha* showcased the most pronounced upregulation post-IL-4 treatment ([New Fig. 6a](#) and [New Extended Data Fig. 14a, b](#)). This observation was further validated through Western blot (WB) and flow cytometry analyses, which confirmed elevated LDHA expression in Fc-IL-4 treated CD8⁺ T_{TE} cells ([New Fig. 6b&c](#) and [New Extended Data Fig. 14c](#)). In addition, LDHA blockade or knock-out completely abrogated the effects of Fc-IL-4 on terminally exhausted CD8⁺ T cells for increased glycolysis, and the subsequent enhancement of effector function and survival in vitro and vivo (previous data, now moved to [Fig. 6d-i](#) and [New Extended Data Fig. 14d-i](#)). All these results suggest that LDHA is indispensable and a primary factor for the upregulated glycolytic activity induced by Fc-IL-4.

LDHA is a crucial enzyme in modulating glycolysis by catalyzing the pyruvate into lactate and maintaining the cycle of NAD⁺ generation⁷ (previous schematic, now moved to [Fig. 6j](#)). CD8⁺ T_{TE} cells exhibited several survival defects⁸, and one contributing factor was the deficiency in NAD⁺⁹. We found that NAD⁺ supplementation could alleviate the cell death of CD8⁺ T_{TE} cells (previous data, now moved to [Extended Data Fig. 15d, f, g](#)). In addition, we showed that the survival enhancement of CD8⁺ T_{TE} cells by Fc-IL-4 treatment also relied on LDHA for the increased cellular NAD⁺ level (previous data, now moved to [Fig. 6k&l](#)), further suggesting the essential role of LDHA for Fc-IL-4 to exert its function.

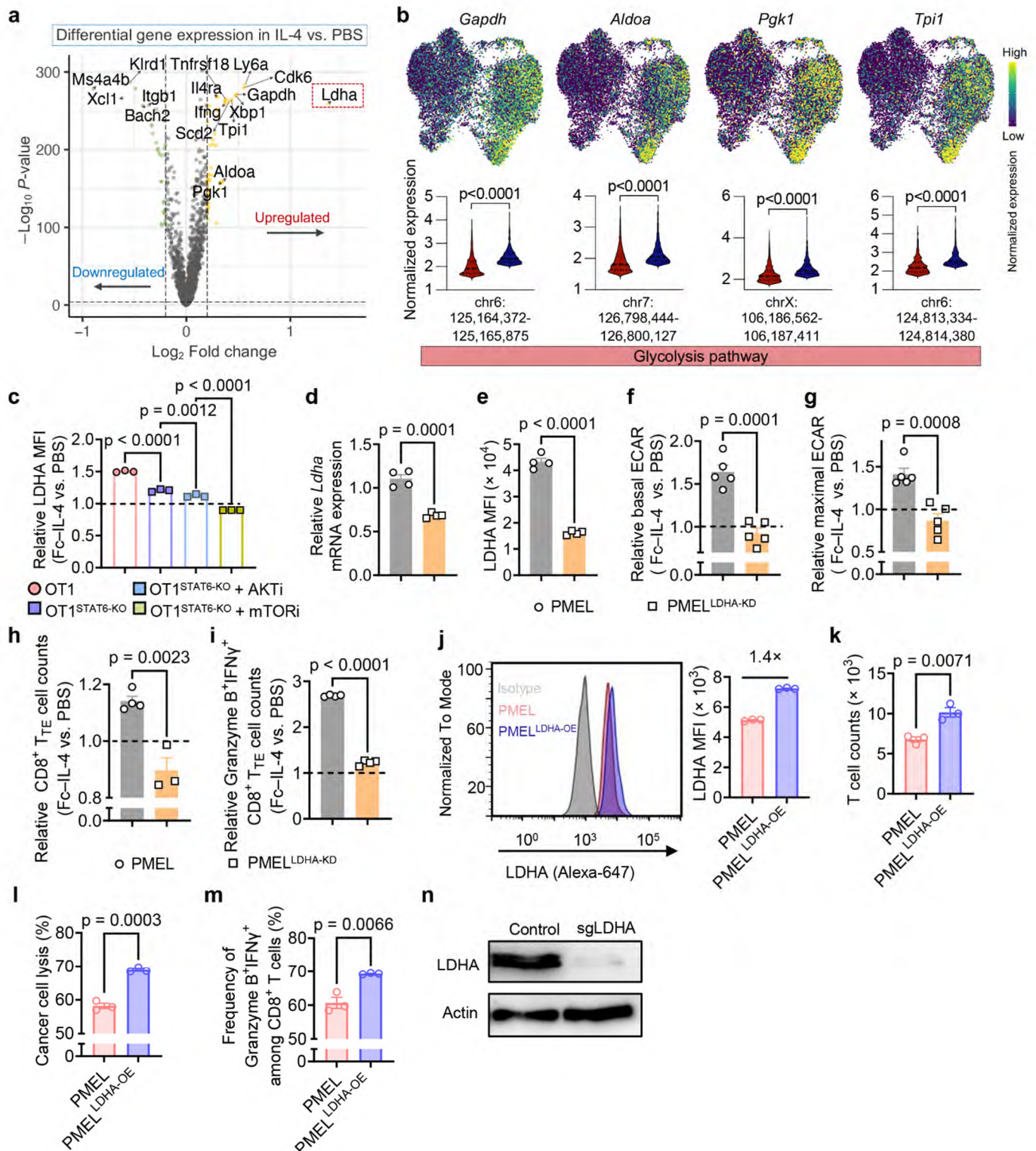
As suggested, we prepared LDHA-overexpressing PMEL T cells and evaluated their function. We found that overexpression of LDHA could enhance the survival, effector function, and antitumor efficacy of CD8⁺ T cells ([New Extended Data Fig. 14j-m](#)).



New Fig. 6 | Fc-IL-4 promotes LDHA-mediated glycolysis and cellular NAD⁺ levels of CD8⁺ T_{TE} cells.

a, Expression of *Ldha* on the joint UMAP in Fig. 5j and pseudo-bulk chromatin accessibility tracks in the genomic region of *Ldha*, depicted separately for IL-4 and PBS conditions. The enhancer element predicted by ENCODE within the region of this gene is highlighted in a light green shade. **b**, **c**, Ex vivo-induced CD8⁺ T_{TE} cells were re-stimulated by dimeric anti-CD3 antibody (0.5 $\mu\text{g ml}^{-1}$) in the presence or absence of Fc-IL-4 for 48 h. ($n = 3$ biological replicates). Shown are the WB images of LDHA (**b**) and LDHA MFI (**c**). **d**, Ex vivo-induced CD8⁺ T_{TE} cells were re-stimulated by dimeric anti-CD3 antibody (0.5 $\mu\text{g ml}^{-1}$) in the presence or absence of Fc-IL-4 for 48 h with a LDHA inhibitor, FX11 (16 μM), or DMSO ($n = 3$ biological replicates). Shown are relative counts of CD8⁺ T_{TE} cells in the Fc-IL-4 treatment group normalized by that in the PBS group. **e-i**, Mice bearing B16-OVA tumors received ACT of activated WT OT1 or OT1^{LDHA-KO} T cells (1×10^6 , i.v.) one-day post lymphodepletion followed by the treatment of Fc-IL-4 (20 μg , p.t.) or PBS every other day for 4 doses in total ($n = 5$ animals). Mice were sacrificed on day 16 and the tumor tissues were collected for analysis by flow cytometry. Shown are the experimental timeline (**e**), counts of tumor-infiltrating OT1 CD8⁺ T_{TE} cells (**f**), MFI of Granzyme B (**g**) and IFN γ (**h**) of tumor-infiltrating OT1 CD8⁺ T_{TE} cells, and average tumor growth curves (**i**) of mice. **j**, Schematic of LDHA mediated NAD⁺/NADH recycling. **k**, Experimental setting was described in Fig. 6b. Shown is the cellular NAD⁺ level of CD8⁺ T_{TE} cells. **l**, Ex vivo-induced WT PMEL and PMEL^{LDHA-KD} CD8⁺ T_{TE} cells were re-stimulated by dimeric anti-CD3 antibody (0.5 $\mu\text{g ml}^{-1}$) in the presence or absence of Fc-IL-4. Shown is relative NAD⁺

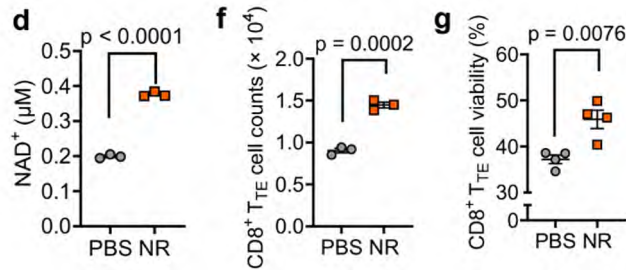
level in the Fc-IL-4 group normalized by that in the PBS group. **m**, Real-time ECAR analysis of ex vivo-induced CD8⁺ T_{TE} cells re-stimulated by dimeric anti-CD3 antibody (0.5 μg ml⁻¹) for 48 h in the presence or absence of NR (100 μM). Data are one representative of three independent experiments with n = 3-5 biological replicates or n = 5-7 animals. All data represent mean ± s.e.m. and are analyzed by unpaired two-sided Student's t-test (**c**, **d**, **k**, and **l**), or one-way ANOVA and Tukey's test (**f-i**).



New Extended Data Fig. 14 | Fc-IL-4 reinvigorates CD8⁺ T_{TE} cells by enhancing LDHA-dependent glycolysis.

a, Experimental setting was described in **Fig. 5i**. Shown is volcano plot showing differential gene expression between IL-4 vs. PBS-treated PMEL CD8⁺ T_{TE} cells. **b**, Expression of glycolysis pathway gene markers on the joint UMAP in **Fig. 5j**, along with comparisons of corresponding accessible peaks between conditions. **c**, Experimental setting was described in **Fig. 5m**. Shown is the relative expression of LDHA in the Fc-IL-4 treatment group normalized by that in

the PBS group. **d-i**, WT PMEL or PMEL^{LDHA-KD} T cells were re-stimulated by dimeric anti-CD3 antibody (0.5 $\mu\text{g ml}^{-1}$) in the presence or absence of Fc-IL-4. Shown are the relative transcriptome level of LDHA (**d**) and protein expression level of LDHA (**e**) in PMEL^{LDHA-KD} T cells, and the relative basal (**f**) and maximal ECAR (**g**), relative counts of CD8⁺ T_{TE} cells (**h**), and Granzyme B⁺IFN γ ⁺ polyfunctional CD8⁺ T_{TE} cells (**i**) in the Fc-IL-4 treatment group normalized by that in the PBS group. **j-m**, WT PMEL or PMEL^{LDHA-OE} T cells were co-cultured with B16F10 for 48 h. Shown are representative flow cytometry plots and LDHA MFI (**j**), T cell counts (**k**), percent of cancer cell lysis (**l**), and frequencies of Granzyme B⁺IFN γ ⁺ (**m**) among PMEL^{LDHA-OE} T cells. **n**, WB images of LDHA showing the LDHA knock-out in OT1^{LDHA-KO} T cells. Data are one representative of three independent experiments with n = 3-5 biological replicates. All data represent mean \pm s.e.m. and are analyzed by One-way ANOVA and Tukey's test (**c**), or unpaired two-sided Student's t-test (**d-m**).



Extended Data Fig. 15d, f, g. **d**, The cellular NAD⁺ level of ex vivo-induced CD8⁺ T_{TE} cells with supplementation of a NAD⁺ precursor, NR (100 μM). **f, g**, Ex vivo-induced CD8⁺ T_{TE} cells were re-stimulated by dimeric anti-CD3 antibody (0.5 $\mu\text{g ml}^{-1}$) for 48 h in the presence or absence of NR (100 μM). Shown are the counts (**f**) and cell viability (**g**) of CD8⁺ T_{TE} cells. All data represent mean \pm s.e.m. and are analyzed by unpaired two-sided Student's t-test.

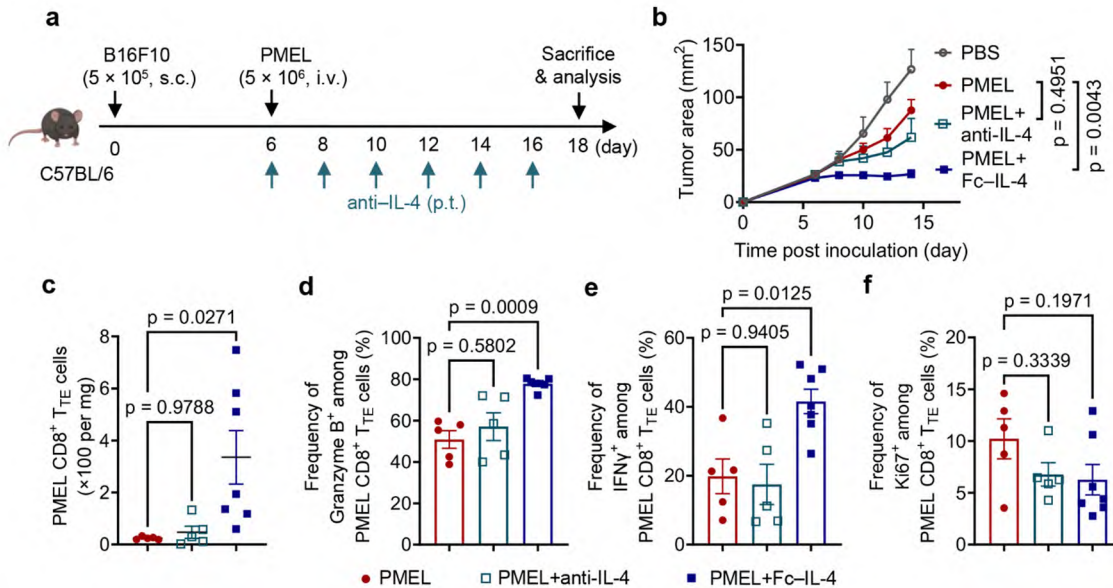
3) The study did not assess the role of endogenous IL-4. While the authors demonstrated that Fc-IL-4 enhances antitumor immunity, this prompts the question of whether blocking the production of endogenous IL-4 impairs antitumor immunity. Furthermore, it remains unclear which cells are responsible for producing IL-4 in normal tumor responses.

We neutralized intratumoral IL-4 using anti-IL-4 antibody and observed that this had negligible effects on the antitumor efficacy of the ACT therapy using PMEL T cells. Tumor infiltration and effector function of tumor-infiltrating PMEL T cells remained unaffected by IL-4 neutralization ([New Extended Data Fig. 8](#)). One of the possible reasons is that the physiological level of endogenous IL-4 (around 1 pg/ml in the human serum² and <5 pg/ml in the tumor tissues³) is substantially lower compared to the injected exogenous Fc-IL-4 (20 μg every injection, equivalent to 2-20 $\mu\text{g/ml}$ assuming tumor volume is 1 cm^3 ; $\sim 10^3$ - 10^6 times higher concentration than the physiological level).

We added the discussion of endogenous IL-4 in the revised manuscript:

“We also discovered that endogenous IL-4, typically present at substantially lower concentrations compared to exogenously injected Fc-IL-4, had negligible impact on the anti-tumor immunity of ACT with PMEL T cells. This was evidenced by minimal effects on the expansion, cytotoxicity, effector function, or proliferative capability of tumor-infiltrating CD8⁺ T_{TE} cells upon neutralizing endogenous IL-4 through p.t. administration of anti-IL-4 antibody (Extended Data Fig. 8). Overall, these findings strongly suggest that the exogenous type 2 cytokine Fc-IL-4, administered at 20 μg per injection (a concentration much higher than endogenous IL-4) primarily drives the enrichment of CD8⁺ T_{TE} cells by enhancing their survival.”

We would like to respectfully clarify that IL-4 producing cells have been extensively investigated and reported in previous studies¹⁰. The expression level of intratumoral IL-4 varies significantly across different types of tumors. In primary epithelial cancer cells, such as those found in human colon, breast and lung carcinomas, IL-4 is primarily produced by these cells³. In bladder and prostate carcinoma, immune cells including eosinophils, basophils, and type 2 CD4⁺ T cells are identified as the major sources of IL-4 production¹¹. However, as we explained above, the physiological levels of endogenous IL-4 in the tumor microenvironment are nearly negligible compared to the injected dose of Fc-IL-4. Thus, its relevance in the context of Fc-IL-4 therapy is minimal.



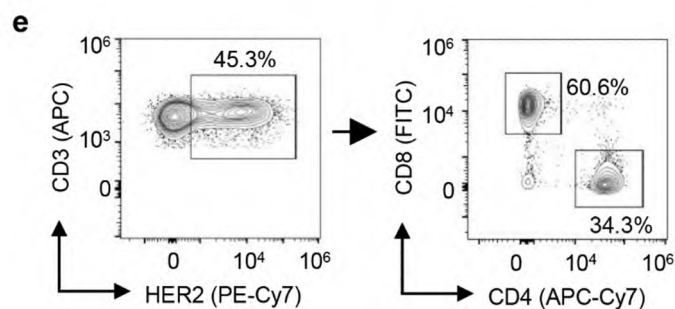
New Extended Data Fig. 8 | Endogenous IL-4 exhibits negligible effects on tumor-infiltrating CD8⁺ T_{TE} cells.

B16F10 tumor-bearing mice received ACT of PMEL T cells (5×10^6 , i.v.) followed by administration of anti-IL-4 antibody (200 μ g, p.t.), or Fc-IL-4 (20 μ g, p.t.), or PBS every other day for 6 doses in total. Mice were sacrificed on day 18 and the tumor tissues were collected for analysis by flow cytometry. Shown are the experimental timeline (a), average tumor growth curves (b), counts of tumor-infiltrating PMEL CD8⁺ T_{TE} cells (c), frequencies of Granzyme B⁺ (d), IFN γ ⁺ (e), and Ki67⁺ (f) among tumor-infiltrating PMEL CD8⁺ T_{TE} cells. Data are one representative of two independent experiments with n = 5-7 animals. All data represent mean \pm s.e.m. and are analyzed by one-way ANOVA and Tukey's test.

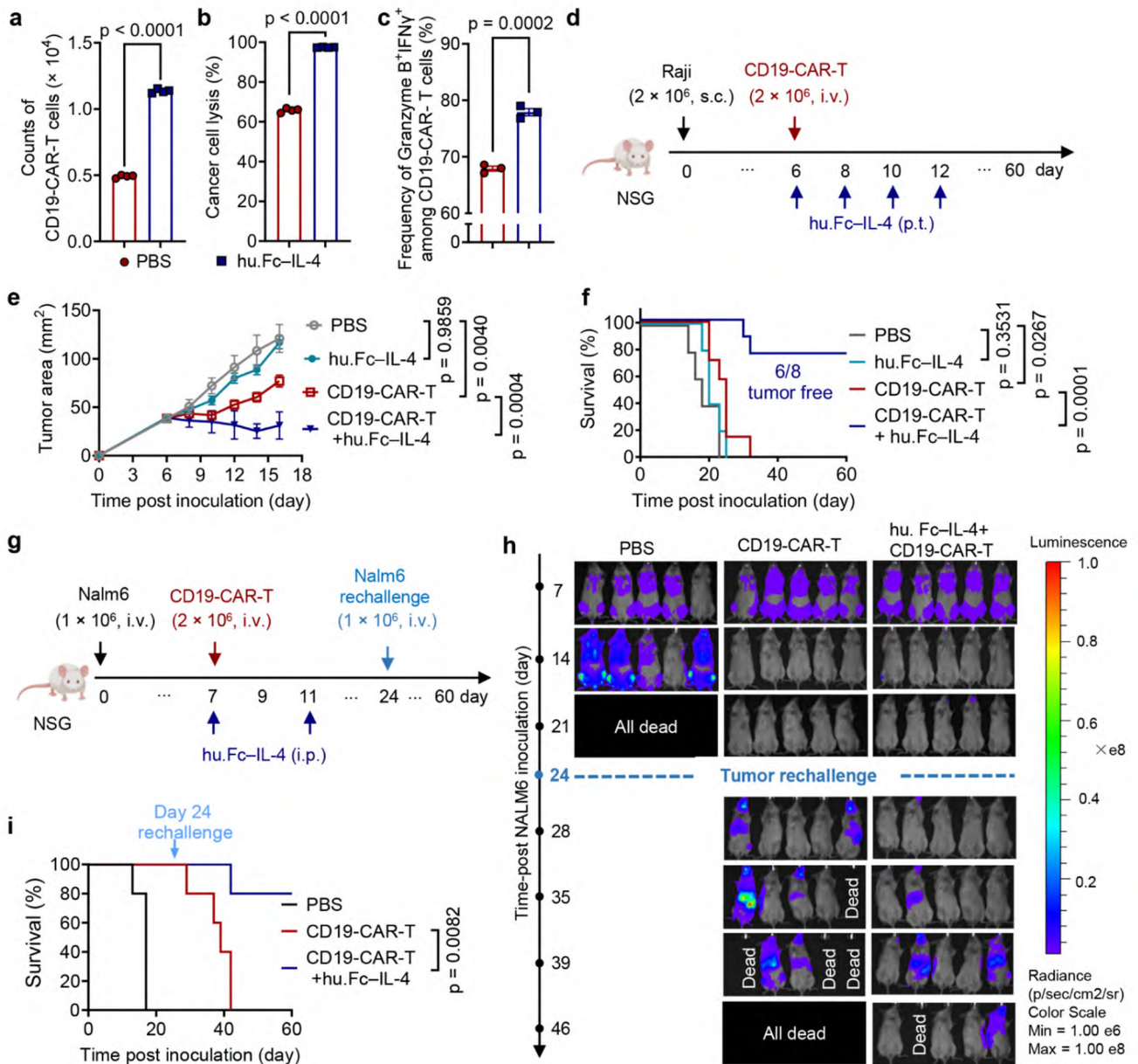
4) In figure 3, it is unclear from the methods and legends if the CAR T cells were composed of CD8 T cells only or a mix of CD4 and CD8 as used in patients. CD4 CAR T cells are known to be cytotoxic and when tested individually are better than CAR CD8 T cells alone. The authors should precise the composition of the CAR T cell used in figure 3.

The HER2-CAR-T cells used in our study comprise both CD4⁺ and CD8⁺ T cells, with the ratio of CD4⁺ CAR-T cells ~34% and CD8⁺ CAR-T cells ~61% (New Extended Data Fig. 4e).

To heighten the clinical relevance of our study, we performed new experiments to assess the combination therapy of human Fc-IL-4 and human CD19-CAR-T cells in both the solid Raji tumor model and recurrent leukemia model. The results demonstrated that human Fc-IL-4 dramatically enhanced the antitumor efficacy of CD19-CAR-T cells and prolonged mouse survival (New Fig. 3). The composition of CD4⁺ and CD8⁺ cells in the human CAR-T was also provided (New Extended Data Fig. 6a).

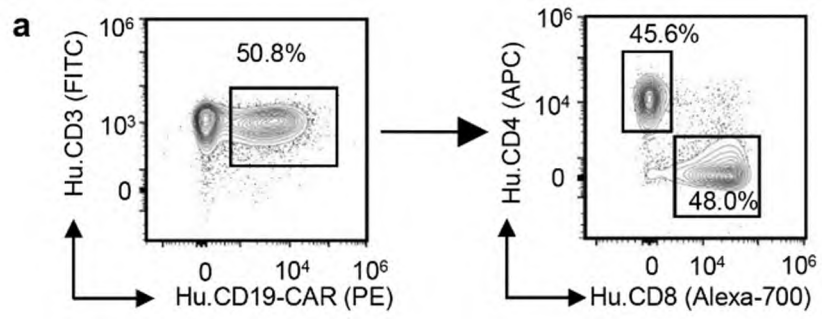


New Extended Data Fig. 4e. Representative flow cytometry plots showing the frequency of CD4⁺ and CD8⁺ T cells among HER2-CAR-T cells.



New Fig. 3 | hu.Fc-IL-4 enhances human CD19-CAR-T cell immunotherapy in xenograft models.

a-c, Human CD19-CAR-T cells restimulated with K562 cells were co-cultured with Nalm6 cells at an effector/target (E/T) ratio of 1:8 for 4 days in the presence or absence of hu.Fc-IL-4 (20 ng ml^{-1}) ($n = 3$ or 4 biological replicates). Shown are the counts of CD19-CAR-T cells (**a**), percent of cancer cell lysis (**b**), and frequencies of Granzyme B⁺IFN γ ⁺ among CD19-CAR-T cells (**c**). **d-f**, NSG mice were inoculated with Raji lymphoma cells (2×10^6 , s.c.). Tumor-bearing mice received ACT of CD19-CAR-T (2×10^6 , i.v.) followed by administration of hu.Fc-IL-4 ($20 \mu\text{g}$, p.t.) or PBS every other day for 4 doses in total. Mice receiving injections of PBS only and hu.Fc-IL-4 ($20 \mu\text{g} \times 4$, p.t.) only served as controls. Shown are the experimental timeline (**d**), average tumor growth curves (**e**) and Kaplan-Meier survival curves (**f**) of mice. **g-i**, NSG mice were inoculated with Nalm6-luciferase leukemia cells (1×10^6 , i.v.). Tumor-bearing mice received ACT of CD19-CAR-T cells (2×10^6 , i.v.) followed by administration of hu.Fc-IL-4 (100 ng , p.t.) or PBS every four days for 2 doses in total. The survivor mice were rechallenged with Nalm6-luciferase cells (1×10^6 , i.v.) on day 24. The tumor burden was monitored using IVIS Spectrum In Vivo Imaging System (PerkinElmer). Shown are the experimental timeline (**g**), bioluminescence images representing the tumor burden (**h**), and Kaplan-Meier survival curves (**i**) of mice. All data represent mean \pm s.e.m. and are analyzed by two-sided unpaired Student's t-test (**a-c**), one-way ANOVA and Tukey's test for tumor growth curves (**e**), or log-rank test for survival curves (**f, i**).



New Extended Data Fig. 6a. Representative flow cytometry plots showing the frequency of CD4⁺ and CD8⁺ T cells among CD19-CAR-T cells.

Referee #3 (Remarks to the Author):

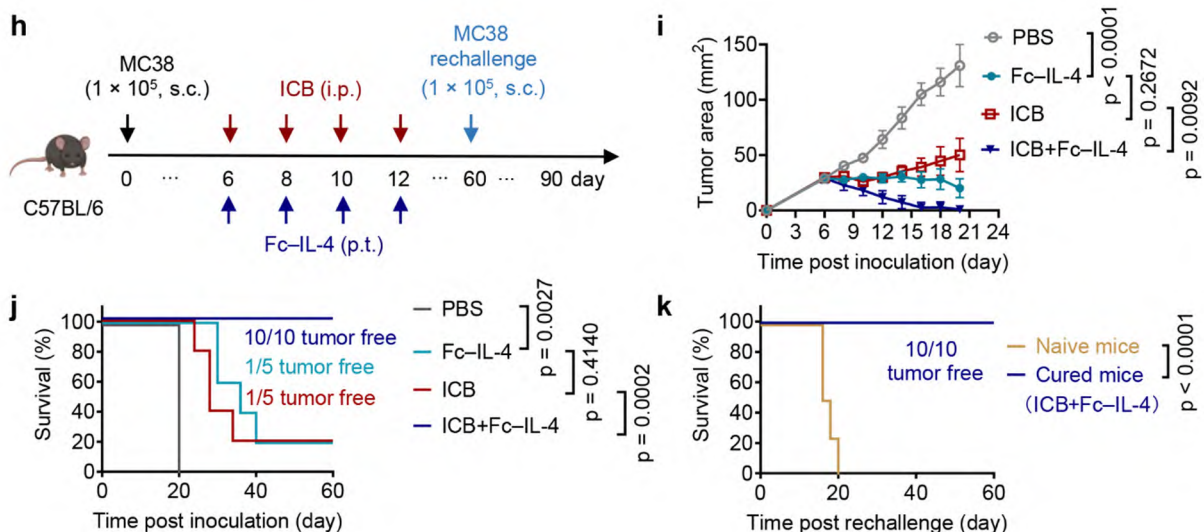
Feng et al. show that IL-4Fc fusion protein strongly promotes anti-tumor activity by both endogenous CD8 T cells and adoptively transferred ex vivo activated T cells. Although the described effects are very interesting, there are several points that slightly limit my enthusiasm for the present manuscript. These include the lack of mechanistic evidence how the IL4 impact occurs and how this alters the function of cells.

We thank the reviewer for the positive and helpful comments. We have thoroughly addressed all points concerning mechanistic evidence, as outlined below in detail.

Major points:

1. There are many reports praising new strategies for their anti-tumor efficacy that later turn out to be less impressive. For me, it is therefore very important to see how a new effect compares to existing strategies. My question is therefore how effective is the IL-4Fc approach compared to anti-PD1 blockade or combined anti-PD1/anti-CTLA4 treatment. Are there synergistic effects between anti-PD-1 and IL-4 FC in this context?

We assessed the antitumor efficacy of Fc-IL-4 in combination with ICB therapy (anti-PD-1 plus anti-CTLA-4) in a MC38 model. The results showed that while Fc-IL-4 monotherapy achieved similar tumor regression effects as the ICB therapy, most strikingly, the combination of Fc-IL-4 and ICB therapy eradicated the tumors in all the treated tumor-bearing mice (10 out of 10). Notably, all cured mice from the treatment group of Fc-IL-4 and ICB rejected the second challenge of MC38 tumor cells. These new results are added in the revised version ([New Fig. 2h-k](#)).



New Fig. 2h-k. C56BL/6 mice were inoculated with MC38 colon adenocarcinoma cells (1 × 10⁵, s.c.). Tumor-bearing mice received the combinatory treatment of ICB (anti-PD-1 (100 µg, i.p.) plus anti-CTLA-4 (100 µg, i.p.)) and Fc-IL-4 (20 µg, p.t.) every other day for 4 doses in total. Mice receiving injections of PBS, Fc-IL-4 (20 µg × 4) only, or ICB only served as controls. Cured mice from groups receiving the combinatory treatment of ICB and Fc-IL-4 were re-challenged with MC38 (1 × 10⁵, s.c.) cells two months post primary tumor inoculation. Shown are the experimental timeline (h), the average tumor growth curves (i) and Kaplan-Meier survival curves (j) of tumor-bearing mice, and Kaplan-Meier survival curves of naïve or cured mice re-challenged with MC38 tumor cells (k). All data represent mean ± s.e.m. and are analyzed by One-way ANOVA and Tukey's test (i) or log-rank test for survival curves (j, k).

2. What I find less convincing are the metabolic studies included into the manuscript. The authors argue that IL-4 induced metabolic reprogramming and that this is critical for the re-activation of cells. However, the authors present only correlative evidence and it remains unclear what it the driving event. T cell activation goes typically along with metabolic changes. It is therefore equally likely that IL-4 somehow activates the cells which then translates into metabolic changes.

A similar problem arises with the conclusions drawn from the LDHA studies. In my opinion, it is an

essential enzyme at the end of the glycolysis pathways. We know that glycolysis is required for effector T cell function. Is this enzyme dispensable under other conditions where effector cells are formed? I suspect that it is not, but then the proposed mechanism would have nothing to do specifically with IL-4-induced activation but rather with T-cell activity in general.

Thus, a shortcoming of the manuscript are the limited mechanistic insights how IL-4 enhances the anti-tumor activity of CD8 T cells. In particular, this relates to how IL-4 promotes recruitment and why it increases the expression of cytokines and granzymes in tumors. Does IL-4FC cause a different signal quality or just a stronger signal because the lifespan is extended by the use of a fusion construct?

Thanks for the comprehensive comments. We believe there are 4 sub-points in this feedback, and we have responded to each point individually as follows:

2(a) The relationship between metabolism and activation/differentiation of T cells.

We fully understand there is a long debate in the general field of immune metabolism, whether metabolic programming is a cause or merely a correlation^{12,13,14,15}. We hope to point out that growing evidence suggests that metabolic changes are important driving forces for T cell differentiation, exhaustion, and reactivation^{16,17}. In this study, we showed evidence that general blockade of glycolysis using 2-DG completely abrogated the effects of Fc-IL-4 (previous data, now moved to [Fig. 5g&h](#) and [Extended Data Fig 9m&n](#)), suggesting that glycolysis enhancement mediated by Fc-IL-4 was a causal effect.

To further validate this observation, we prepared LDHA-overexpressing PMEL T cells and evaluated their functionality. We found that overexpression of LDHA alone in T cells (without any Fc-IL-4 treatment) enhanced the survival, effector function, and antitumor efficacy of CD8⁺ T cells ([New Extended Data Fig. 14j-m](#)), providing additional evidence that metabolic reprogramming could reinvigorate CD8⁺ T_{TE} cells.

As pointed out by the reviewer, LDHA is a crucial enzyme in modulating glycolysis by catalyzing the pyruvate into lactate and maintaining the cycle of NAD⁺ generation⁷ (previous schematic, now moved to [Fig. 6j-m](#)). CD8⁺ T_{TE} cells exhibited severe survival defects⁸, and one contributing factor was the deficiency in NAD⁺⁹. As an alternative, we found that NAD⁺ supplementation, as a direct metabolic modulation, could also alleviate the survival defect of CD8⁺ T_{TE} cells (previous data, now moved to [Extended Data Fig. 15d-i](#)) and enhance their function.

With various datasets presented, including those from general and specific blockade of glycolysis, over-expressing LDHA, and feeding cells with NAD⁺ supplementation, we show that the glycolysis enhancement mediated by Fc-IL-4 was a causal effect of the observed phenotypes.

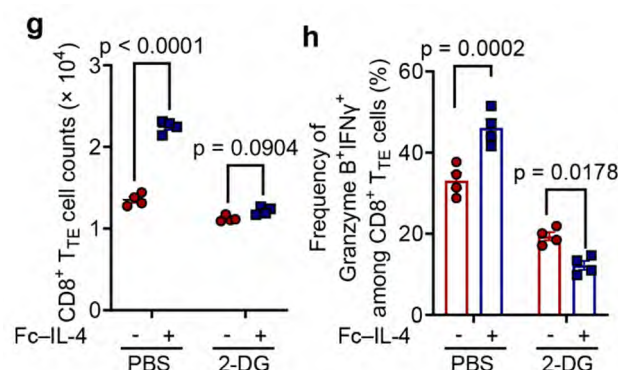
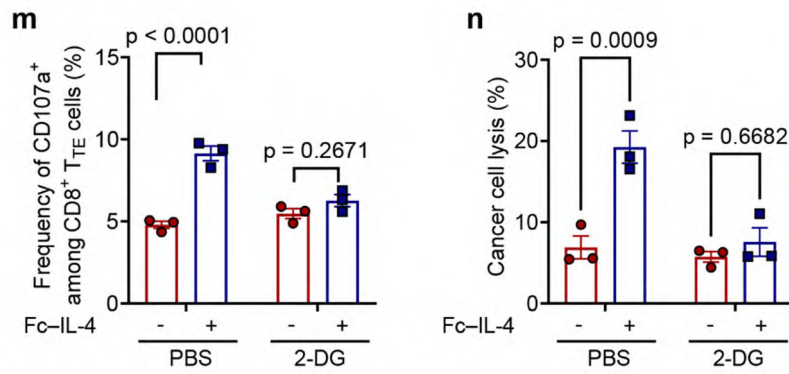
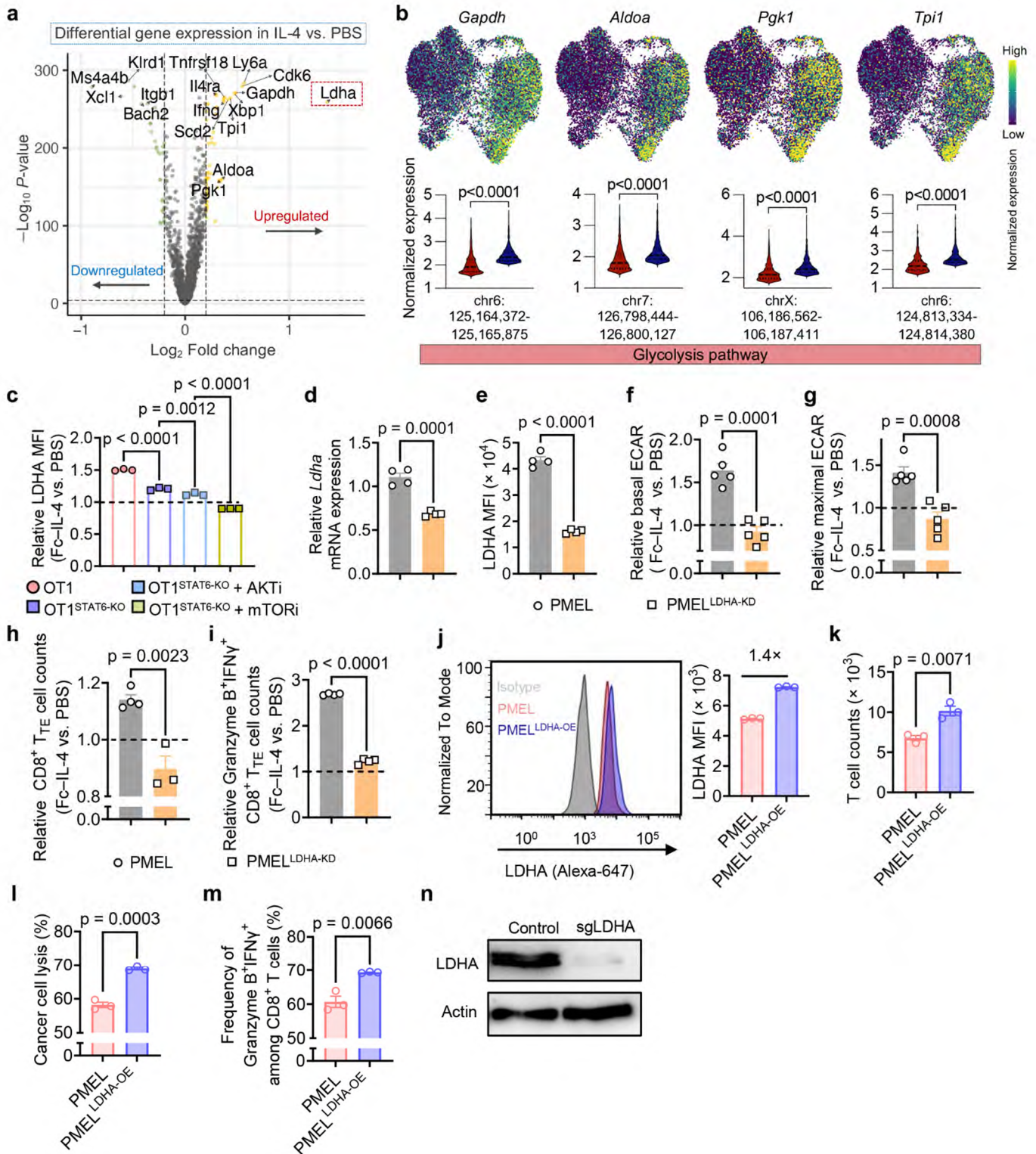


Fig. 5g, h. Ex vivo-induced CD8⁺ T_{TE} cells were pre-treated with Fc-IL-4 for 24 h and re-stimulated by dimeric anti-CD3 antibody in the presence or absence of a glycolysis inhibitor, 2-DG (10 mM). Shown are CD8⁺ T_{TE} cell counts (**g**) and frequencies of Granzyme B⁺IFN γ ⁺ among CD8⁺ T_{TE} cells (**h**). Data are one representative of three independent experiments with n = 4 biological replicates. All data represent mean ± s.e.m. and are analyzed by unpaired two-sided Student's t-test.



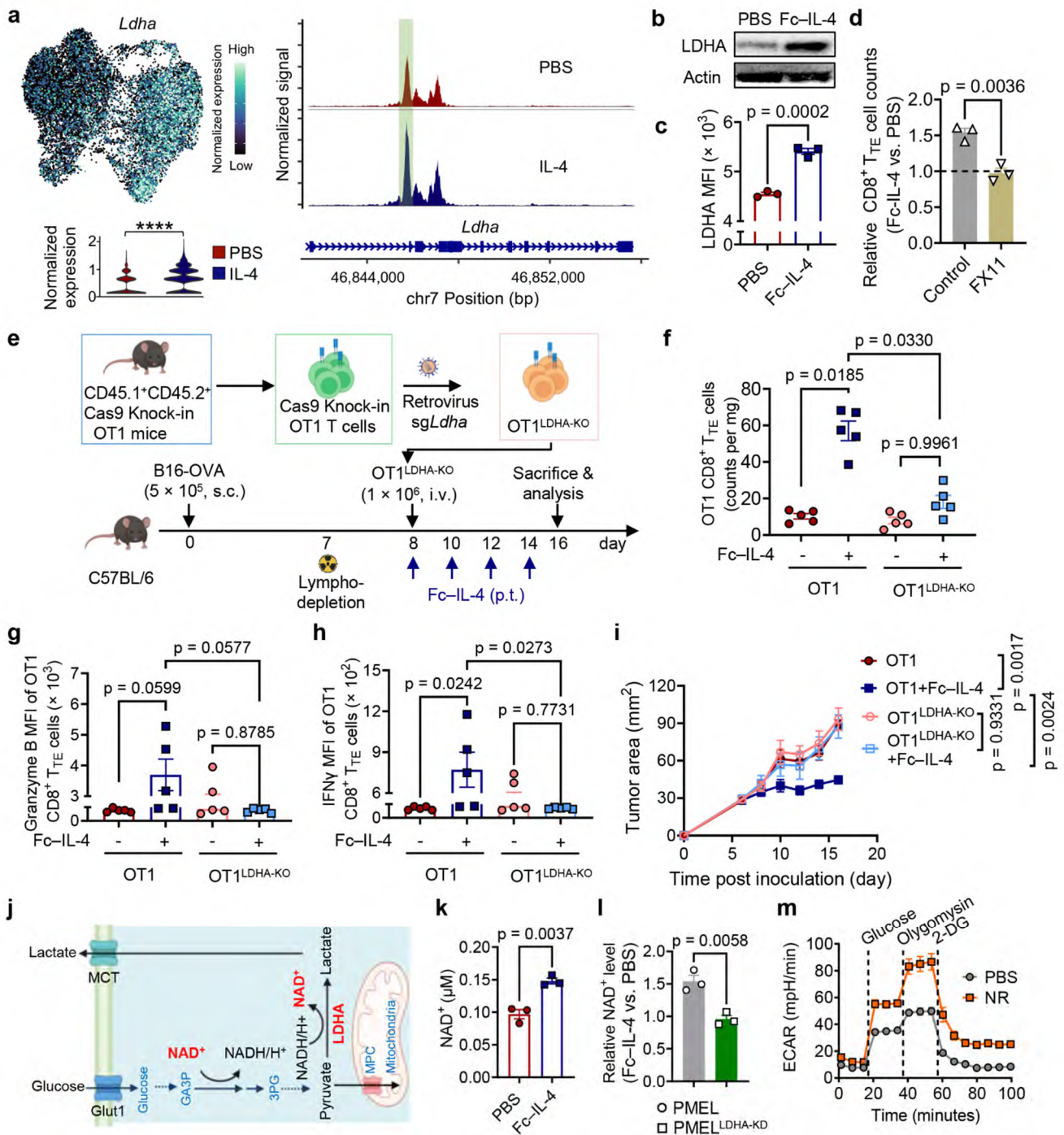
Extended Data Fig. 9m, n. B16F10 tumor cells were co-cultured with ex vivo-induced CD8⁺ T_{TE} cells in the presence or absence of Fc-IL-4 with or without the treatment of 2-DG (10 mM). Shown are the frequencies of CD107a⁺ among CD8⁺ T_{TE} cells (**m**) and percent of cancer cell lysis (**n**). Data are one representative of three independent experiments with n = 3 biological replicates. All data represent mean ± s.e.m. and are analyzed by unpaired two-sided Student's t-test.



New Extended Data Fig. 14 | Fc-IL-4 reinvigorates CD8⁺ T_{TE} cells by enhancing LDHA-dependent glycolysis.

a, Experimental setting was described in Fig. 5i. Shown is volcano plot showing differential gene expression between IL-4 vs. PBS-treated PMEL CD8⁺ T_{TE} cells. **b**, Expression of glycolysis pathway gene markers on the joint UMAP in Fig. 5j, along with comparisons of corresponding accessible peaks between conditions. **c**, Experimental setting was described in Fig. 5m. Shown is the relative expression of LDHA in the Fc-IL-4 treatment group normalized by that in the PBS group. **d-i**, WT PMEL or PMEL^{LDHA-KD} T cells were re-stimulated by dimeric anti-CD3 antibody (0.5 $\mu\text{g ml}^{-1}$) in the presence or absence of Fc-IL-4. Shown are the relative transcriptome level of LDHA (**d**) and protein expression level of LDHA (**e**) in PMEL^{LDHA-KD} T cells, and the relative basal (**f**) and maximal ECAR (**g**), relative counts of CD8⁺ T_{TE} cells (**h**), and Granzyme B⁺IFN γ ⁺ polyfunctional CD8⁺ T_{TE} cells (**i**) in the Fc-IL-4 treatment group normalized by that in the PBS group. **j-m**, WT PMEL or PMEL^{LDHA-OE} T cells were co-cultured with B16F10 for 48 h. Shown are representative flow cytometry plots and LDHA MFI (**j**), T cell counts (**k**), percent of cancer cell lysis (**l**), and frequencies of Granzyme

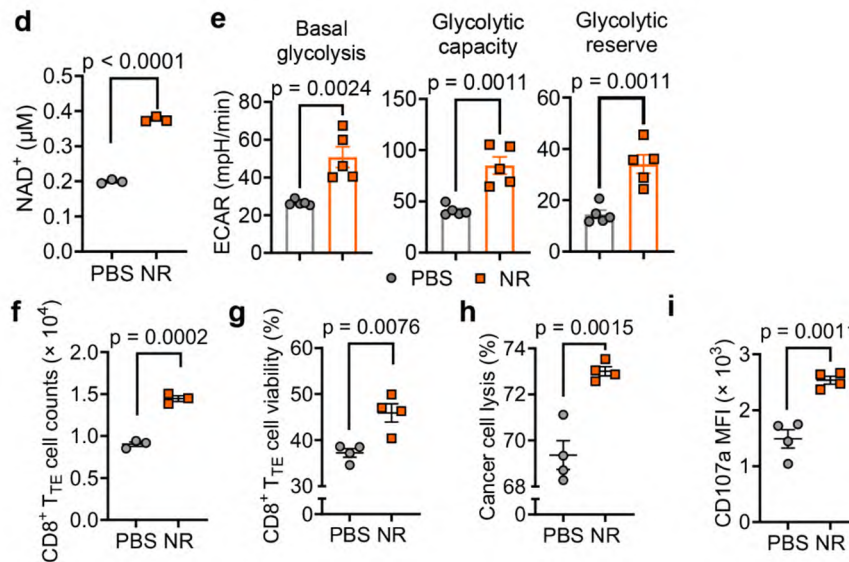
B⁺IFN γ ⁺ (m) among PMEL^{LDHA-OE} T cells. n, WB images of LDHA showing the LDHA knock-out in OT1^{LDHA-KO} T cells. Data are one representative of three independent experiments with n = 3-5 biological replicates. All data represent mean \pm s.e.m. and are analyzed by One-way ANOVA and Tukey's test (c), or unpaired two-sided Student's t-test (d-m).



New Fig. 6 | Fc-IL-4 promotes LDHA-mediated glycolysis and cellular NAD⁺ levels of CD8⁺ T_{TE} cells.

a, Expression of *Ldha* on the joint UMAP in Fig. 5j and pseudo-bulk chromatin accessibility tracks in the genomic region of *Ldha*, depicted separately for IL-4 and PBS conditions. The enhancer element predicted by ENCODE within the region of this gene is highlighted in a light green shade. **b**, **c**, Ex vivo-induced CD8⁺ T_{TE} cells were re-stimulated by dimeric anti-CD3 antibody (0.5 μ g ml⁻¹) in the presence or absence of Fc-IL-4 for 48 h. (n = 3 biological replicates). Shown are the WB images of LDHA (**b**) and LDHA MFI (**c**). **d**, Ex vivo-induced CD8⁺ T_{TE} cells were re-stimulated by dimeric anti-CD3 antibody (0.5 μ g ml⁻¹) in the presence or absence of Fc-IL-4 for 48 h with a LDHA inhibitor, FX11 (16 μ M), or DMSO (n = 3 biological replicates). Shown are relative counts of CD8⁺ T_{TE} cells in the Fc-IL-4 treatment group normalized by that in the PBS group. **e-i**, Mice bearing B16-OVA tumors received ACT of activated WT OT1 or OT1^{LDHA-KO} T cells (1 $\times 10^6$, i.v.) one-day post lymphodepletion followed by the treatment of Fc-IL-4 (20 μ g, p.t.) or PBS every other day for 4 doses in total (n = 5 animals). Mice were sacrificed on day 16 and the tumor tissues were collected for analysis by flow cytometry. Shown are the experimental timeline (**e**), counts of tumor-infiltrating OT1 CD8⁺ T_{TE} cells (**f**),

MFI of Granzyme B (**g**) and IFN γ (**h**) of tumor-infiltrating OT1 CD8⁺ T_{TE} cells, and average tumor growth curves (**i**) of mice. **j**, Schematic of LDHA mediated NAD⁺/NADH recycling. **k**, Experimental setting was described in **Fig. 6b**. Shown is the cellular NAD⁺ level of CD8⁺ T_{TE} cells. **l**, Ex vivo-induced WT PMEL and PMEL^{LDHA-KD} CD8⁺ T_{TE} cells were re-stimulated by dimeric anti-CD3 antibody (0.5 $\mu\text{g ml}^{-1}$) in the presence or absence of Fc-IL-4. Shown is relative NAD⁺ level in the Fc-IL-4 group normalized by that in the PBS group. **m**, Real-time ECAR analysis of ex vivo-induced CD8⁺ T_{TE} cells re-stimulated by dimeric anti-CD3 antibody (0.5 $\mu\text{g ml}^{-1}$) for 48 h in the presence or absence of NR (100 μM). Data are one representative of three independent experiments with $n = 3-5$ biological replicates or $n = 5-7$ animals. All data represent mean \pm s.e.m. and are analyzed by unpaired two-sided Student's t-test (**c**, **d**, **k**, and **l**), or one-way ANOVA and Tukey's test (**f-i**).



Extended Data Fig. 15d-i. **d**, The cellular NAD⁺ level of ex vivo-induced CD8⁺ T_{TE} cells with supplementation of a NAD⁺ precursor, NR (100 μM). **e**, Average basal glycolysis, glycolytic capacity, and glycolytic reserve analyzed from **Fig. 6m**. **f**, **g**, Ex vivo-induced CD8⁺ T_{TE} cells were re-stimulated by dimeric anti-CD3 antibody (0.5 $\mu\text{g ml}^{-1}$) for 48 h in the presence or absence of NR (100 μM). Shown are the counts (**f**) and viability (**g**) of CD8⁺ T_{TE} cells. **h**, **i**, Ex vivo-induced CD8⁺ T_{TE} cells were co-cultured with B16F10 tumor cells for 48 h in the presence or absence of NR (100 μM). Shown are the percent of cancer cell lysis (**h**) and CD107a MFI (**i**) of CD8⁺ T_{TE} cells. Data are one representative of three independent experiments with $n = 3-5$ biological replicates. All data represent mean \pm s.e.m. and are analyzed by unpaired two-sided Student's t-test.

2(b) The essential role of LDHA in glycolysis enhancement mediated by Fc-IL-4.

We fully agree with the reviewer that LDHA is an indispensable enzymes involved in glycolysis for effector T cell differentiation and its effector function¹⁸. We believe LDHA is an essential factor for the effects of Fc-IL-4 for the following reasons:

First, to assess the involvement of key enzymes in Fc-IL-4-induced glycolysis enhancement, we performed single-cell ATAC and transcriptome co-profiling of ex vivo-induced CD8⁺ T_{TE} cells. Unsupervised analysis revealed alterations in chromatin accessibility associated with several glycolytic enzymes, among which *Ldha* showcased the most pronounced upregulation post-IL-4 treatment (**New Fig. 6a** and **New Extended Data Fig. 14a, b**). This observation was further validated through Western blot (WB) and flow cytometry analyses, which confirmed elevated LDHA expression in Fc-IL-4 treated CD8⁺ T_{TE} cells (**New Fig. 6b&c** and **New Extended Data Fig. 14c**, please see both figures above);

Second, LDHA blockade or knock-out completely abrogated the effects of Fc-IL-4 on terminally exhausted CD8⁺ T cells for increased glycolysis, and the subsequent enhancement of effector function and survival in vitro and vivo (previous data, now move to **Fig. 6d-i** and **Extended Data Fig. 14d-i, n**, please see both figures above);

Third, as we mentioned above, LDHA overexpression enhanced the survival and effector function of CD8⁺ T

cells ([New Extended Data Fig. 14j-m](#), please see both figures above);

Forth, it remains unknown regarding the relationship between glycolysis and survival of T cells (although glycolysis is known to be required for effector function as the reviewer pointed out). CD8⁺ T_{TE} cells exhibit severe survival defects⁸, in part due to the lack of NAD⁺⁹. We found that NAD⁺ supplementation, as a metabolic modulation, could alleviate the survival defect of CD8⁺ T_{TE} cells and enhance their function (previous data, now moved to [Extended Data Fig. 15d-i](#), please see the figure above). The survival enhancement of CD8⁺ T_{TE} cells mediated by Fc-IL-4 also depended on LDHA (previous data, now moved to [Fig. 6j-m](#), please see the figures above). This is consistent with literature report as LDHA is known to be crucial for NAD⁺ recycling⁷.

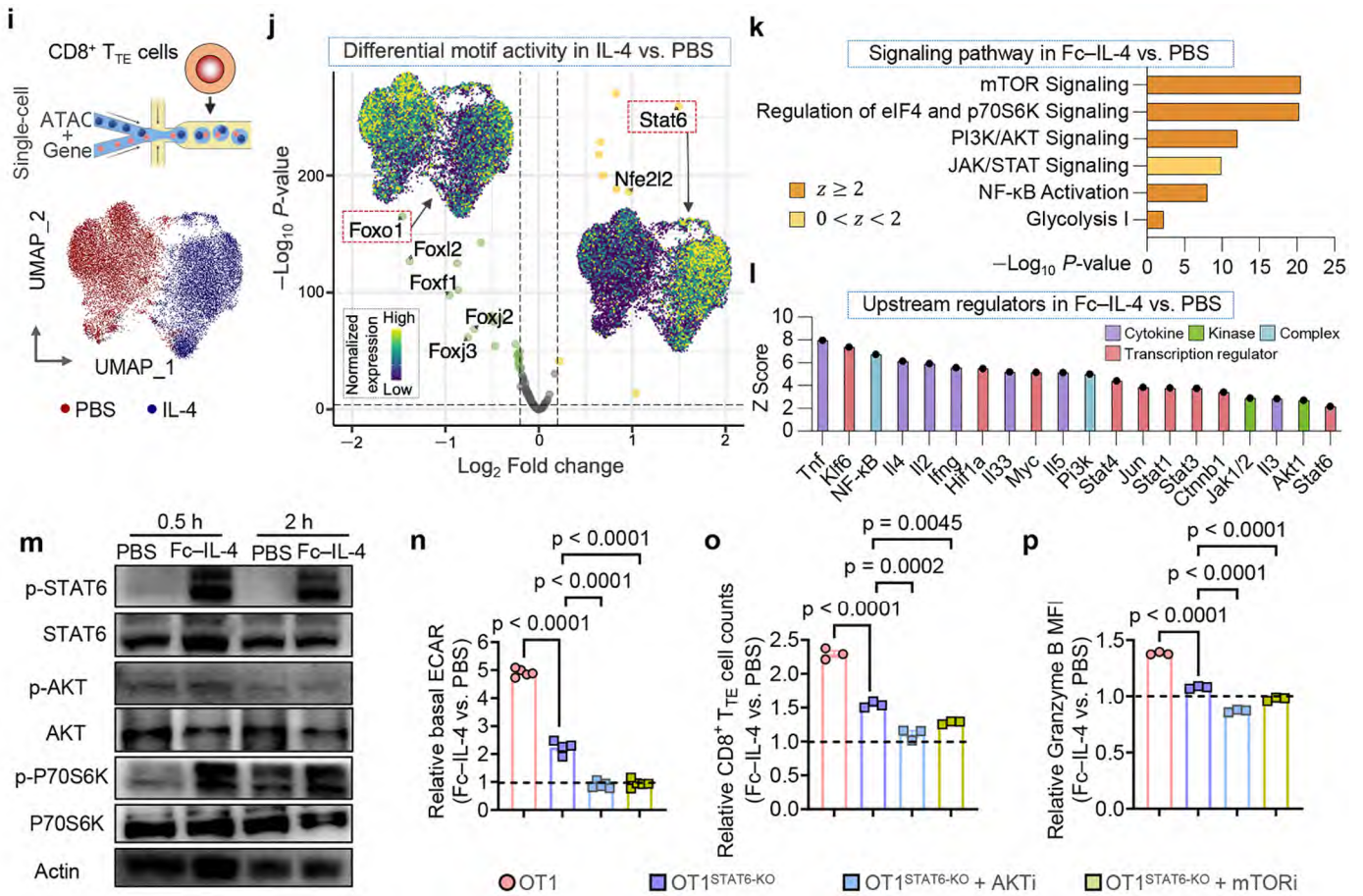
All these datasets collectively represent our efforts to elucidate the role of LDHA in glycolysis enhancement mediated by Fc-IL-4.

2(c) The mechanistic insights in to how Fc-IL-4 enhances the anti-tumor activity of CD8 T cells.

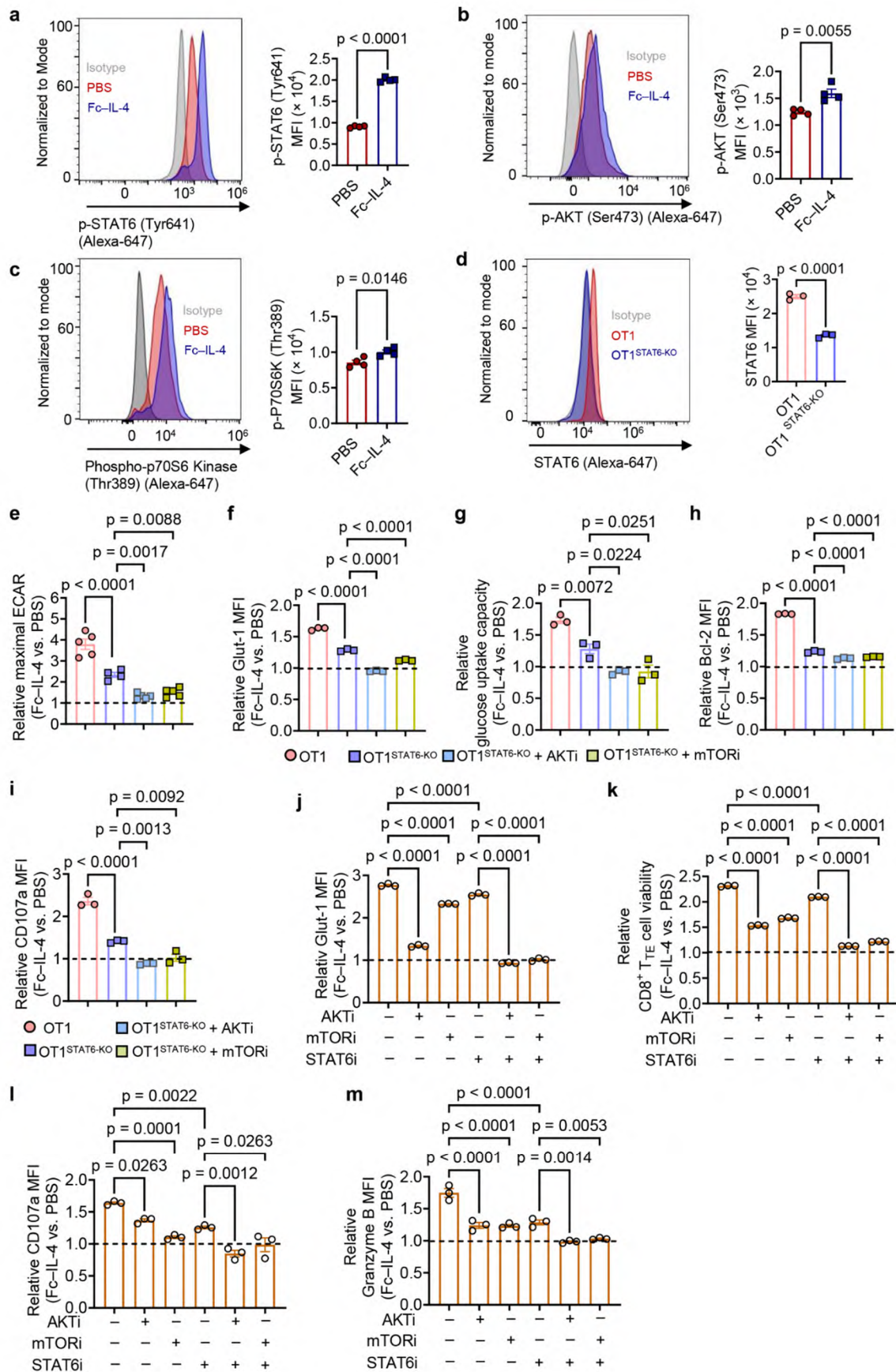
To further elucidate the molecular mechanisms driving the heightened glycolysis induced by Fc-IL-4, we performed single-cell ATAC and transcriptome co-profiling of ex vivo-induced CD8⁺ T_{TE} cells ([New Fig. 5i](#)). The integrated UMAP analysis merging ATAC and transcriptome datasets revealed distinct molecular profiles in T_{TE} cells between the two conditions, suggesting an intrinsic regulatory impact on this specific cell type due to the inclusion of IL-4 ([New Fig. 5i, bottom panel](#)). We performed a differential motif analysis using ATAC data to identify potential transcription factor binding sites within open chromatin regions. In IL-4 treated CD8⁺ T_{TE} cells compared to the PBS condition, Stat6 emerged as the most significantly enhanced motif, while Foxo1, a canonical negative regulator of mTOR, exhibited the highest degree of reduction ([New Fig. 5j](#)). We also investigated the signaling pathways regulated by differentially expressed genes (DEGs) within CD8⁺ TILs obtained from B16F10 tumors in mice subjected to Fc-IL-4 combined ACT, in comparison to the PBS control. The analysis revealed a significant upregulation of mTOR signaling, eIF4 and p70S6 signaling, and PI3K/AKT signaling in Fc-IL-4 treated cells, along with the upregulation of JAK/STAT signaling, NF-κB activation and glycolysis ([New Fig. 5k](#)). Upstream regulator analysis based on the DEGs identified multiple functional molecules predicted to be upregulated in the Fc-IL-4 group, particularly NF-κB, Myc, Pi3K, Akt1, and Stat6 ([New Fig. 5l](#)).

These findings prompted us to delve deeper into the role of the PI3K-AKT-mTOR axis and STAT6 in the heightened glycolytic activities observed following Fc-IL-4 treatment. Through flow cytometry and western blot analysis, we confirmed an elevation in the phosphorylation levels of AKT, P70S6K, and STAT6 following Fc-IL-4 treatment ([New Fig. 5m](#) and [New Extended Data Fig. 12a-c](#)). In an ex vivo stimulation assay, the partial attenuation of Fc-IL-4 treatment benefits, including glycolysis level, T cell counts, enhanced effector function, increased Glut-1 expression, glucose uptake capacity, and upregulation of Bcl-2 and CD107a, was observed in STAT6 knockout OT1 cells (OT1 STAT6-KO). However, the complete abrogation of Fc-IL-4 benefits occurred exclusively when AKT or mTOR signaling was concurrently blocked ([New Fig. 5n-p](#) and [New Extended Data Fig. 12d-i](#)). Additionally, co-inhibition of STAT6 along with either AKT or mTOR signaling using chemical inhibitors yielded similar outcomes ([New Extended Data Fig. 12j-m](#)).

Altogether, these results indicate that Fc-IL-4 enhances glycolysis, survival, and effector function of CD8⁺ T_{TE} cells through STAT6 signaling and PI3K-AKT-mTOR axis.



New Fig. 5i-p. i, j, Schematic illustration of single-cell ATAC and gene co-profiling of ex vivo-induced CD8⁺ T_{TE} cells in the presence or absence of IL-4. Shown is a joint ATAC-gene UMAP of all the single cells, with cells color-coded by their respective conditions (i), and volcano plot showing differentially active motifs between IL-4 vs. PBS-treated T_{TE} cells (j). The expression intensity for the top upregulated and downregulated motifs was displayed. k, l, Experimental setting was described in Fig. 1g. Shown are signaling pathways regulated by DEGs in Fc-IL-4 vs. PBS-treated PMEL CD8⁺ TILs. Pathway terms are ranked by -log₁₀ (p-value) (k), and top 20 ranked upstream regulators predicted from DEGs in Fc-IL-4 vs. PBS-treated PMEL CD8⁺ TILs, categorized by molecule type (l). In k and l, z score is computed and used to reflect the predicted activation level (z > 0, activated/upregulated; z < 0, inhibited/downregulated; z ≥ 2 or z ≤ -2 can be considered significant). m, Ex vivo-induced CD8⁺ T_{TE} cells were re-stimulated by dimeric anti-CD3 antibody (0.1 μg ml⁻¹) in the presence or absence of Fc-IL-4 (n = 4 biological replicates) for 0.5 h or 2 h. Shown are the WB images of phosphorylated STAT6, AKT (Ser473), and p-P70S6K (Thr389). n-p, Ex vivo-induced OT1 and OT1^{STAT6-KO} CD8⁺ T_{TE} cells were re-stimulated by dimeric anti-CD3 antibody (0.5 μg ml⁻¹), and treated with AKT inhibitor VIII (HY-10355, 1 μM) or mTOR inhibitor (Rapamycin, 100 nM) in the presence or absence of Fc-IL-4 for 24 h. Shown are the relative basal glycolysis (n), CD8⁺ T_{TE} cell counts (o), and Granzyme B MFI (p) in the Fc-IL-4 treatment group normalized by that in the PBS group. Data are one representative of three independent experiments with n = 3-5 biological replicates. All data represent mean ± s.e.m. and are analyzed by one-way ANOVA and Tukey's test (n, o, and p).



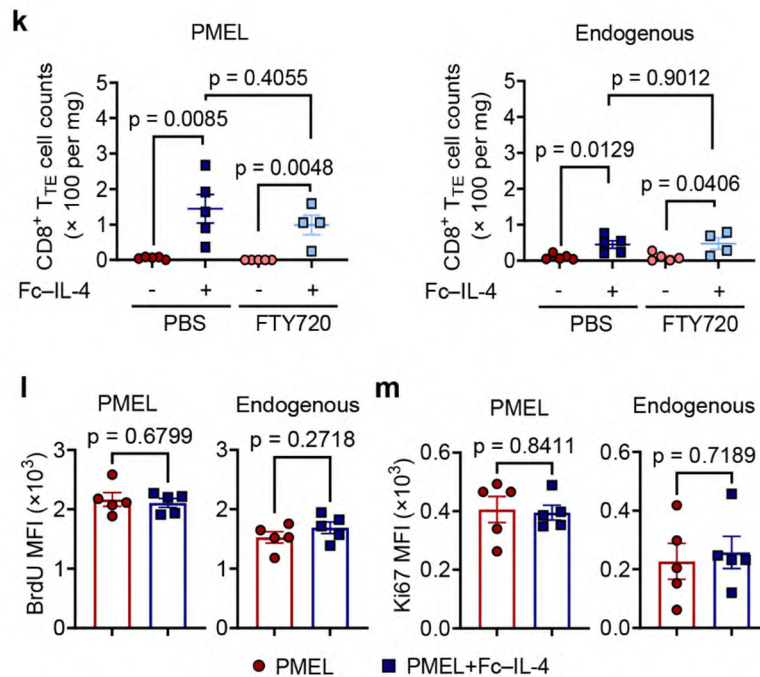
New Extended Data Fig. 12 | Fc-IL-4 enhances the glycolytic metabolism of CD8⁺ T_{TE} cells through STAT6 signaling and PI3K-AKT-mTOR axis.

a-c, Ex vivo-induced PMEL CD8⁺ T_{TE} cells were re-stimulated by dimeric anti-CD3 antibody (0.1 $\mu\text{g ml}^{-1}$) in the presence or absence of Fc-IL-4 ($n = 4$ biological replicates) for 0.5 h. Shown are the representative flow cytometry plots and MFI

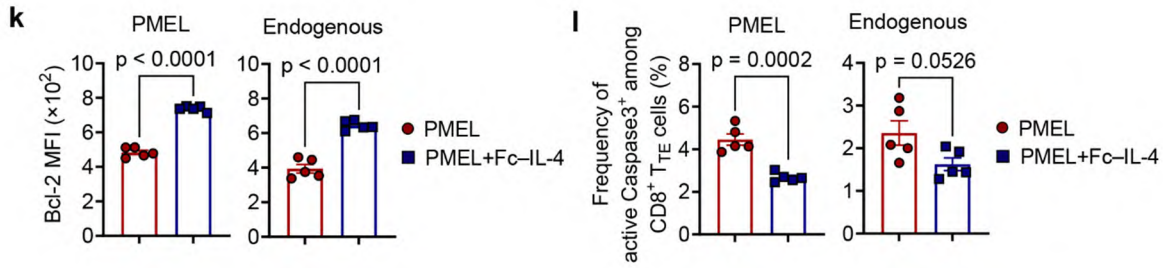
of p-STAT6 (a), p-AKT (Ser473) (b), p-P70S6K (Thr389) (c). d, The STAT6 was knock-out in OT1 T cells using CRISPR-Cas9 gene editing. Shown are representative flow cytometry plots and MFI of STAT6. e-i, Experimental setting was described in Fig. 4n. Shown are relative maximal ECAR (e), relative expression of Glut-1 (f), relative glucose uptake capacity (g), and relative expression of Bcl-2 (h) and CD107a (i) in the Fc-IL-4 treatment group normalized by that in the PBS group. j-m, Ex vivo-induced PMEL CD8⁺ T_{TE} cells were re-stimulated by dimeric anti-CD3 antibody (0.5 μg ml⁻¹) and treated with AKT inhibitor VIII (HY-10355, 1 μM), mTOR inhibitor (Rapamycin, 100 nM), or STAT6 inhibitor (AS1517499, 50 nM) in the presence or absence of Fc-IL-4 for 24 h. Shown are relative expression of Glut-1 (j), relative T cell viability (k), and relative expression of CD107a (l) and Granzyme B (m) in the Fc-IL-4 treatment group normalized by that in the PBS group. Data are one representative of three independent experiments with n = 3-5 biological replicates. All data represent mean ± s.e.m. and are analyzed by unpaired two-sided Student's t-test (a-d), or by one-way ANOVA and Tukey's test (e-m).

2(d) How did Fc-IL-4 enrich the CD8⁺ T_{TE} cells in tumor?

We investigated potential mechanisms by which Fc-IL-4 could enrich the CD8⁺ T_{TE} cells in tumor. First, we observed that blocking T cell egress from lymphoid organs with FTY720 did not affect the enrichment of both transferred and endogenous CD8⁺ T cells (New Extended Data Fig. 7k). Second, we found that the proliferative capacity of CD8⁺ T_{TE} cells was not increased by Fc-IL-4 by measuring Ki67 expression and BrdU incorporation (New Extended Data Fig. 7l&m). Third, we found that Fc-IL-4 could directly act on CD8⁺ T_{TE} cells through IL-4Rα and significantly promote the survival of CD8⁺ T_{TE} cells by alleviating T cell apoptosis (New Fig. 4k&l). In summary, our findings suggest that Fc-IL-4 enriches functional CD8⁺ T_{TE} cells primarily by enhancing their survival.



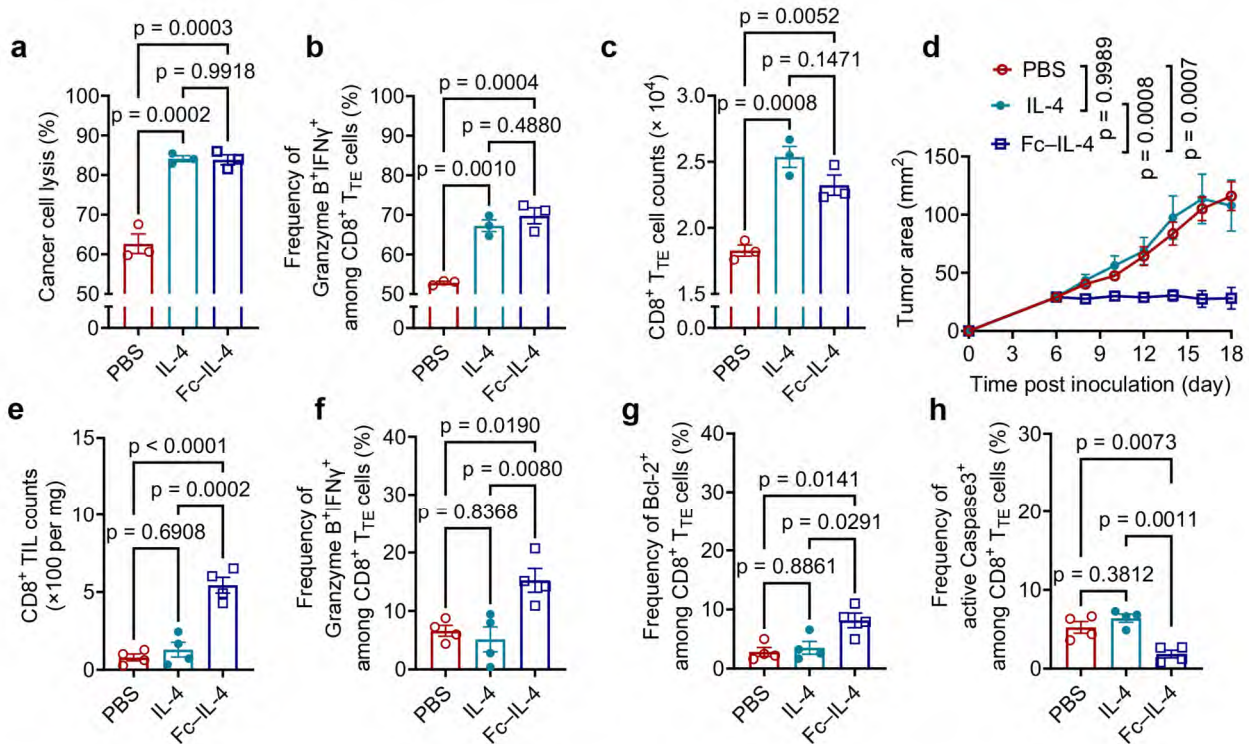
New Extended Data Fig. 7k-m. k, B16F10 tumor-bearing mice were treated with ACT of PMEL T cells (5×10^6 , i.v.) (day 6) followed by administration of Fc-IL-4 (20 μg, p.t.) or PBS every other day for 6 doses in total, and injection of FTY720 (40 μg, i.p.) every day for 9 doses in total. Mice were euthanized on day 16 to collect the tumor tissues for flow cytometry analysis. Shown are counts of PMEL and endogenous CD8⁺ T_{TE} cells in the tumor (n = 4 or 5 animals). l, m, Experimental setting was described in Fig. 4k. Shown are BrdU MFI (l), and Ki67 MFI (m) of PMEL and endogenous CD8⁺ T_{TE} cells (n = 5 animals). All data represent mean ± s.e.m. and are analyzed by One-way ANOVA and Tukey's test (k), or unpaired two-sided Student's t-test (l, m).



New Fig. 4k, l. Experimental setting was similar as described in **Fig. 1a** except that BrdU (1 mg, i.p.) was injected 24 h before tumor tissue collection. Shown are Bcl-2 MFI (**k**), and frequencies of active Caspase3⁺ (**l**) among PMEL and endogenous CD8⁺ T_{TE} cells (n = 5 animals). All data represent mean \pm s.e.m. and are analyzed by unpaired two-sided Student's t-test.

2(e) Possible signaling difference between IL-4 and Fc-IL-4.

We compared the effects of IL-4 and Fc-IL-4 on ex-vivo-induced terminally exhausted CD8⁺ T cells and found that both reagents showed similar function and effects in vitro, including the enhancement of the effector function and survival of CD8⁺ T_{TE} cells in vitro. However, the administration of IL-4 in vivo with an equivalent dose showed negligible effects as compared to Fc-IL-4 (**RL-only Fig. II**). These results indicate the necessity of Fc fusion protein for IL-4 to achieve therapeutic effects in vivo.



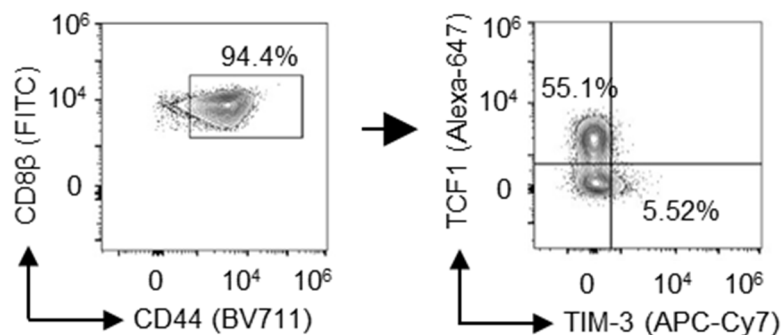
RL-only Fig. II. Comparing the native IL-4 and Fc-IL-4. **a-c**, B16F10 tumor cells were co-cultured with ex-vivo-induced PMEL CD8⁺ T_{TE} cells for 2 days in the presence of IL-4 (3.6 ng/ml, corresponding to 0.53 units/ml) or Fc-IL-4 (20 ng/ml, corresponding to 0.52 units/ml). Shown are the percent of cancer cell lysis (**a**), frequency of Granzyme B⁺IFN γ ⁺CD8⁺ T_{TE} cells (**b**), and counts of CD8⁺ T_{TE} cells (**c**). **d-h**, MC38 tumor-bearing mice received the treatment of Fc-IL-4 (p.t. 20 μ g per injection, corresponding to 520 units per injection) or IL-4 (p.t. 3.6 μ g per injection, corresponding to 529 units per injection) every other day for 6 doses in total. Mice were sacrificed on day 18 and the tumor tissues were collected for analysis by flow cytometry. Shown are the tumor growth curves (**d**), the cell counts of CD8⁺ TILs (**e**), frequencies of Granzyme B⁺IFN γ ⁺ (**f**), Bcl-2⁺ (**g**), and active Caspase3⁺ (**h**) among CD8⁺ T_{TE} cells. All data represent mean \pm s.e.m. and are analyzed by One-way ANOVA and Tukey's test.

3. The authors conclude that progenitor cells are not required for the IL-4-induced effects. However, the authors write in the methods section that the cells were activated for 2-3 days. I am not sure how many progenitor cells are present after this short culture, but long-term cultures usually do not contain T_{pex}. Therefore, could the authors provide evidence that T_{pex} were transferred? If such cells are not present, then the depletion approach provides no evidence. Moreover, the absence of T_{pex} would even leave unanswered the question of whether there is a possible effect on T_{pex}?

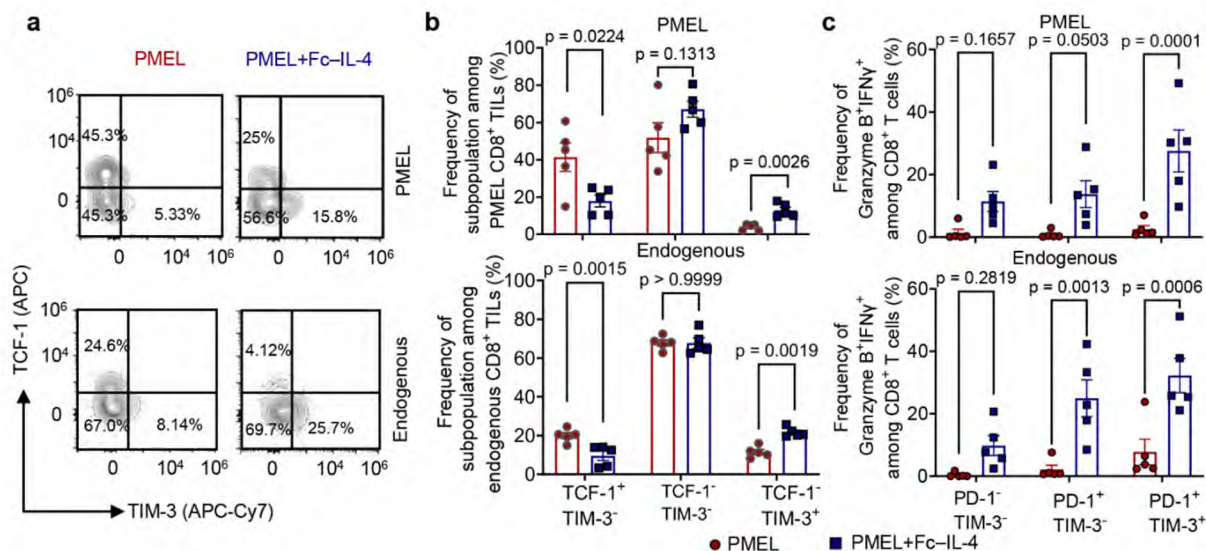
Ex vivo cultures with IL-2 tend to raise nonexhausted T cells, implying that IL-4 treatment of previously ex vivo activated cells enhances the response of nonexhausted cells. Now, one could argue that endogenous T cells also respond to IL-4 treatment and that IL-4 treatment alone (without cell transfer) has significant antitumor effects in the B16 and MC38 models. Nevertheless, the question remains whether depleted or nonexhausted cells respond under these conditions. Therefore, clear evidence that nonexhausted cells can be reactivated would be crucial to support the message put forward by the authors.

Progenitor exhausted T cells (both transferred and endogenous) were consistently involved in the ACT experiments. First, the activated T cells used for adoptive transfer comprised ~55% progenitor CD8⁺ T cells (TCF1⁺) ([New Extended Data Fig. 1f](#)). It is important to note that when we refer to “progenitor exhausted” T cells, we are highlighting a subset that shares certain properties of the normal progenitor/memory T cells but is distinct^{19,20}. Among the intratumoral endogenous CD8⁺ T cells, progenitor exhausted CD8⁺ T cells were also present ([New Extended Data Fig. 2a, b](#)). This observation aligns with findings reported in the literatures, particularly at the early stage of tumor progress^{21,22,23}. In the DT depletion experiment reported here, we also noticed a notable decrease in the frequencies of progenitor exhausted CD8⁺ T cells following DT treatment ([New Extended Data Fig. 7b-f](#)), providing additional evidence for our findings.

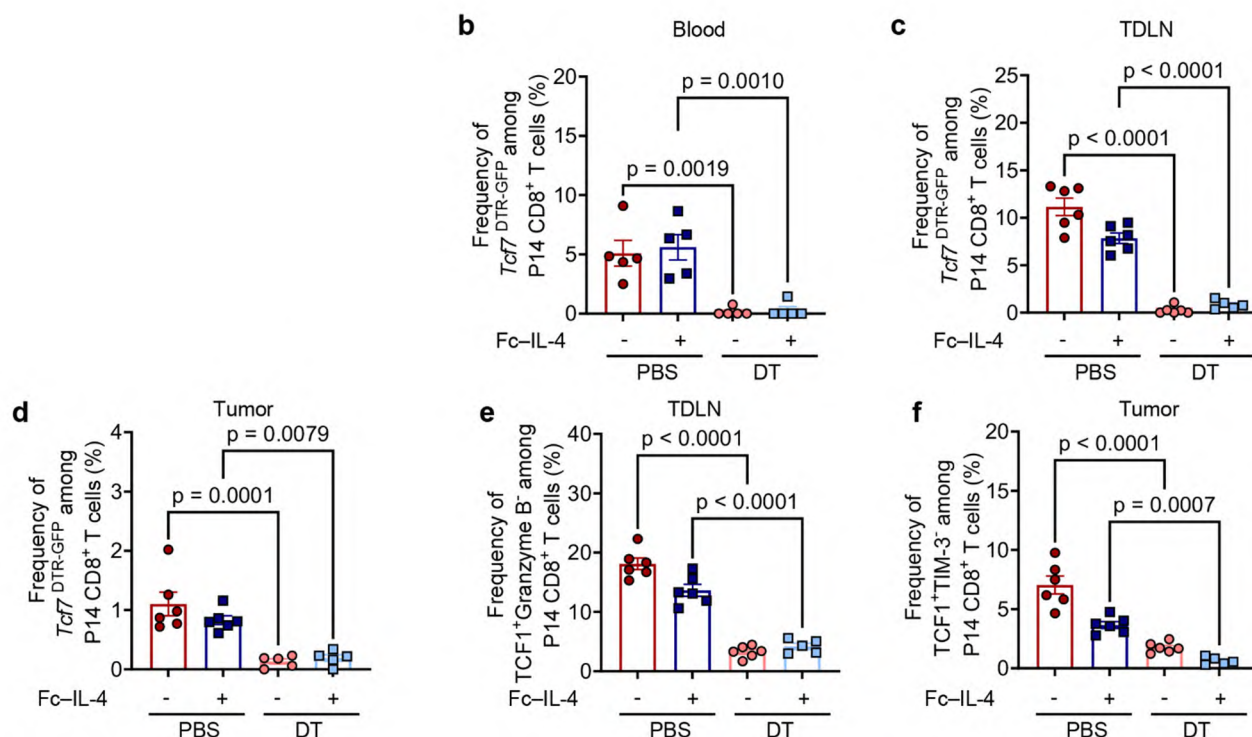
We indeed found that both endogenous and transferred CD8⁺ T cells responded to the Fc-IL-4 treatment ([Fig. 1a-d](#) and [New Extended Data Fig. 2a-c](#)). However, the responses of the CD8⁺ T_{TE} cells were more pronounced compared to the progenitor exhausted CD8⁺ T cells. Following Fc-IL-4 treatment, the counts of progenitor exhausted CD8⁺ T cells (defined as TCF1⁺TIM-3⁻, which should also be contained in the PD-1⁺TIM-3⁻ CD8⁺ T cell subset) were not significantly increased ([Fig. 1a-d](#), [New Extended Data Fig. 2a&b](#)). Nonetheless, we observed enhancement in their effector function upon Fc-IL-4 treatment ([New Extended Data Fig. 2c](#)).



New Extended Data Fig. 1f. The phenotype of in vitro-activated PMEL before infusion.



New Extended Data Fig. 2a-c. Experimental setting was described in Fig. 1a. Shown are the representative flow cytometry plots (a) and the frequencies (b) of CD8⁺ T_{TE} cells (TCF1-TIM-3⁺) among PMEL or endogenous CD8⁺ TILs, and frequencies of Granzyme B⁺IFNγ⁺ among different subpopulations of PMEL or endogenous CD8⁺ TILs (c). All data represent mean ± s.e.m. and are analyzed by Two-way ANOVA and Sidak multiple comparisons test.



New Extended Data Fig. 7b-f. Experimental setting was similar as described in Fig. 4a except that mice were sacrificed on day 12 and the tumor-draining lymph node (TDLN), spleen, blood, and tumor tissues were collected for analysis by flow cytometry. Shown are the frequencies of Tcf7^{DTR-GFP+} progenitor exhausted T cells among transferred P14 T cells in the peripheral blood (b), TDLN (c), and tumor (d), and frequencies of TCF1⁺Granzyme B⁺ among transferred P14 T cells in the TDLN (e), and frequencies of TCF1⁺TIM-3⁻ among transferred P14 T cells in the tumor (f). All data represent mean ± s.e.m. and are analyzed by One-way ANOVA and Tukey's test.

Minor points:

Perhaps the authors can find other wording in the abstract for "a type 2 cytokine that acts directly on CD8⁺ T cells via the IL-4 receptor and specifically enriches functional, nonexhausted CD8⁺ T cells (CD8⁺ TTE) in the tumor independently of the exhausted progenitor CD8⁺ T cells. resulting in

dramatically increased antitumor efficacy and durable cure in multiple solid tumor models when combined with adoptive T cell transfer therapies targeting type 1 immunity. " The length of the sentence and the terminology are very confusing to a broader audience, especially when referring to "functional, terminally exhausted" cells that have superior antitumor function.

We apologize for the technical language and the lengthy sentence. The "terminally exhausted" T cell (TCF1⁺TIM-3⁺) is a terminology broadly used in the field of T cell exhaustion. Upon the treatment of Fc-IL-4, we were able to enhance and maintain their effector function and cytotoxicity. Therefore, we could "enrich functional 'terminally exhausted' T cells". We have modified this description into the following version:

"Here, we show that an interleukin-4 fusion protein (Fc-IL-4), a typical type 2 cytokine, directly acts on CD8⁺ T cells and enriches functional terminally exhausted CD8⁺ T (CD8⁺ T_{TE}) cells in the tumor. When combined with type 1 immunity-centric adoptive T cell transfer (ACT) and immune checkpoint blockade (ICB) therapies, Fc-IL-4 remarkably enhances anti-tumor efficacy and induces durable cures in multiple syngeneic and xenograft tumor models. "

As for the list of author contributions, it is surprising to read that a senior scientist (i.e., W.H.) performed experiments without analyzing them.

We apologize for this oversight. Dr. Werner Held indeed analyzed the data and this information has been updated in the "Author contribution" section.

"CD8⁺ TTE cells have higher cytotoxicity than nonexhausted progenitor CD8⁺ T cells and therefore contribute directly to the elimination of cancer cells." I do not think it is useful to specifically highlight that differentiated cells have higher cytotoxic potential than their progenitor cells, which are related to memory cells.

We would like to respectfully specify these two subsets of exhausted cells in this study. Other studies have reported that terminally exhausted subsets (CD8⁺ T_{TE}) exhibit higher cytotoxicity than the progenitor exhausted subset^{23,24}. Here, the tumor-infiltrating progenitor exhausted T cells (PD-1⁺TCF1⁺) are not typical progenitor or memory cells as they are still "exhausted" cells¹². To streamline this description, we have revised the sentence to "CD8⁺ T_{TE} cells possess superior cytotoxicity and directly contribute to elimination of cancer cells", along with proper citation.

Referee #4 (Remarks to the Author):

Type 2 cytokine Fc-IL-4 reinvigorates terminally exhausted CD8+ T cells to potentiate anticancer immunotherapy.

In this manuscript, Feng et al. show that treating tumor-responding T cells with IL-4 promotes an advanced exhaustion differentiation state (PD-1+, TIM-3+) that has increased functional capacities and tumor controlling ability. Upon administration of IL-4, there is a selective increase in the number of TIM-3+ CD8 T cells responding to tumor challenge and these cells also possess increased granzyme and cytokine producing capacity. This result is striking as these more differentiated cell types in the T cell exhaustion differentiation lineage are thought to be relatively less plastic and less responsive to conventional ICB compared to the less-differentiated, progenitor differentiation state. The authors show that these more terminally exhausted T cells are the responders to the IL-4 treatment by utilizing a system that allows for selective depletion of the progenitor differentiation state. This experimental system showed that a lack of progenitors did not abrogate the IL-4 treatment phenotype (increased tumor control). The IL-4 treatment increased glycolytic capacity of the tumor-responding CD8 T cells, which is notable as glycolytic activity is known to be critical for both functional capacities of T cells (like IFN γ production) as well as their proliferative potential. In summary, this study claimed that IL-4 treatment increases TIL functionality and tumor-controlling capacity.

This study strengthens the notion that certain type-2 cytokines can be beneficial for reprogramming tumor-responding T cells and tumor control, however, the conceptual rationale for why this would be the case and how this could relate to human ICB responses is limited in this paper. The relevance is also not entirely clear given that the entire manuscript rests entirely on the treatment of murine models of subcutaneous implanted tumors and is lacking clinical correlates. Also, what are the clinical contexts wherein IL-4 would be associated with a good prognosis in tumors as there are decades of reports showing that this does not have a positive correlation with patient outcome. That doesn't mean that the IL-4 therapy couldn't have paradoxical effects on promoting anti-tumor immunity like IL-10, but it would require that the authors identify the physiological settings for when IL-4 would naturally be associated with promoting function and reversing exhaustion of CD8+ T cells. Furthermore, given the group recently showed similar effects of IL-10 on TILs it would be important to extend from this to understand how IL-4 and IL-10 operate independently or cooperatively of one another. Thus, at this stage, while an interesting and well done study, it lacks the overall physiological and clinical relevance needed to have a larger impact on the field, and would be more suited for a more specialized journal.

We are grateful for the reviewer's comments. As sparsely reported in some studies (certainly not the mainstream in the tumor immunology field), it is true that "certain type-2 cytokines might be beneficial for reprogramming tumor-responding T cells and tumor control,". However, which specific cytokine can be used for therapeutic intervention, how to use it (native or fusion protein? monotherapy? combination therapy and with what?), how they work, and which cells/molecules they act on remains largely unknown in the field. Here, for the first time, we clearly present that Fc-IL-4, as a type 2 cytokine, can be used in combination with several ACT therapies or ICB therapy (new data added) to substantially improve the curative response rate in several syngeneic and xenograft tumor models (new data added including human CAR-T cells) and thoroughly elucidate the cellular, metabolic, and molecular (new data added) mechanisms by which it achieves such effects. We firmly believe that the results reported here have strong clinical translation potential, and provide new insights into the synergy of type 1 and 2 immune responses for cancer immunotherapy, a critical but unsolved question. In light of the reviewer's observation that "there are decades of reports showing that this does not have a positive correlation with patient outcome", the potent antitumor effect of Fc-IL-4 reported in this manuscript is truly surprising and novel.

The novelty and clinical relevance of this study have also received unanimous support from other reviewers. Comments include "a very impressive study, revealing a novel role for IL-4 in activating CD8 T cells", "bring a significant discovery to the cancer immunotherapy field", "a captivating report focusing on the use of type 2 cytokines", "has the potential to advance the field of adoptive cell therapy (ACT)", "the enhancement of antitumor activity by Fc-IL4 was surprising", and "This discovery is poised to have a profound impact on the field of immunotherapy".

As the reviewer correctly noted, our lab previously reported the anti-tumor effect and mechanism of **IL-10** (*Nat. Immunol.* 2021, 22, 746-756; *Nat. Biotechnol.* 2024. <https://doi.org/10.1038/s41587-023-02060-8>). Currently, several ongoing clinical trials are testing IL-10-secreting CAR-T cell therapy in patients, which is based on our discoveries (ClinicalTrials.gov ID: NCT05715606, NCT05747157, NCT06120166). *This manuscript serves as a foundational pre-clinical study, marking the initial stride towards orchestrating type 1 and 2 immune factors to potentiate cancer immunotherapy, a new strategy that is unexplored.* We aim to ultimately tackle the question of “identifying the physiological settings for when IL-4 would naturally be associated with promoting function” in patients. However, achieving this goal will require years of rigorous clinical studies and beyond the scope of present study.

In the revised manuscript, we have also included a discussion comparing the effects of IL-4 and IL-10. Notably, this study offers another compelling demonstration of reinvigorating terminally exhausted T cells to boost the potential of cancer immunotherapy against solid tumors, employing mechanisms distinct from those of IL-10.

To further address the question raised by the reviewer, we have added a number of *new results (listed collectively on the first page of this response letter)*. We believe the new datasets provide valuable insights into the mechanism by which IL-4 could achieve the observed benefits (“why this would be the case”).

Major Comments:

1) Overall, the authors showed a very interesting effect of IL-4 on controlling both functional capacities of tumor-responsive T cells as well as the differentiation program they adopt. There has only been a small amount of work suggesting that the non-progenitor subsets of tumor-responding T cells could be “rejuvenated” to the degree that the authors show here and the effects of tumor controlling capacity by the IL-4 treatment are exciting. However, the novelty of this finding is dampened by the previous work done by Tang group showing that another Type-2 cytokine (IL-10) treatment increases tumor controlling capacity of T cells through a similar mechanism (increased functional TIM-3⁺ T cells). What would be the rationale for terminally exhausted cells become more responsive to type 2 cytokines if indeed they promote their anti-tumor activities? How does this differ from the conventional roles of IL-4-STAT-6 and IL-10-STAT3 in suppressing Type-I IFN γ -inducing immune responses? How STAT3 and STAT6 operate uniquely from one another or cooperatively in CD8 TILs would be important to understand.

Thanks for reviewer’s encouraging feedback and for acknowledging the study as “interesting” and “exciting”. We have carefully addressed the comments raised from the following 4 perspectives:

1a. novelty and differentiation from previous work on IL-10

The current work on IL-4 has several major differences from our previous report on IL-10²⁷.

First, IL-4 and IL-10 are cytokines from two different cytokine families and have distinct immunological function and mechanisms^{28,29}. IL-4 is typically considered to induce type 2 immune responses, resulting in resistance to parasite infection, promoting wound healing, and exacerbating allergic diseases. IL-10 functions to suppress pro-inflammatory responses, safeguarding tissues from damage caused by inflammatory reactions, including those associated with type 1, type 2, and type 17 inflammatory responses.

Second, while we observed the action of both cytokines on terminally exhausted T cells (TCF1-TIM3⁺), their mechanisms differed significantly. IL-10-Fc promotes the proliferation of CD8⁺ T_{TE} cells, whereas *Fc-IL-4 promotes the survival of CD8⁺ T_{TE} cells instead of inducing proliferation* (**New Fig. 4k, l** and **New Extended Data Fig. 7l, m**).

Third, regarding the metabolic programming, IL-10-Fc promotes OXPHOS, while *Fc-IL-4 significantly enhances glycolysis of CD8⁺ T_{TE} cells* (previous data, now move to **Fig. 5a-h** and **Extended Data Fig. 9**).

Forth, IL-10-Fc signals through STAT3 pathway²⁷, while *Fc-IL-4 exerts the effects on CD8⁺ T_{TE} cells through STAT6 and mTOR pathways as evidenced by multiple datasets provided in this revised version* (**New Fig. 5i-p** and **New Extended Fig. 12**).

Altogether, **for the first time**, we conclusively demonstrate the efficacy of Fc–IL-4, a type 2 cytokine, when combined with various ACT therapies or ICB therapy, in significantly enhancing the curative response rate across multiple syngeneic and xenograft tumor models. Moreover, we elucidate the cellular, molecular, metabolic, transcriptomic, and epigenomic mechanisms underlying this potent therapeutic effect. We firmly believe that our findings represent a significant contribution to the field, offering not only **a potential new immunotherapy with high clinical relevance**, but also **unveiling a novel mechanism for reinvigorating terminally exhausted T cells through metabolic modulation**.

1b. What would be the rationale for terminally exhausted cells become more responsive to type 2 cytokines?

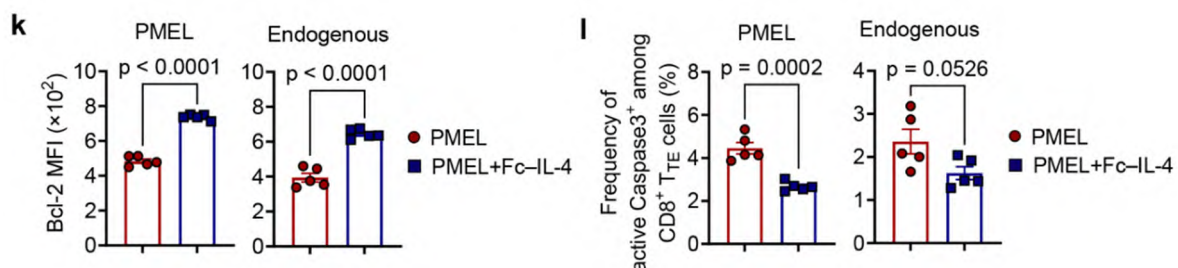
The enhanced responsiveness of CD8⁺ T_{TE} cells to IL-4 is likely attributed to their higher expression level of IL-4R α , as detailed in our manuscript (previous data, now moved to **Extended Data Fig. 7i**). This observation suggests a potential self-rescue mechanism employed by exhausted cells to sustain their survival.

1c. How does this differ from the conventional roles of IL-4-STAT-6 and IL-10-STAT3 in suppressing Type-I IFN γ -inducing immune responses?

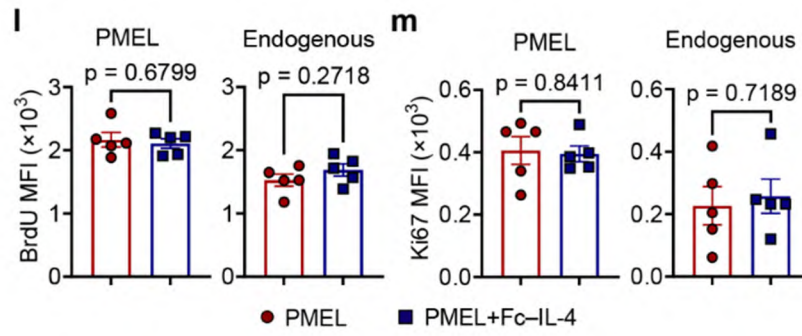
IL-4-STAT6 and IL-10-STAT3 signaling function to suppress Type-I IFN γ -inducing immune responses, mainly mediated by myeloid cells such as macrophages^{30,31}, or to promote the differentiation of naive T cells into type 2 immune cells³². Distinct from previous understanding, our manuscript presents substantial evidence demonstrating that **IL-4 directly acts on exhausted CD8⁺ T cells** (activated and antigen-experienced) in the tumor microenvironment. This direct interaction leads to a significant enhancement in their cytotoxicity and effector function, as evidence by increased IFN γ production. This discovery sheds light on a **novel role of IL-4**, previously unrecognized in the context of rejuvenating exhausted T cell function. Hence, the functionality of pleiotropic cytokines like IL-4 is profoundly influenced by various contextual factors, including concentration, the specific type and differentiation status of responding cells, the nature of the disease being addressed, and other pertinent variables.

1d. How STAT3 and STAT6 operate uniquely from one another or cooperatively in CD8 TILs would be important to understand.

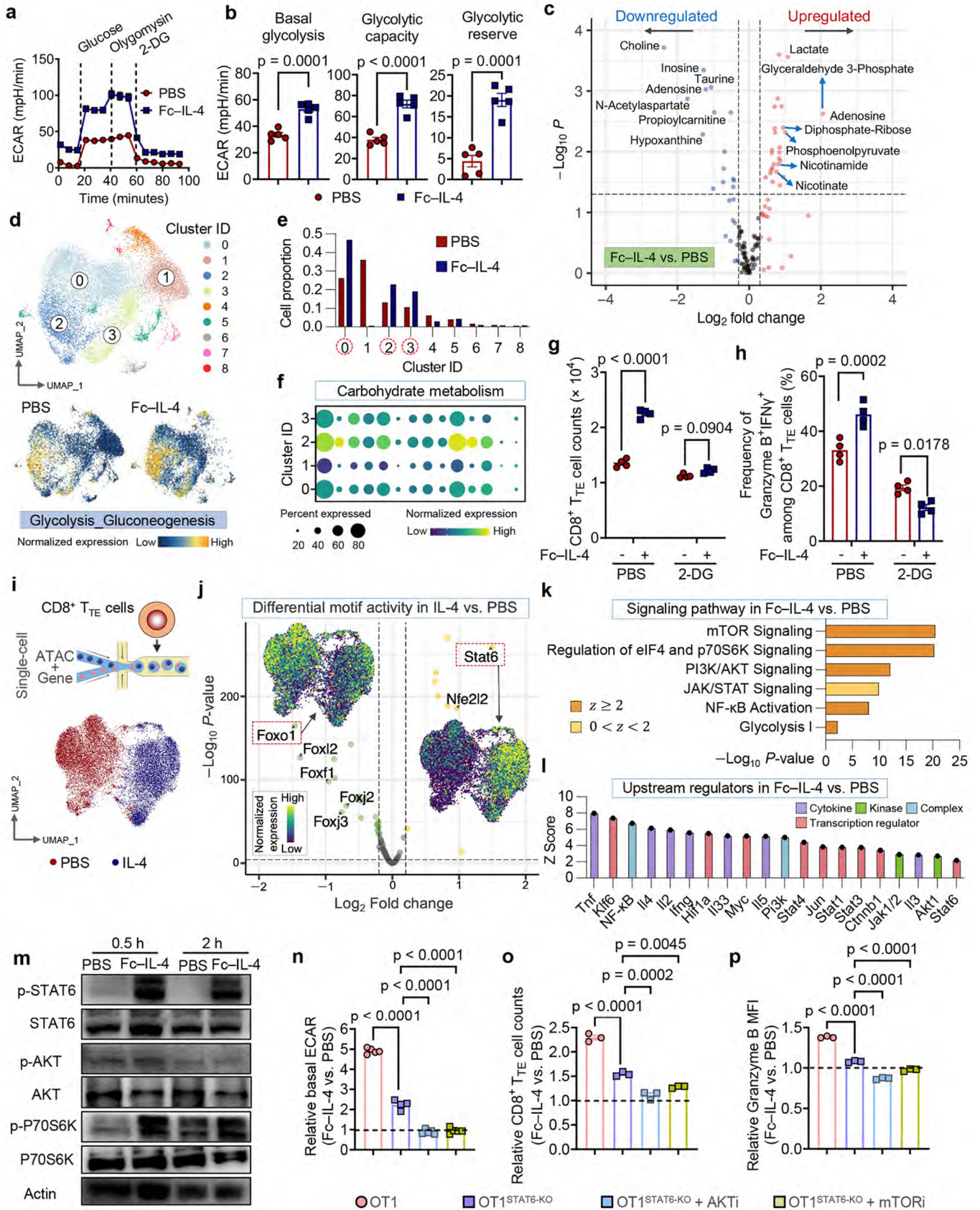
We agree with the reviewer that this is an interesting and important question. In our previous study, IL-10 was found to stimulate STAT3 to enhance the effector function and OXPHOS level of CD8⁺ T cells²¹. In this study, we elucidated the role of Fc–IL-4 in modulating the CD8⁺ T_{TE} cells by promoting their glycolysis, survival, and effector function through STAT6 signaling and PI3K–AKT–mTOR axis (**New Fig. 5i-p** and **New Extended Fig. 12**). In the present manuscript, our primary focus lies in elucidating the function and mechanism of Fc–IL-4. While comparing the STAT3 and STAT6 signaling pathways is beyond the scope of this study, it certainly remains an area of interest for our future investigations.



New Fig. 4k, l. Experimental setting was similar as described in **Fig. 1a** except that BrdU (1 mg, i.p.) was injected 24 h before tumor tissue collection. Shown are Bcl-2 MFI (**k**) of PMEL and endogenous CD8⁺ T_{TE} cells, and frequencies of active Caspase3⁺ among PMEL and endogenous CD8⁺ T_{TE} cells (**l**) (n = 5 animals). All data represent mean \pm s.e.m. and are analyzed by unpaired two-sided Student's t-test.



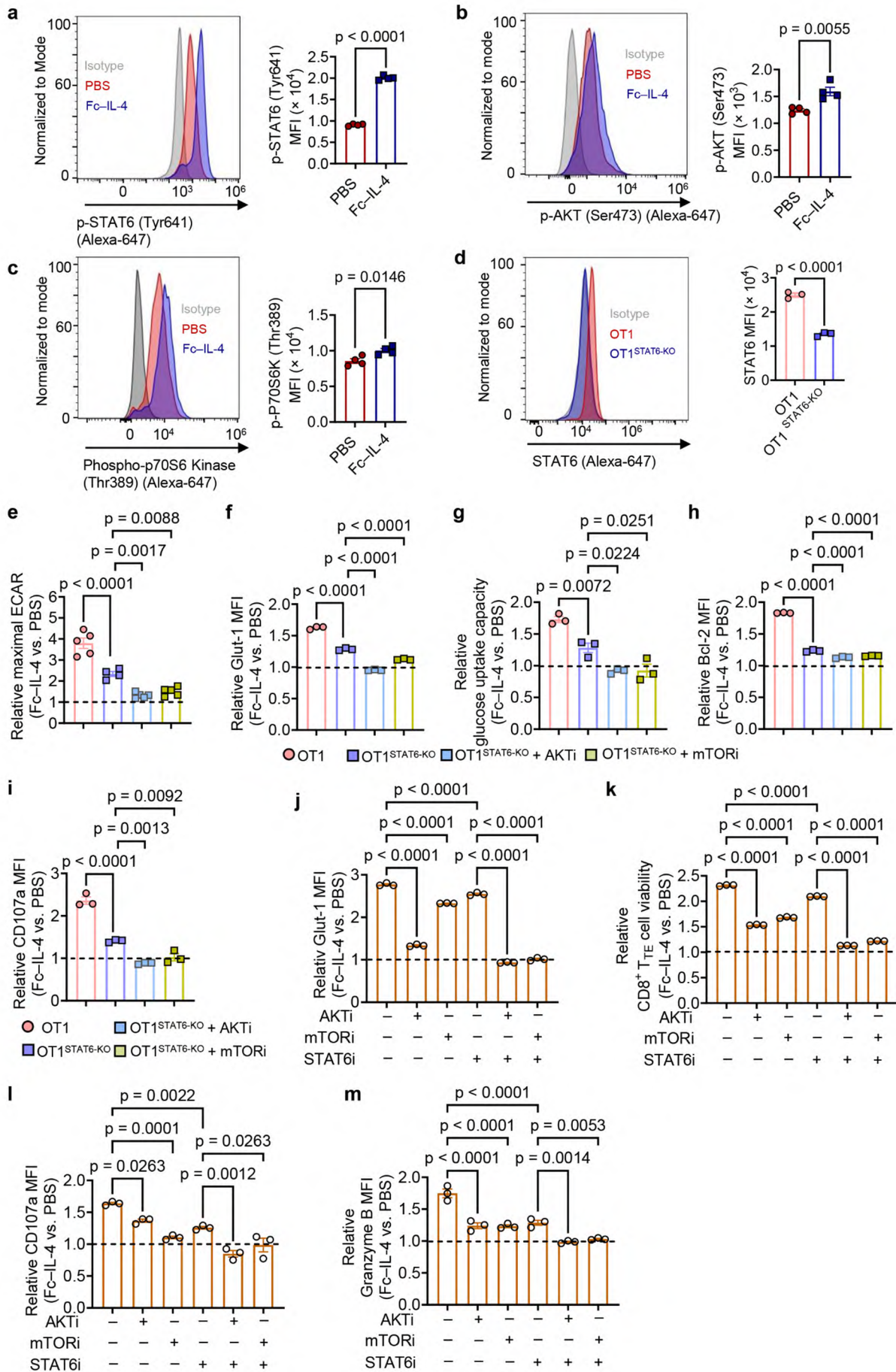
New Extended Data Fig. 7l, m. Experimental setting was described in **Fig. 4k**. Shown are BrdU MFI (**I**), and Ki67 MFI (**m**) of PMEL and endogenous CD8⁺ T_{TE} cells (n = 5 animals). All data represent mean \pm s.e.m. and are analyzed by unpaired two-sided Student's t-test (**I, m**).



New Fig. 5 | Fc-IL-4 enhances glycolytic metabolism of CD8⁺ T_{TE} cells through STAT6 signaling and PI3K-AKT-mTOR axis.

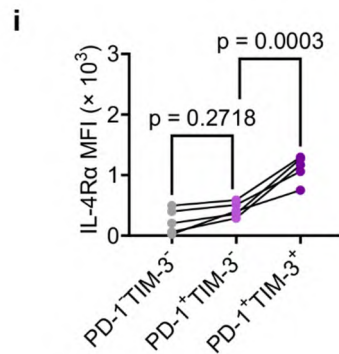
a, Real-time ECAR analysis of ex vivo-induced CD8⁺ T_{TE} cells re-stimulated by dimeric anti-CD3 antibody (0.5 μg ml⁻¹) for 48 h in the presence or absence of Fc-IL-4. **b**, Average basal glycolysis, glycolytic capacity, and glycolytic reserve analyzed from **a**. **c**, Metabolomic analysis was utilized to analyze the metabolites from CD8⁺ T_{TE} cells re-stimulated by

dimeric anti-CD3 antibody ($0.5 \mu\text{g ml}^{-1}$) and treated with Fc-IL-4 ($n = 4$ biological replicates) or PBS ($n = 3$ biological replicates). Shown is the volcano plot of upregulated or downregulated metabolites in cells treated with Fc-IL-4 vs. PBS. **d**, Experimental setting was described in **Fig. 1g**. Shown is unsupervised UMAP clustering of PMEL CD8⁺ TILs sorted from tumors in mice treated with Fc-IL-4 or PBS based on the 1667 genes involved in KEGG-defining metabolic pathways. A higher expression level of Glycolysis_Gluconeogenesis was observed in TILs treated with Fc-IL-4. **e**, Comparison of cell proportion in each cluster identified in **d**. Fc-IL-4 group showed notably higher proportions in clusters 0, 2, and 3, while cells in the PBS group were enriched in cluster 1. **f**, Systematic expression comparison of carbohydrate metabolisms between the top 4 clusters identified in **d**. Each column is one metabolic pathway. The size of the circle represents the proportion of single cells expressing the pathway, and the color shade indicates the normalized expression level. **g, h**, Ex vivo-induced CD8⁺ T_{TE} cells were pre-treated with Fc-IL-4 for 24 h and re-stimulated by dimeric anti-CD3 antibody in the presence or absence of a glycolysis inhibitor, 2-DG (10 mM). Shown are CD8⁺ T_{TE} cell counts (**g**) and frequencies of Granzyme B⁺IFN γ ⁺ among CD8⁺ T_{TE} cells (**h**). **i, j**, Schematic illustration of single-cell ATAC and gene co-profiling of ex vivo-induced CD8⁺ T_{TE} cells in the presence or absence of IL-4. Shown is a joint ATAC-gene UMAP of all the single cells, with cells color-coded by their respective conditions (**i**), and volcano plot showing differentially active motifs between IL-4 vs. PBS-treated T_{TE} cells (**j**). The expression intensity for the top upregulated and downregulated motifs was displayed. **k, l**, Experimental setting was described in **Fig. 1g**. Shown are signaling pathways regulated by DEGs in Fc-IL-4 vs. PBS-treated PMEL CD8⁺ TILs. Pathway terms are ranked by $-\log_{10}$ (p-value) (**k**), and top 20 ranked upstream regulators predicted from DEGs in Fc-IL-4 vs. PBS-treated PMEL CD8⁺ TILs, categorized by molecule type (**l**). In **k** and **l**, z score is computed and used to reflect the predicted activation level ($z > 0$, activated/upregulated; $z < 0$, inhibited/downregulated; $z \geq 2$ or $z \leq -2$ can be considered significant). **m**, Ex vivo-induced CD8⁺ T_{TE} cells were re-stimulated by dimeric anti-CD3 antibody ($0.1 \mu\text{g ml}^{-1}$) in the presence or absence of Fc-IL-4 ($n = 4$ biological replicates) for 0.5 h or 2 h. Shown are the WB images of phosphorylated STAT6, AKT (Ser473), and p-P70S6K (Thr389). **n-p**, Ex vivo-induced OT1 and OT1^{STAT6-KO} CD8⁺ T_{TE} cells were re-stimulated by dimeric anti-CD3 antibody ($0.5 \mu\text{g ml}^{-1}$), and treated with AKT inhibitor VIII (HY-10355, 1 μM) or mTOR inhibitor (Rapamycin, 100 nM) in the presence or absence of Fc-IL-4 for 24 h. Shown are the relative basal glycolysis (**n**), CD8⁺ T_{TE} cell counts (**o**), and Granzyme B MFI (**p**) in the Fc-IL-4 treatment group normalized by that in the PBS group. Data are one representative of three independent experiments with $n = 3-5$ biological replicates or $n = 5-7$ animals. All data represent mean \pm s.e.m. and are analyzed by two-sided unpaired Student's t-test (**b, g, and h**), or by one-way ANOVA and Tukey's test (**n, o, and p**). In **k** and **l**, the full list of KEGG metabolic pathways and genes defining each pathway are provided in Supplementary Table 1.



New Extended Data Fig. 12 | Fc-IL-4 enhances the glycolytic metabolism of CD8⁺ T_{TE} cells through STAT6 signaling and PI3K-AKT-mTOR axis.

a-c, Ex vivo-induced PMEL CD8⁺ T_{TE} cells were re-stimulated by dimeric anti-CD3 antibody (0.1 µg ml⁻¹) in the presence or absence of Fc-IL-4 (n = 4 biological replicates) for 0.5 h. Shown are the representative flow cytometry plots and MFI of p-STAT6 (**a**), p-AKT (Ser473) (**b**), p-P70S6K (Thr389) (**c**). **d**, The STAT6 was knock-out in OT1 T cells using CRISPR-Cas9 gene editing. Shown are representative flow cytometry plots and MFI of STAT6. **e-i**, Experimental setting was described in **Fig. 4n**. Shown are relative maximal ECAR (**e**), relative expression of Glut-1 (**f**), relative glucose uptake capacity (**g**), and relative expression of Bcl-2 (**h**) and CD107a (**i**) in the Fc-IL-4 treatment group normalized by that in the PBS group. **j-m**, Ex vivo-induced PMEL CD8⁺ T_{TE} cells were re-stimulated by dimeric anti-CD3 antibody (0.5 µg ml⁻¹) and treated with AKT inhibitor VIII (HY-10355, 1 µM), mTOR inhibitor (Rapamycin, 100 nM), or STAT6 inhibitor (AS1517499, 50 nM) in the presence or absence of Fc-IL-4 for 24 h. Shown are relative expression of Glut-1 (**j**), relative T cell viability (**k**), and relative expression of CD107a (**l**) and Granzyme B (**m**) in the Fc-IL-4 treatment group normalized by that in the PBS group. Data are one representative of three independent experiments with n = 3-5 biological replicates. All data represent mean ± s.e.m. and are analyzed by unpaired two-sided Student's t-test (**a-d**), or by one-way ANOVA and Tukey's test (**e-m**).



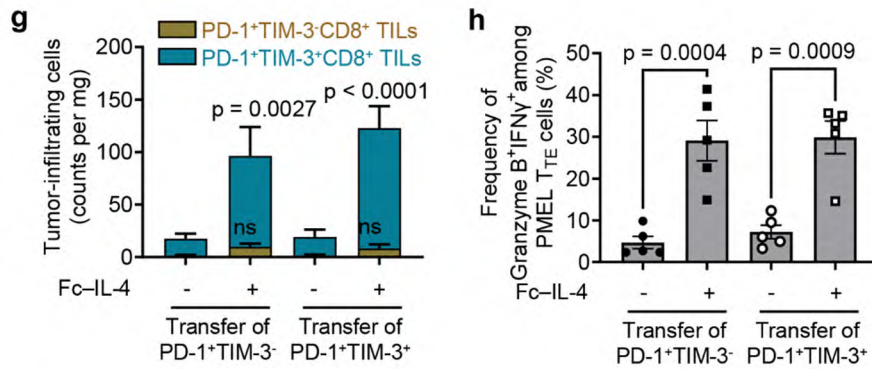
Extended Data Fig. 7i. MFI of IL-4Rα expression among different subsets of tumor-infiltrating CD8⁺ T cells. All data represent mean ± s.e.m. and are analyzed by One-way ANOVA and Tukey's test.

2) Importantly, the authors suggest that IL-4 acts on the terminal exhausted subsets but there are some concerns with the TCF-DTR model (discussed below). As an alternative, and a potentially more convincing approach, the authors should study the effects of the individual subsets of T cells and their effects on tumor growth with IL-4 treatment, sorting the PD-1⁺ TIM-3⁻ and PD-1⁺ TIM3⁺ subsets and transferring them into separate tumor-bearing recipients would be a strong assay for understanding the effects of the IL-4 treated PD-1⁺ TIM-3⁺ subset specifically.

We thank the reviewer for this valuable suggestion. We sorted the PD1⁺TIM3⁻ and PD1⁺TIM3⁺ subsets and separately transferred them into tumor-bearing mice to directly investigate the effects of Fc-IL-4. Subsequently, we analyzed the tumor-infiltrating transferred antigen-specific T cells ([New Extended Data Fig. 7g&h](#)).

First, consistent with the observations from the TCF-DTR model, our study revealed that Fc-IL-4 directly expanded the population of CD8⁺ T_{TE} cells (PD1⁺TIM3⁺) in tumor-bearing mice, enhancing their cytotoxicity and effector function ([New Extended Data Fig. 7g&h](#));

Second, we found that the transferred PD1⁺TIM3⁻ CD8⁺ T cells (containing progenitor exhausted T cells) can self-expand and differentiate into the CD8⁺ T_{TE} cells (PD1⁺TIM3⁺) ([New Extended Data Fig. 7g](#)), consistent with previous literature report²⁴. Additionally, their effector function can also be enhanced by Fc-IL-4 ([New Extended Data Fig. 7h](#)). (Note: In the [New Extended Data Fig. 7g](#), there was a small population of PD1⁺TIM3⁻ CD8⁺ T cells found in mice with transferred CD8⁺ T_{TE} cells (PD1⁺TIM3⁺). We suspect there was a slight impurity in cell sorting (<5%).



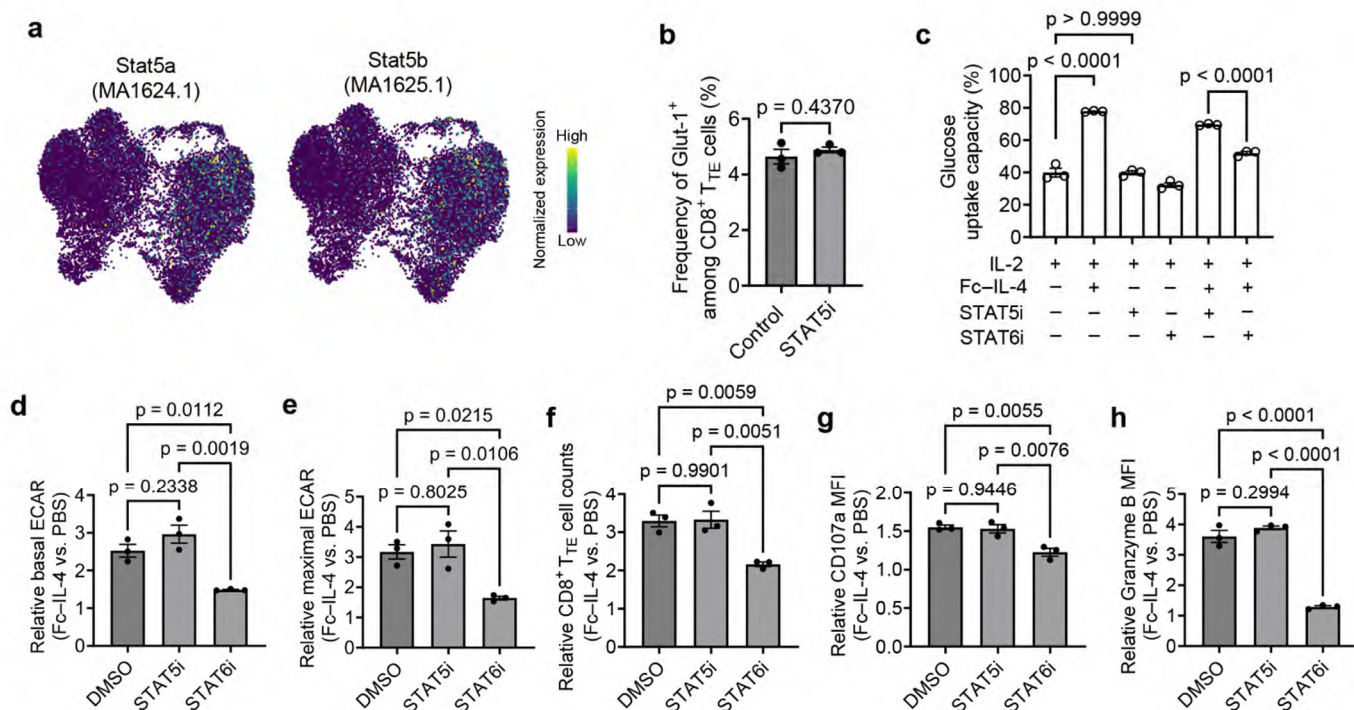
New Extended Data Fig. 7g, h. Mice bearing B16F10 tumors received ACT of PD1⁺TIM-3⁻ (1×10^6 , i.v.) or PD-1⁺TIM-3⁺ PMEL T cells (1×10^6 , i.v.) (day 7), which were sorted from ex vivo-induced PMEL T cells, one day post lymphodepletion (day 6) followed by the treatment of Fc-IL-4 (20 μ g, p.t.) or PBS every other day starting from day 7 for 4 doses in total (n = 5 animals). Mice were sacrificed on day 15 and the tumor tissues were collected for analysis by flow cytometry. Shown are the counts of PMEL T cells (**g**) and frequency of Granzyme B⁺IFN γ ⁺ among PMEL CD8⁺ T_{TE} cells (**h**). All data represent mean \pm s.e.m. and are analyzed by One-way ANOVA and Tukey's test.

3) The claimed mechanism from the authors by which IL-4 treatment is achieving increased T cell functionality and tumor-controlling capacity is through an induction of glycolytic flux. Work from Hashimoto et al. (Nature, 2022) and Mo et al. (Nature, 2021) show that IL-2 treatment can increase glycolytic flux (with certain engineered IL-2 variants increased glycolysis more than others) can also increase tumor controlling capacity of CD8 T cells. However, the mechanism by which this is achieved is through an enrichment and reinvigoration of progenitor-like cells, not terminally exhausted cells. So, if increased glycolysis is truly the mechanism driving the phenotypes seen here with IL-4 treatment, it is at odds with the observations that IL-2 treatment (which also increases glycolysis) does not achieve the same differentiation effects. Can the authors deconvolute these different effects of IL4 and IL-2?

We thank the reviewer for raising this interesting point. While both cytokines increase glycolytic activities in T cells, IL-2 and IL-4 act on different subsets of exhausted T cells via different signaling pathways, resulting in distinct phenotypes and ultimately leading to divergent therapeutic outcomes.

Our findings demonstrate that Fc-IL-4 enriches functional terminally exhausted CD8⁺ T cells by enhancing glycolysis, as these cells express higher levels of IL-4R α compared to the progenitor subset (previous data, now moved to [Extended Data Fig. 7i](#), please see figure above). Many studies, including those referenced by the reviewer, have shown that IL-2 increases glycolysis in progenitor exhausted CD8⁺ T cells, promoting their differentiation into effector T cells³³. However, IL-2 failed to re-activate the terminally exhausted CD8⁺ T cells or enhance its glycolytic metabolism³⁴. Moreover, chronic stimulation by IL-2 has been reported to drive CD8⁺ T cell dysfunction through aryl hydrocarbon receptors³⁵. Therefore, many strategies have been developed to reduce the conventional IL-2 signaling (including the Mo et al. Nature, 2021 paper) to generate more memory T cells for ACT therapy.

In addition, IL-2 typically activates STAT5 but not STAT6³⁶. While IL-4 is a member of the gamma c cytokine family and activates both STAT5 and STAT6 signaling pathways. Our study revealed that Fc-IL-4 enhances the glycolysis primarily through the STAT6 and mTOR pathways (mainly reported in [New Fig. 5i-p](#) and [New Extended Data Fig. 12](#), please see figures above). We performed additional experiments to explore the involvement of STAT5 and STAT6 signaling pathways in the reinvigoration of CD8⁺ T_{TE} cells ([New Extended Data Fig. 13](#)). From single-cell chromatin accessibility dataset, we found that the activity of Stat6, instead of Stat5a/b, was dramatically enriched in CD8⁺ T_{TE} cells treated with IL-4 ([New Fig. 5j](#), please see the figure above and [New Extended Data Fig. 13a](#)). Blocking STAT5 signaling did not hinder the increase in Glut-1 expression, glucose uptake, or glycolysis enhancement mediated by Fc-IL-4 ([Extended Data Fig. 13b-e](#)). In contrast, inhibition of STAT6 notably attenuated the effects of Fc-IL-4 on promoting glycolytic metabolism, as well as enhancing expansion and cytotoxicity ([New Fig. 5m-p](#), please see figures above and [New Extended Data Fig. 13d-h](#)). These results suggest that STAT6, rather than STAT5, is crucial for the observed phenotypes induced by Fc-IL-4, highlighting a major distinction from IL-2.



Extended Data Fig. 13 | Fc-IL-4 mediated glycolysis enhancement of CD8⁺ T_{TE} cells is not dependent on STAT5 signaling.

a, Visualization of motif activity expression for Stat5a (MA1624.1) and Stat5b (MA1625.1) on the joint UMAP in **Fig. 5j**. **b-h**, Ex vivo-induced PMEL CD8⁺ T_{TE} cells were re-stimulated by dimeric anti-CD3 antibody (0.5 μg ml⁻¹), and treated with inhibitors for STAT6 (STAT6i, AS1517499, 50 nM) or STAT5 (STAT5i, Bestellnummer 573108, 25 μM) in the presence or absence of Fc-IL-4 (n = 3 biological replicates). Shown are frequency of Glut-1⁺ among PMEL CD8⁺ T_{TE} cells (**b**), glucose uptake capacity of PMEL CD8⁺ T_{TE} cells (**c**), and relative level of basal ECAR (**d**), relative level of maximal ECAR (**e**), relative T cell counts (**f**), and relative MFI of CD107a (**g**) and Granzyme B (**h**) expression in the Fc-IL-4 treatment group normalized by that in the PBS group (**h**). Data are one representative of three independent experiments with n = 3-4 biological replicates. All data represent mean ± s.e.m. and are analyzed by unpaired two-sided Student's t-test (**b**), or One-way ANOVA and Tukey's test (**c-h**).

4) Though the authors have very convincing data showing that IL-4 controls tumor-responsive T cell differentiation, there are a few areas that could be strengthened. Given that there is an increase in function of the TIM-3⁺ CD8 T cell population with IL-4 treatment, further investigation into the mechanism by which this is occurring would be valuable. The work presented here relies heavily on the loss of LDHA to abrogate IL-4 treatment phenotypes. This may indicate that increased glycolysis is one component driving the IL-4 treatment phenotypes, however, loss of LDHA significantly compromises effector T cell expansion and function. This makes interpreting the mechanistic experiments done with LDHA knockout difficult to interpret as this would be the expected result of LDHA KO cells. Does a constitutively active STAT4 prevent exhaustion or rescue an LDHA KO? An orthogonal approach could be to see if IL-4r expression or downstream signaling is lost in LDHA knockout T cells. In that same idea, deeper analysis of the sequencing results on the TIM-3⁺ subset of CD8 T cells could reveal a novel transcriptional program allowing the restoration of function in these cells, which would be exciting and build a more complete understanding of the mechanism of IL-4 treatment.

We have extensively investigated the potential mechanisms underlying how Fc-IL-4 enhances the antitumor activity of CD8⁺ T_{TE} cells, scrutinizing factors across tissue, cellular, metabolic, molecular, transcriptomic, and epigenomic levels.

4a. The role of LDHA and molecular mechanism

We fully agree with the reviewer that LDHA is an indispensable enzyme involved in glycolysis for effector T cell differentiation and its effector function¹⁸. LDHA was identified as an essential factor mediating the effects of Fc-IL-4 due to the following reasons:

First, to assess the involvement of key enzymes in Fc-IL-4-induced glycolysis enhancement, we analyzed single-cell ATAC and transcriptome co-profiling datasets, revealing alterations in chromatin accessibility associated with several glycolytic enzymes, among which *Ldha* showcased the most pronounced upregulation post-IL-4 treatment (**New Fig. 6a** and **New Extended Data Fig. 14a, b**). This observation was further validated through Western blot (WB) and flow cytometry analyses, which confirmed elevated LDHA expression in Fc-IL-4 treated CD8⁺ T_{TE} cells (**New Fig. 6b&c** and **New Extended Data Fig. 14c**).

Second, LDHA blockade or knock-out completely abrogated the effects of Fc-IL-4 on terminally exhausted CD8⁺ T cells for increased glycolysis, and the subsequent enhancement of effector function and survival in vitro and vivo (previous data, now moved to **Fig. 6d-i** and **New Extended Data Fig. 14d-i, n**).

Third, LDHA overexpression could enhance the survival, effector function and antitumor efficacy of CD8⁺ T cells (**New Extended Data Fig. 14j-m**);

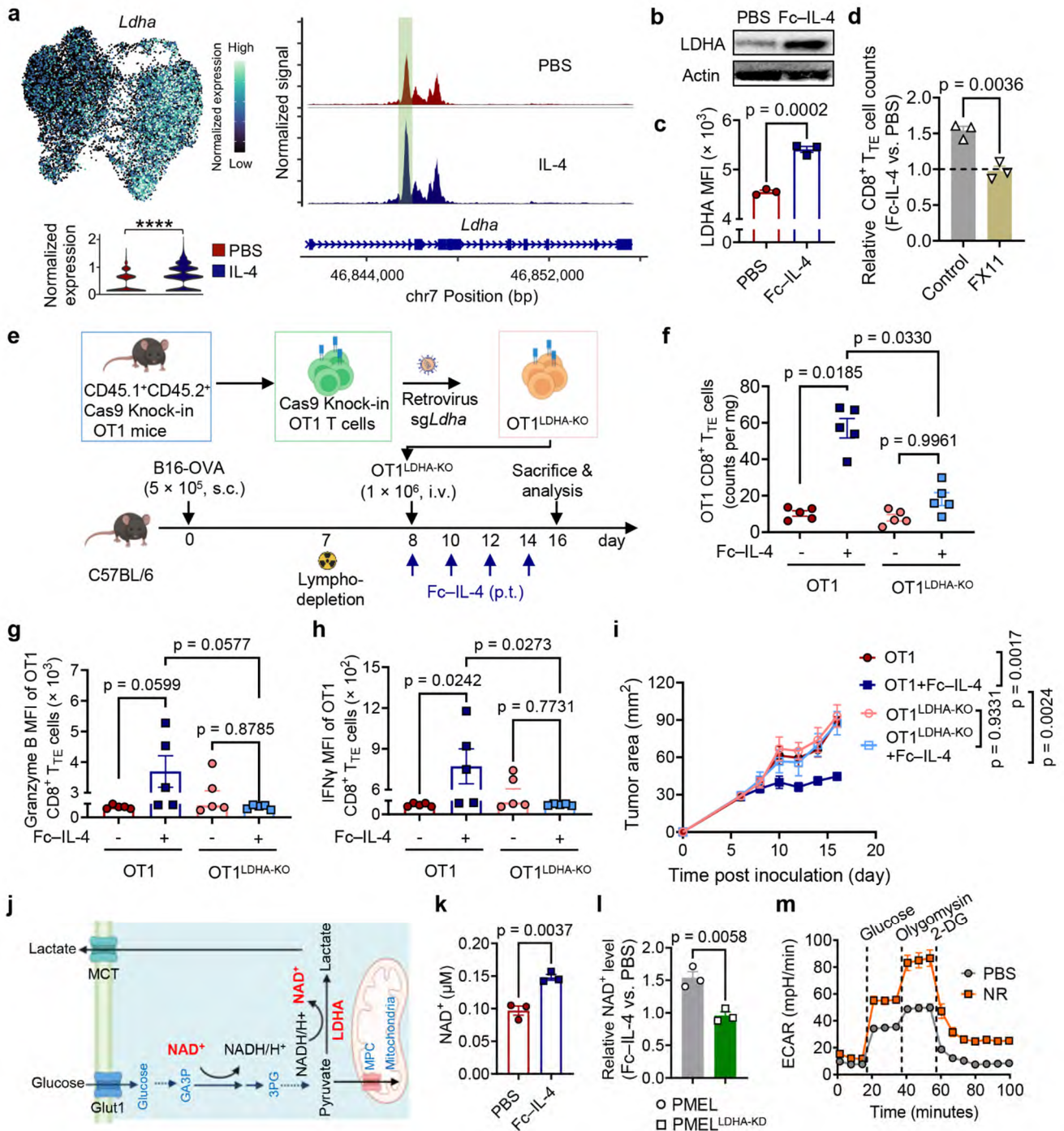
Fourth, the relationship between glycolysis and T cell survival remains uncertain, despite the acknowledged necessity of glycolysis for effector function, as noted by the reviewer. CD8⁺ T_{TE} cells exhibit severe survival defects⁸, and one contributing factor was the deficiency in NAD⁺⁹. We found that NAD⁺ supplementation, as a metabolic modulation, could alleviate the survival defect of CD8⁺ T_{TE} cells and enhance their function (previous data and moved to **Extended Data Fig. 15d-i**). The survival enhancement of CD8⁺ T_{TE} cells mediated by Fc-IL-4 also depended on LDHA (**New Fig. 6. j-m**). This is consistent with the literature reports as LDHA is known to be crucial for NAD⁺ recycling⁷.

4b. The mechanistic insights into how Fc-IL-4 enhances the anti-tumor activity of CD8 T cells (please see figures above)

To elucidate the molecular mechanisms driving the heightened glycolysis induced by Fc-IL-4, we performed single-cell ATAC and transcriptome co-profiling of ex vivo-induced CD8⁺ T_{TE} cells (**New Fig. 5i**). The integrated UMAP analysis merging ATAC and transcriptome datasets revealed distinct molecular profiles in T_{TE} cells between the two conditions, suggesting an intrinsic regulatory impact on this specific cell type due to the inclusion of IL-4 (**New Fig. 5i, bottom panel**). We performed a differential motif analysis using ATAC data to identify potential transcription factor binding sites within open chromatin regions. In IL-4 treated CD8⁺ T_{TE} cells compared to the PBS condition, Stat6 emerged as the most significantly enhanced motif, while Foxo1, a canonical negative regulator of mTOR, exhibited the highest degree of reduction (**New Fig. 5j**). We also investigated the signaling pathways regulated by differentially expressed genes (DEGs) within CD8⁺ TILs obtained from B16F10 tumors in mice subjected to Fc-IL-4 combined ACT, in comparison to the PBS control. The analysis revealed a significant upregulation of mTOR signaling, eIF4 and p70S6 signaling, and PI3K/AKT signaling in Fc-IL-4 treated cells, along with the upregulation of JAK/STAT signaling, NF-κB activation and glycolysis (**New Fig. 5k**). Upstream regulator analysis based on the DEGs identified multiple functional molecules predicted to be upregulated in the Fc-IL-4 group, particularly NF-κB, Myc, Pi3K, Akt1, and Stat6 (**New Fig. 5l**).

These findings prompted us to delve deeper into the role of the PI3K-AKT-mTOR axis and STAT6 in the heightened glycolytic activities observed following Fc-IL-4 treatment. Through flow cytometry and western blot analysis, we confirmed an elevation in the phosphorylation levels of AKT, P70S6K, and STAT6 following Fc-IL-4 treatment (**New Fig. 5m** and **New Extended Data Fig. 12a-c**). In an ex vivo stimulation assay, the partial attenuation of Fc-IL-4 treatment benefits, including glycolysis level, T cell counts, enhanced effector function, increased Glut-1 expression, glucose uptake capacity, and upregulation of Bcl-2 and CD107a, was observed in STAT6 knockout OT1 cells (OT1^{STAT6-KO}). However, the complete abrogation of Fc-IL-4 benefits occurred exclusively when AKT or mTOR signaling was concurrently blocked alongside STAT6 knockout (**New Fig. 5n-p** and **New Extended Data Fig. 12d-i**). Additionally, co-inhibition of STAT6 along with either AKT or mTOR signaling using chemical inhibitors yielded similar outcomes (**New Extended Data Fig. 12j-m**).

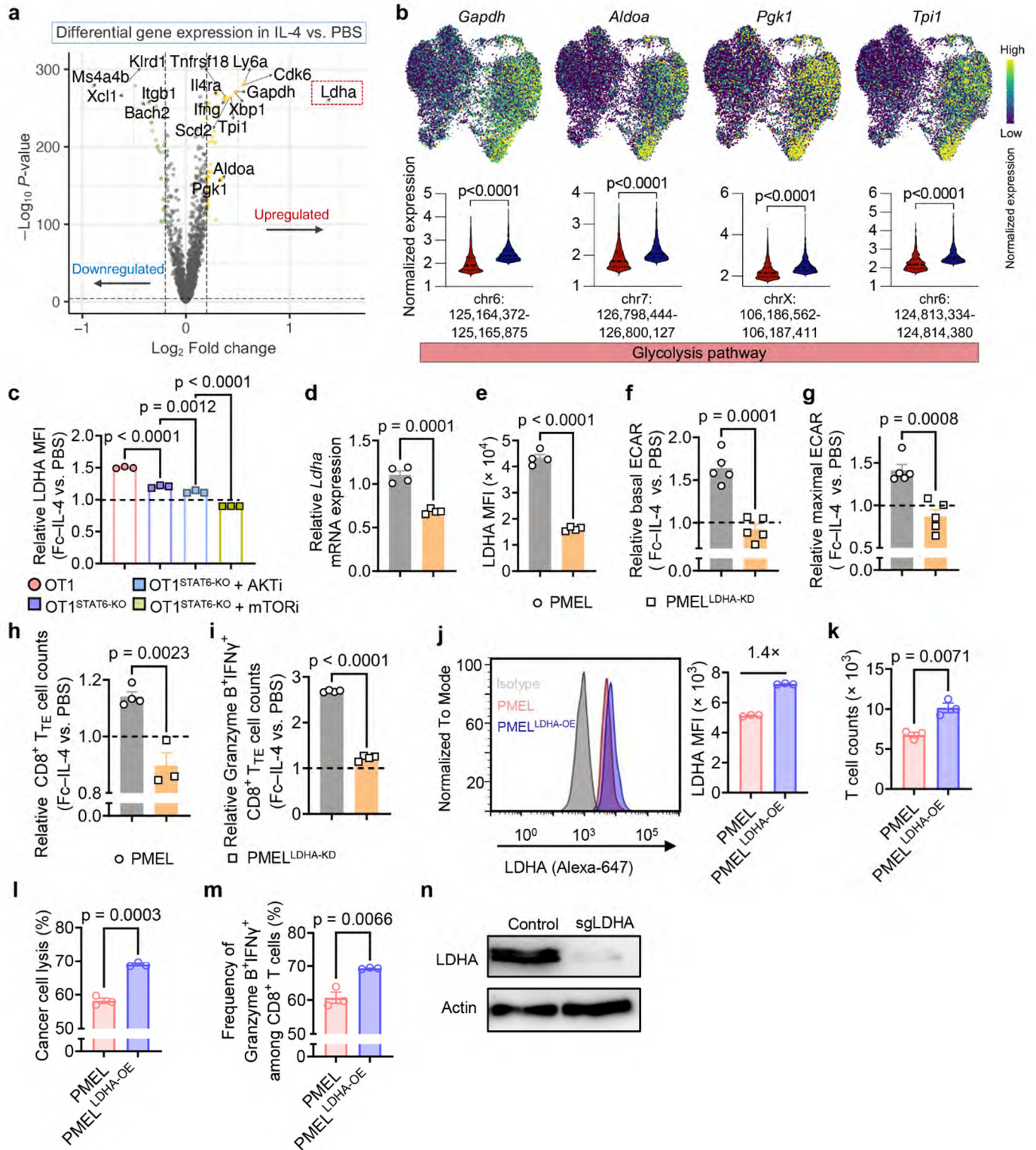
Altogether, these results indicate that Fc-IL-4 enhances glycolysis, survival, and effector function of CD8⁺ T_{TE} cells through STAT6 signaling and PI3K-AKT-mTOR axis.



New Fig. 6 | Fc-IL-4 promotes LDHA-mediated glycolysis and cellular NAD⁺ levels of CD8⁺ T_{TE} cells.

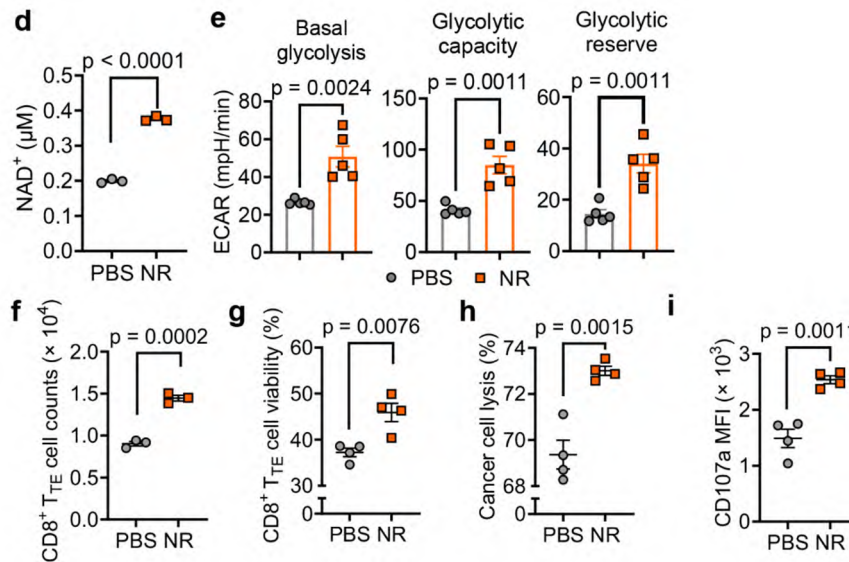
a, Expression of *Ldha* on the joint UMAP in **Fig. 5j** and pseudo-bulk chromatin accessibility tracks in the genomic region of *Ldha*, depicted separately for IL-4 and PBS conditions. The enhancer element predicted by ENCODE within the region of this gene is highlighted in a light green shade. **b, c**, Ex vivo-induced CD8⁺ T_{TE} cells were re-stimulated by dimeric anti-CD3 antibody (0.5 μg ml⁻¹) in the presence or absence of Fc-IL-4 for 48 h. (n = 3 biological replicates). Shown are the WB images of LDHA (**b**) and LDHA MFI (**c**). **d**, Ex vivo-induced CD8⁺ T_{TE} cells were re-stimulated by dimeric anti-CD3 antibody (0.5 μg ml⁻¹) in the presence or absence of Fc-IL-4 for 48 h with a LDHA inhibitor, FX11 (16 μM), or DMSO (n = 3 biological replicates). Shown are relative counts of CD8⁺ T_{TE} cells in the Fc-IL-4 treatment group normalized by that in the PBS group. **e-i**, Mice bearing B16-OVA tumors received ACT of activated WT OT1 or OT1^{LDHA-KO} T cells (1 × 10⁶, i.v.) one-day post lymphodepletion followed by the treatment of Fc-IL-4 (20 μg, p.t.) or PBS every other day for 4 doses in total (n = 5 animals). Mice were sacrificed on day 16 and the tumor tissues were collected for analysis by flow cytometry. Shown are the experimental timeline (**e**), counts of tumor-infiltrating OT1 CD8⁺ T_{TE} cells (**f**), MFI of Granzyme B (**g**) and IFNγ (**h**) of tumor-infiltrating OT1 CD8⁺ T_{TE} cells, and average tumor growth curves (**i**) of

mice. **j**, Schematic of LDHA mediated NAD⁺/NADH recycling. **k**, Experimental setting was described in **Fig. 6b**. Shown is the cellular NAD⁺ level of CD8⁺ T_{TE} cells. **l**, Ex vivo-induced WT PMEL and PMEL^{LDHA-KD} CD8⁺ T_{TE} cells were re-stimulated by dimeric anti-CD3 antibody (0.5 μg ml⁻¹) in the presence or absence of Fc-IL-4. Shown is relative NAD⁺ level in the Fc-IL-4 group normalized by that in the PBS group. **m**, Real-time ECAR analysis of ex vivo-induced CD8⁺ T_{TE} cells re-stimulated by dimeric anti-CD3 antibody (0.5 μg ml⁻¹) for 48 h in the presence or absence of NR (100 μM). Data are one representative of three independent experiments with n = 3-5 biological replicates or n = 5-7 animals. All data represent mean ± s.e.m. and are analyzed by unpaired two-sided Student's t-test (**c**, **d**, **k**, and **l**), or one-way ANOVA and Tukey's test (**f**-**i**).



New Extended Data Fig. 14 | Fc-IL-4 reinvigorates CD8⁺ T_{TE} cells by enhancing LDHA-dependent glycolysis. **a**, Experimental setting was described in **Fig. 5i**. Shown is volcano plot showing differential gene expression between IL-4 vs. PBS-treated PMEL CD8⁺ T_{TE} cells. **b**, Expression of glycolysis pathway gene markers on the joint UMAP in **Fig.**

5j, along with comparisons of corresponding accessible peaks between conditions. **c**, Experimental setting was described in **Fig. 5m**. Shown is the relative expression of LDHA in the Fc-IL-4 treatment group normalized by that in the PBS group. **d-i**, WT PMEL or PMEL^{LDHA-KD} T cells were re-stimulated by dimeric anti-CD3 antibody (0.5 µg ml⁻¹) in the presence or absence of Fc-IL-4. Shown are the relative transcriptome level of LDHA (**d**) and protein expression level of LDHA (**e**) in PMEL^{LDHA-KD} T cells, and the relative basal (**f**) and maximal ECAR (**g**), relative counts of CD8⁺ T_{TE} cells (**h**), and Granzyme B⁺IFNγ⁺ polyfunctional CD8⁺ T_{TE} cells (**i**) in the Fc-IL-4 treatment group normalized by that in the PBS group. **j-m**, WT PMEL or PMEL^{LDHA-OE} T cells were co-cultured with B16F10 for 48 h. Shown are representative flow cytometry plots and LDHA MFI (**j**), T cell counts (**k**), percent of cancer cell lysis (**l**), and frequencies of Granzyme B⁺IFNγ⁺ (**m**) among PMEL^{LDHA-OE} T cells. **n**, WB images of LDHA showing the LDHA knock-out in OT1^{LDHA-KO} T cells. Data are one representative of three independent experiments with n = 3-5 biological replicates. All data represent mean ± s.e.m. and are analyzed by One-way ANOVA and Tukey's test (**c**), or unpaired two-sided Student's t-test (**d-m**).



Extended Data Fig. 15d-i. d, The cellular NAD⁺ level of ex vivo-induced CD8⁺ T_{TE} cells with supplementation of a NAD⁺ precursor, NR (100 µM). **e**, Average basal glycolysis, glycolytic capacity, and glycolytic reserve analyzed from **Fig. 6m**. **f, g**, Ex vivo-induced CD8⁺ T_{TE} cells were re-stimulated by dimeric anti-CD3 antibody (0.5 µg ml⁻¹) for 48 h in the presence or absence of NR (100 µM). Shown are the counts (**f**) and viability (**g**) of CD8⁺ T_{TE} cells. **h, i**, Ex vivo-induced CD8⁺ T_{TE} cells were co-cultured with B16F10 tumor cells for 48 h in the presence or absence of NR (100 µM). Shown are the percent of cancer cell lysis (**h**) and CD107a MFI (**i**) of CD8⁺ T_{TE} cells. Data are one representative of three independent experiments with n = 3-5 biological replicates. All data represent mean ± s.e.m. and are analyzed by unpaired two-sided Student's t-test.

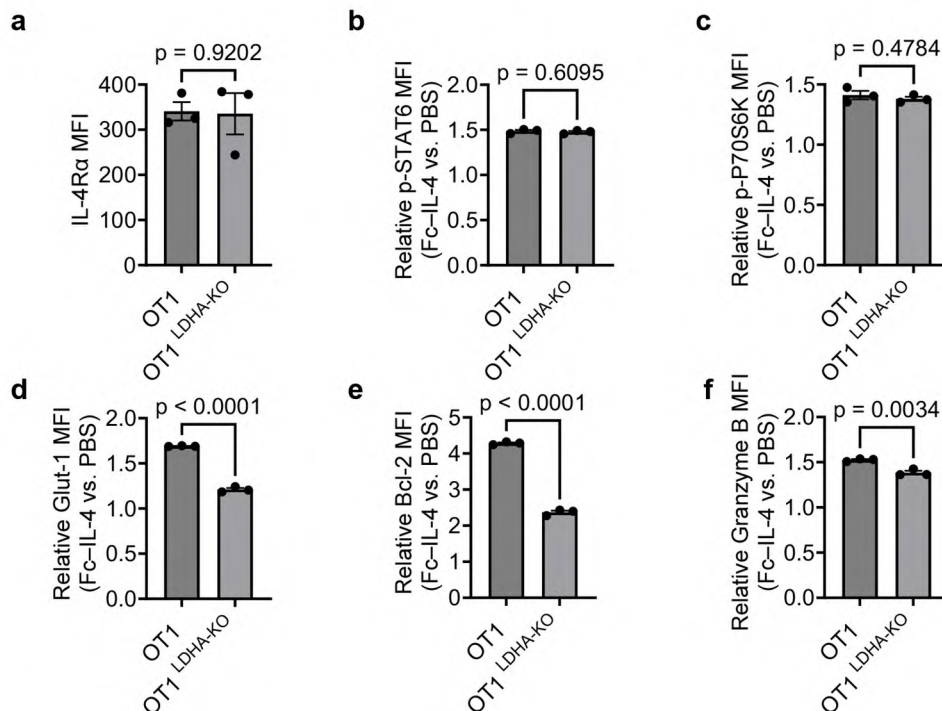
4c. Does a constitutively active STAT4 (we think the reviewer meant STAT6) prevent exhaustion or rescue an LDHA KO?

We agree that it is an interesting idea to investigate whether a constitutively active STAT6 signal could rescue the dysfunction of LDHA-KO T cells. However, we believe that while the constitutive STAT6 signal may provide some degree of compensation, it may not be sufficient to entirely substitute for the roles of LDHA due to two reasons. *First*, our STAT6-KO experiment and pharmacological inhibition studies reveal that both STAT6 and mTOR signaling pathways act synergistically to up-regulate LDHA and enhance glycolysis (**New Fig. 5i-p** and **New Extended Data Fig. 12** and **New Extended Data Fig. 14a&c** please see the figures above). So STAT6 signaling alone may not be enough. *Second*, we have demonstrated that LDHA is essential for Fc-IL-4-induced elevation of cellular NAD⁺ level and the promotion of T cell survival (**New Fig. 6j-l**, please see figures above). Therefore, STAT6 signal unlikely rescues the LDHA-KO T cells.

4d. An orthogonal approach could be to see if IL-4r expression or downstream signaling is lost in LDHA knockout T cells.

We investigated IL-4Rα expression and downstream signaling in OT1^{LDHA-KO} T cells, and observed that the

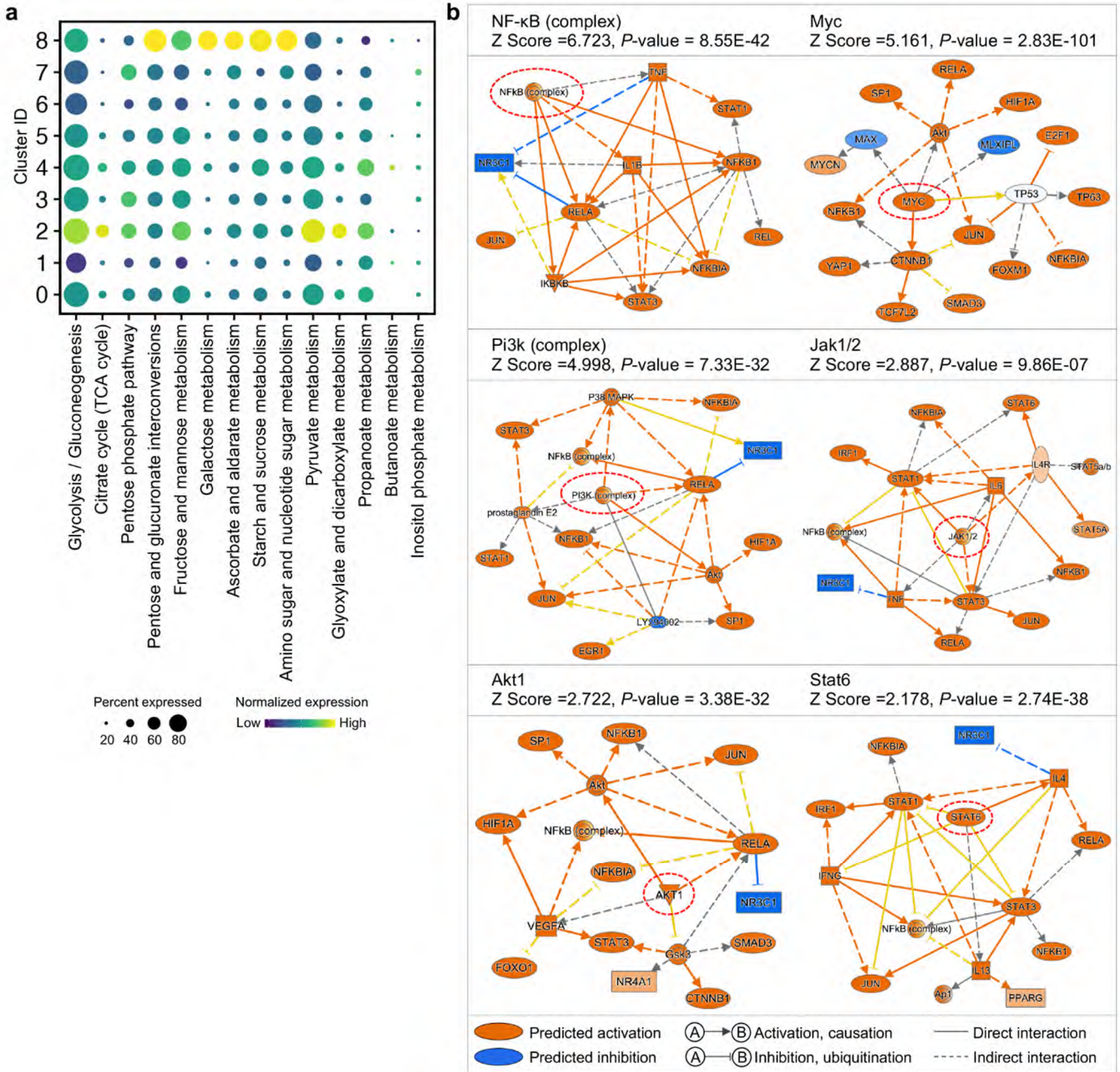
expression of IL-4R α in CD8⁺ T cells remained unchanged upon LDHA knockout (**RL-only Fig. IIIa**). The downstream signaling of IL-4R α , including STAT6 and mTOR pathways, remained activatable by Fc-IL-4 despite LDHA knockout (**RL-only Fig. IIIb&c**). However, Fc-IL-4 failed to increase Glut-1, Bcl-2, and Granzyme B expression (**RL-only Fig. IIId-f**), underscoring the crucial role of LDHA in these processes.



RL-only Fig. III. LDHA is dispensable for IL-4R α expression and downstream signaling transduction of Fc-IL-4. **a**, The IL-4R α expression of ex vivo-induced OT1 CD8⁺ T_{TE} and OT1^{LDHA-KO} CD8⁺ T_{TE} cells; **b, c**, OT1 or OT1^{LDHA-KO} T cells were re-stimulated by dimeric anti-CD3 antibody (0.1 $\mu\text{g ml}^{-1}$) in the presence or absence of Fc-IL-4 (n = 3 biological replicates) for 30 mins. Shown are the relative p-STAT6 MFI (**b**) and p-P70S6K (**c**). **d-f**, OT1 or OT1^{LDHA-KO} T_{TE} cells were re-stimulated by dimeric anti-CD3 antibody (0.5 $\mu\text{g ml}^{-1}$) in the presence or absence of Fc-IL-4 (n = 3 biological replicates) for 24 h. Shown are the relative expression of Glut-1 (**d**), Bcl-2 (**e**), and Granzyme B (**f**). All data represent mean \pm s.e.m. and are analyzed by unpaired two-sided Student's t-test.

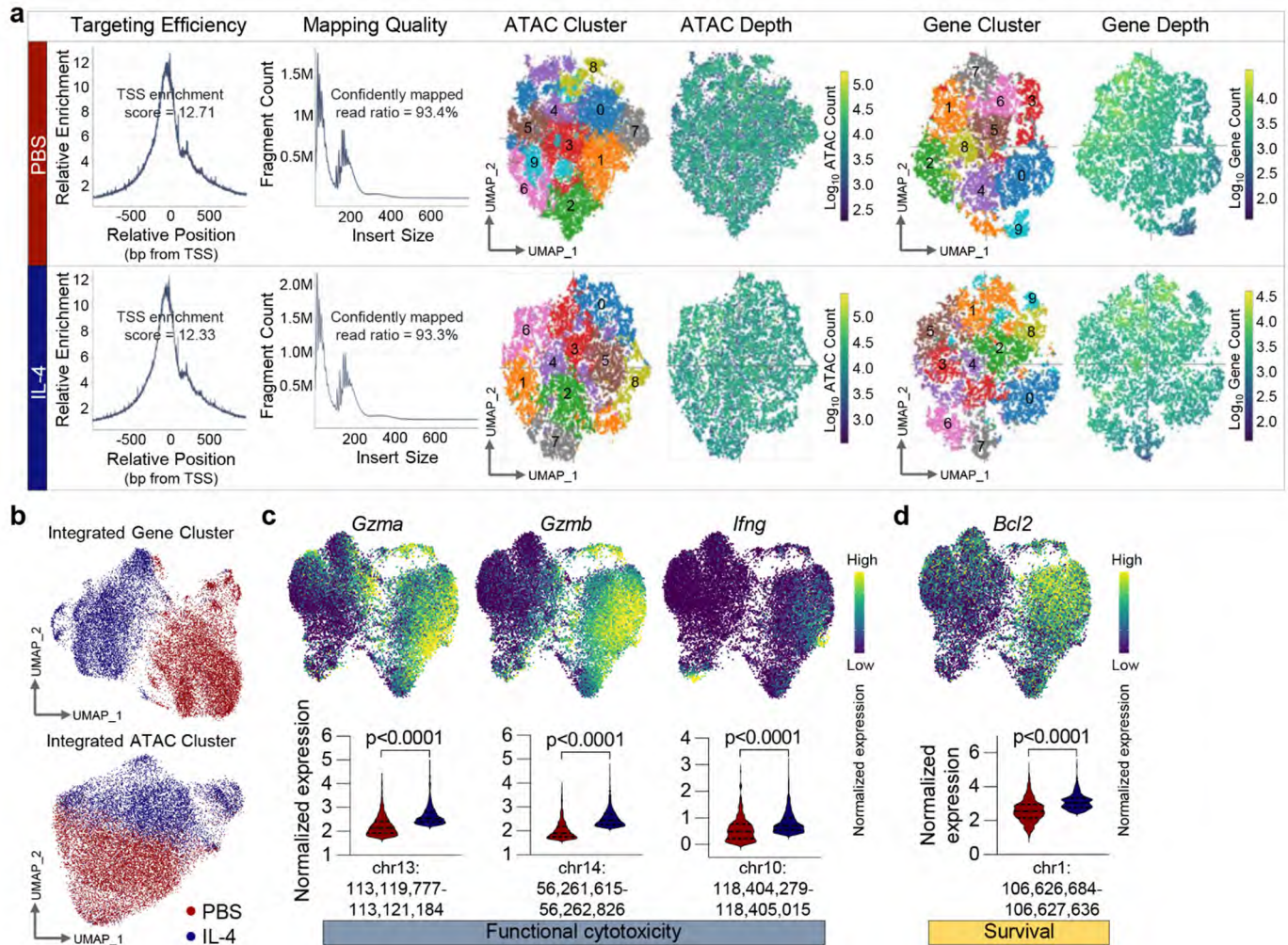
4e. In that same idea, deeper analysis of the sequencing results on the TIM-3⁺ subset of CD8 T cells could reveal a novel transcriptional program allowing the restoration of function in these cells.

Following reviewer's suggestion, in the revised manuscript, we conducted an in-depth analysis of single-cell RNA-seq data to delineate the signaling pathway profile of CD8⁺ T_{TE} cells treated with Fc-IL-4 (**New Fig. 5k&l**, please see figures above and also **New Extended Data Fig. 10**). We also performed single-cell ATAC and transcriptome co-profiling of CD8⁺ T_{TE} cells to particularly investigate the chromatin accessibility alterations induced by IL-4 treatment (**New Fig. 5i&j**, please see figures above and also **New Extended Data Fig. 11**). Through comprehensive analysis of these datasets, we have confirmed that the activation of STAT6 and mTOR pathways by Fc-IL-4 significantly contributes to the augmentation of glycolytic metabolism, effector function, and survival of CD8⁺ T_{TE} cells mediated by Fc-IL-4.



New Extended Data Fig. 10 | Single-cell metabolism and upstream regulator analysis based on scRNA-seq results.

Experimental setting was described in **Fig. 1g. a**, Systematic expression comparison of carbohydrate metabolisms across all identified clusters in **Fig. 5d**, with each metabolic pathway name indicated. The size of circle represents proportion of single cells expressing the pathway, and the color shade indicates normalized expression level. Genes defining each pathway are provided in Supplementary Table 1. **b**, Mechanistic networks associated with the significant activation of selected upstream regulators in Fc-IL-4 treated PMEL CD8⁺ TILs relative to the PBS condition. z score is computed and used to reflect the predicted activation level (z > 0, activated/upregulated; z < 0, inhibited/downregulated; z ≥ 2 or z ≤ -2 can be considered significant).



New Extended Data Fig. 11 | Single-cell ATAC and gene co-profiling analysis of IL-4 treated PMEL CD8+ TTE cells.

a, Quality assessment of sequenced data from IL-4 or PBS conditions, featuring TSS enrichment score, insert size distribution, unsupervised clustering analysis of ATAC and gene datasets, and corresponding count distribution. Consistent performance is observed with negligible batch effect. **b**, Gene or ATAC expression UMAP of all the single cells color-coded by their respective conditions. **c**, **d**, Expression of functional cytotoxicity (**c**), and survival (**d**) gene markers on the joint UMAP in **Fig. 5i**, along with comparisons of corresponding accessible peaks between conditions. Statistical analyses are performed using unpaired two-sided Student's t-test.

5) It would also be important to know what cell types are naturally producing IL-4 in the TME in humans and mice.

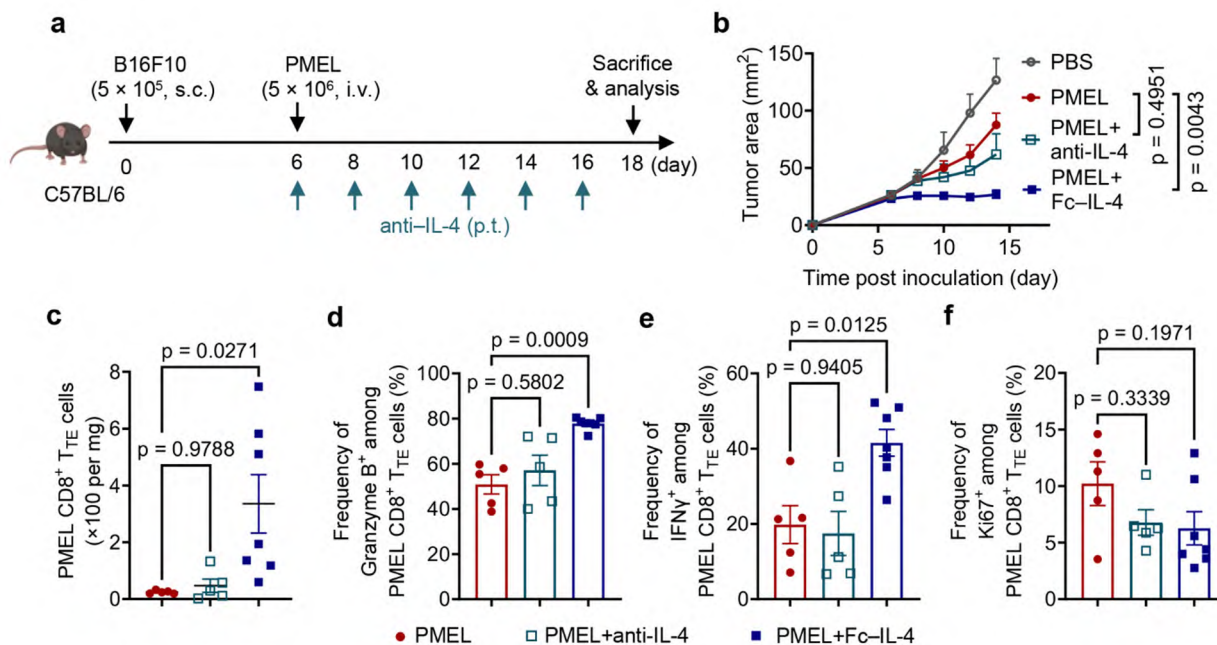
To probe the role of endogenous IL-4, we neutralized endogenous IL-4 using anti-IL-4 antibody and observed that this had negligible effects on the antitumor efficacy of the ACT therapy using PMEL T cells. Tumor infiltration and effector function of tumor-infiltrating PMEL T cells remained unaffected by IL-4 neutralization (**New Extended Data Fig. 8**). One of the possible reasons is that the physiological level of endogenous IL-4 (around 1 pg/ml in the human serum² and <5 pg/ml in the tumor tissues³) is substantially lower compared to the injected exogenous Fc-IL-4 (20 µg every injection, equivalent to 2-20 µg/ml assuming tumor volume is 1 cm³; ~10³-10⁶ times higher concentration than the physiological level).

We would like to respectfully clarify that IL-4 producing cells have been extensively investigated and reported in previous studies¹⁰. The expression level of intratumoral IL-4 varies significantly across different types of tumors. In primary epithelial cancer cells, such as those found in human colon, breast and lung carcinomas, IL-4 is primarily produced by these cancer cells³. In bladder and prostate carcinoma, immune cells including eosinophils, basophils, and type 2 CD4⁺ T cells are identified as the major sources of IL-4 production¹¹. However, as we explained above, the physiological levels of endogenous IL-4 in the tumor microenvironment

are nearly negligible compared to the injected dose of Fc-IL-4. Thus, its relevance in the context of Fc-IL-4 therapy is minimal.

We added the discussion of endogenous IL-4 in the revised manuscript:

“We also discovered that endogenous IL-4, typically present at substantially lower concentrations compared to exogenously injected Fc-IL-4, had negligible impact on the anti-tumor immunity of ACT with PMEL T cells. This was evidenced by minimal effects on the expansion, cytotoxicity, effector function, or proliferative capability of tumor-infiltrating CD8⁺ T_{TE} cells upon neutralizing endogenous IL-4 through p.t. administration of anti-IL-4 antibody (Extended Data Fig. 8). Overall, these findings strongly suggest that the exogenous type 2 cytokine Fc-IL-4, administered at 20 μg per injection (a concentration much higher than endogenous IL-4) primarily drives the enrichment of CD8⁺ T_{TE} cells by enhancing their survival.”



Extended Data Fig. 8 | Endogenous IL-4 exhibits negligible effects on tumor-infiltrating CD8⁺ T_{TE} cells.

B16F10 tumor-bearing mice received ACT of PMEL T cells (5 × 10⁶, i.v.) followed by administration of anti-IL-4 antibody (200 μg, p.t.), or Fc-IL-4 (20 μg, p.t.), or PBS every other day for 6 doses in total. Mice were sacrificed on day 18 and the tumor tissues were collected for analysis by flow cytometry. Shown are the experimental timeline (a), average tumor growth curves (b), counts of tumor-infiltrating PMEL CD8⁺ T_{TE} cells (c), frequencies of Granzyme B⁺ (d), IFN γ ⁺ (e), and Ki67⁺ (f) among tumor-infiltrating PMEL CD8⁺ T_{TE} cells. Data are one representative of two independent experiments with n = 5-7 animals. All data represent mean ± s.e.m. and are analyzed by one-way ANOVA and Tukey's test.

Minor Points:

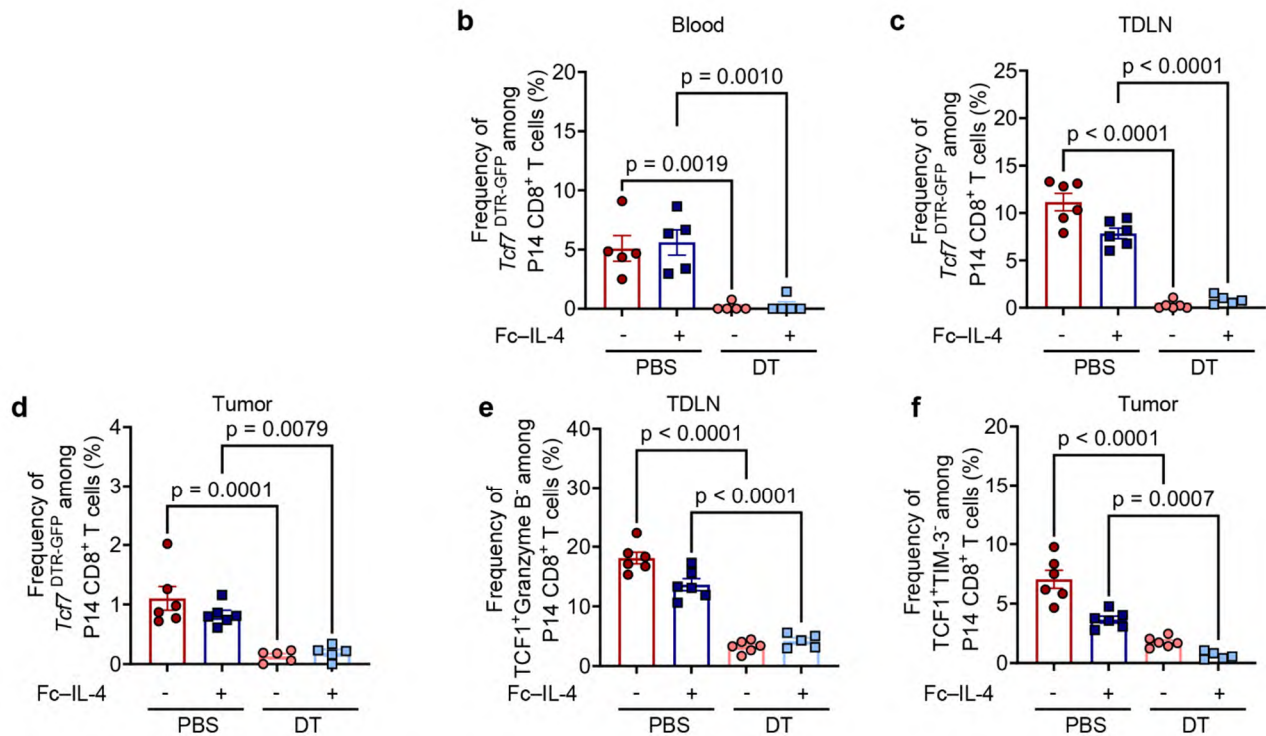
-In figure 2, panel C, it would be helpful to see stacked bar graphs in order to more easily see the relative contribution of each treatment group to each defined subset

Thanks for this suggestion, and we have implemented the modifications to this figure in the revised version (now moved to [Fig. 1i](#)).

-Regarding figure 4 and the DT treatment, it is difficult to see whether the DT treatment truly depleted the PD-1⁺ TIM-3⁻ subset (presumably the TCF7 expressing cells), including a day 12 time point showing loss of this population is suggested. Also, the authors should demonstrate this is occurring directly in the tumors and draining lymph nodes. There are very few TCF7⁺ cells in the blood that is used as a proxy, and so it is not clear if all the progenitor TEX cells are truly depleted in the tissues and tumors where it matters more.

As suggested, we have included data on the detection of progenitor exhausted CD8⁺ T cells on day 12 post DT treatment in different organs. Progenitor exhausted CD8⁺ T cells were characterized as Tcf7^{DTR-GFP} positive subset or TCF1⁺Granzyme B⁻ subset in the TDLN, or TCF1⁺TIM-3⁻ subset in the tumor²². We found

that DT effectively depleted *Tcf7*^{DTR-GFP} positive P14 T cells in the blood, TDLN, and tumor tissue ([New Extended Data Fig. 7b-d](#)). Moreover, TCF1⁺ T cells in the TDLN and tumor tissues, where their presence is particularly relevant, were also substantially depleted ([New Extended Data Fig. 7e&f](#)), confirming the effective depletion of progenitor exhausted CD8⁺ T cells by DT treatment.



New Extended Data Fig. 7b-f. Experimental setting was similar as described in [Fig. 4a](#) except that mice were sacrificed on day 12 and the tumor-draining lymph node (TDLN), spleen, blood, and tumor tissues were collected for analysis by flow cytometry. Shown are the frequencies of *Tcf7*^{DTR-GFP} progenitor exhausted T cells among transferred P14 T cells in the peripheral blood (**b**), TDLN (**c**), and tumor (**d**), and frequencies of TCF1⁺Granzyme B⁺ among transferred P14 T cells in the TDLN (**e**), and frequencies of TCF1⁺TIM3⁻ among transferred P14 T cells in the tumor (**f**). All data represent mean ± s.e.m. and are analyzed by One-way ANOVA and Tukey's test.

-Similarly, regarding the profiling of the TILs in figure 4, the T cell population analysis by PD-1 and TIM-3 should be included for the TCF7 DTR and IL-4r KO experiment

We respectfully clarify that in the *Tcf7* conditional KO experiment ([Fig. 4b-d](#)), we have already utilized *Tcf7*^{DTR-GFP}-PD-1⁺TIM-3⁺ subset to profile P14 CD8⁺ T_{TE} cells. Similarly, in the IL-4-Rα KO experiment ([Fig. 4g-i](#)), PD-1⁺TIM-3⁺ subset was employed to profile OT1 CD8⁺ T_{TE} cells.

References

1. Ju, G. *et al.* Conversion of the interleukin 1 receptor antagonist into an agonist by site-specific mutagenesis. *Proc. Natl. Acad. Sci. U.S.A.* . **88**, 2658–2662 (1991).
2. Eini, P., Majzoobi, M. M., Ghasemi Basir, H. R., Moosavi, Z. & Moradi, A. Comparison of the serum level of interleukin-4 in patients with brucellosis and healthy controls. *J. Clin.Lab. Anal.* **34**, e23267 (2020).
3. Todaro, M. *et al.* Apoptosis resistance in epithelial tumors is mediated by tumor-cell-derived interleukin-4. *Cell Death Differ.* **15**, 762–772 (2008).
4. Reinfeld, B. I. *et al.* Cell-programmed nutrient partitioning in the tumour microenvironment. *Nature* **593**, 282–288 (2021).
5. Chang, C. H. *et al.* Metabolic Competition in the Tumor Microenvironment Is a Driver of Cancer Progression. *Cell* **162**, 1229–1241 (2015).
6. Bantug, G. R. *et al.* Mitochondria-Endoplasmic Reticulum Contact Sites Function as Immunometabolic Hubs that Orchestrate the Rapid Recall Response of Memory CD8+ T Cells. *Immunity* **48**, 542–555 (2018).
7. Liu, P. S. *et al.* CD40 signal rewires fatty acid and glutamine metabolism for stimulating macrophage anti-tumorigenic functions. *Nat. Immunol.* **24**, 452–462 (2023).
8. Zhu, J., Petit, P. F. & Van den Eynde, B. J. Apoptosis of tumor-infiltrating T lymphocytes: a new immune checkpoint mechanism. *Cancer Immunol. Immunother.* vol. 68 835–847 (2019).
9. Vardhana, S. A. *et al.* Impaired mitochondrial oxidative phosphorylation limits the self-renewal of T cells exposed to persistent antigen. *Nat. Immunol.* **21**, 1022–1033 (2020).
10. Gadani, S. P., Cronk, J. C., Norris, G. T. & Kipnis, J. IL-4 in the Brain: A Cytokine To Remember. *J.Immunol.* **189**, 4213–4219 (2012).
11. Conticello, C. *et al.* IL-4 Protects Tumor Cells from Anti-CD95 and Chemotherapeutic Agents via Up-Regulation of Antiapoptotic Proteins. *J.Immunol.* **172**, 5467–5477 (2004).
12. DePeaux, K. & Delgoffe, G. M. Metabolic barriers to cancer immunotherapy. *Nat. Rev. Immunol.* vol. 21 785–797 (2021).
13. Maciver, N. J., Michalek, R. D. & Rathmell, J. C. Metabolic regulation of T lymphocytes. *Ann. Rev. Immunol.* **31**, 259–283 (2013).
14. Chapman, N. M., Boothby, M. R. & Chi, H. Metabolic coordination of T cell quiescence and activation. *Nat. Rev. Immunol.* **20**, 55–70 (2020).
15. Park, J., Hsueh, P. C., Li, Z. & Ho, P. C. Microenvironment-driven metabolic adaptations guiding CD8+ T cell anti-tumor immunity. *Immunity* **56**, 32–42 (2023).
16. Giles, J. R., Globig, A. M., Kaech, S. M. & Wherry, E. J. CD8+ T cells in the cancer-immunity cycle. *Immunity* **56**, 2231–2253 (2023).
17. Li, X. *et al.* Navigating metabolic pathways to enhance antitumour immunity and immunotherapy. *Nat. Rev. Clin. Oncol.* **16**, 425–441 (2019).
18. Xu, K. *et al.* Glycolysis fuels phosphoinositide 3-kinase signaling to bolster T cell immunity. *Science* **371**, 405–410 (2021).
19. Blank, C. U. *et al.* Defining ‘T cell exhaustion’. *Nat. Rev. Immunol.* **19**, 665–674 (2019).
20. Giles, J. R. *et al.* Shared and distinct biological circuits in effector, memory and exhausted CD8+ T cells revealed by temporal single-cell transcriptomics and epigenetics. *Nat. Immunol.* **23**, 1600–1613 (2022).
21. Guo, Y. *et al.* Metabolic reprogramming of terminally exhausted CD8+ T cells by IL-10 enhances anti-tumor immunity. *Nat.Immunol.* **22**, 746–756 (2021).
22. Siddiqui, I. *et al.* Intratumoral Tcf1 + PD-1 + CD8 + T Cells with Stem-like Properties Promote Tumor

- Control in Response to Vaccination and Checkpoint Blockade Immunotherapy. *Immunity* **50**, 195–211 (2019).
23. LaFleur, M. W. *et al.* PTPN2 regulates the generation of exhausted CD8⁺ T cell subpopulations and restrains tumor immunity. *Nat. Immunol.* **20**, 1335–1347 (2019).
 24. Miller, B. C. *et al.* Subsets of exhausted CD8⁺ T cells differentially mediate tumor control and respond to checkpoint blockade. *Nat. Immunol.* **20**, 326–336 (2019).
 25. Tulpule, A. *et al.* Interleukin-4 in the treatment of AIDS-related Kaposi's sarcoma. *Ann. Oncol.* **8**, 79–83 (1997).
 26. Goldstein, R. *et al.* Clinical investigation of the role of interleukin-4 and interleukin-13 in the evolution of prostate cancer. *Cancers (Basel)*. **3**, 4281–4293 (2011).
 27. Guo, Y. *et al.* Metabolic reprogramming of terminally exhausted CD8⁺ T cells by IL-10 enhances anti-tumor immunity. *Nat. Immunol.* **22**, 746–756 (2021).
 28. Lloyd, C. M. & Snelgrove, R. J. Type 2 immunity: Expanding our view. *Sci. Immunol.* **3**, eaat1604 (2018).
 29. Ouyang, W., Rutz, S., Crellin, N. K., Valdez, P. A. & Hymowitz, S. G. Regulation and Functions of the IL-10 Family of Cytokines in Inflammation and Disease. *Ann. Rev. Immunol.* **29**, 71–109 (2011).
 30. Wang, H. W. & Joyce, J. A. Alternative activation of tumor-associated macrophages by IL-4: Priming for protumoral functions. *Cell Cycle* vol. 9 4824–4835 (2010).
 31. LaMarche, N. M. *et al.* An IL-4 signalling axis in bone marrow drives pro-tumorigenic myelopoiesis. *Nature* **625**, 166–174 (2023).
 32. Kaplan, M. H., Schindler, U., Smiley, S. T. & Grusby, M. J. Stat6 is required for mediating responses to IL-4 and for the development of Th2 cells. *Immunity* **4**, 313–319 (1996).
 33. Sukumar, M. *et al.* Inhibiting glycolytic metabolism enhances CD8⁺ T cell memory and antitumor function. *J. Clin. Invest.* **123**, 4479–4488 (2013).
 34. Wu, W. *et al.* IL-2R α -biased agonist enhances antitumor immunity by invigorating tumor-infiltrating CD25⁺CD8⁺ T cells. *Nat. Cancer* **4**, 1309–1325 (2023).
 35. Liu, Y. *et al.* IL-2 regulates tumor-reactive CD8⁺ T cell exhaustion by activating the aryl hydrocarbon receptor. *Nat. Immunol.* **22**, 358–369 (2021).
 36. Rochman, Y., Spolski, R. & Leonard, W. J. New insights into the regulation of T cells by γ c family cytokines. *Nat. Rev. Immunol.* vol. 9 480–490 (2009).

Reviewer Reports on the First Revision:

Referees' comments:

Referee #1 (Remarks to the Author):

Feng et al. have invested significant efforts in revising their exciting study on the function of Fc-IL4 as an enhancer of anti-tumor CAR T cell efficacy. I would like to commend them for these efforts and their important research on this subject.

In their revision of Extended Data Figure 2d-g, it is intriguing that the percentages of CD45.1 OT1 cells is significantly higher than that of CD90.1 PME (6.9% vs 1.2% in the representative dot plot). Do the authors have a hypothesis as to why this is the case? Additionally, it would be helpful to add the data for the activated CD90.2+ PMEL to panels f and g.

A very minor comment is that regarding the new exciting data in Extended Data Figure 12, it would be helpful to present the pSTAT6 and STAT6 plots next to each other (i.e. panels a and b (not a and d)). The increase in pSTAT6 following Fc-IL-4 is even more impressive given that there appears to be a compensatory decrease in total STAT6 levels.

The new data on glucose uptake is more convincing to this reviewer than the 2-NBDG studies which pose significant problems due to the difference in affinity of glucose and 2-NBDG for GLUT1. In the opinion of this reviewer, I would include the glucose uptake (extended Figure 9d) in the main figure and not 2-NBDG.

One point is that it will be important for the authors to add a point to their discussion regarding the recent study by S. Kenderian (Stewart et al.) pointing to a negative role of IL-4 in CAR T cell function ("...when CART cells were treated with IL-4, they developed signs of exhaustion, but when CART cells were treated with an IL-4 monoclonal antibody, they showed improved antitumor efficacy and reduced signs of exhaustion in preclinical models. Therefore, our study identified both a novel role for IL-4 on CART cells and the improvement of CART cell therapy through IL-4 neutralization."). This study was presented at both ASH and AACR and the DOI for their bioRxiv manuscript is copied below.

This could be of significant interest in light of your new data showing that prior to transfer (and after Fc-IL4 treatment), your cells exhibited a complete bias to a Th1 phenotype (93% IFN γ secretion, new Extended Figure 1f). Interestingly, the Kenderian study also finds that the function of IL4 is independent of Th2 polarization.

<https://doi.org/10.1101/2023.09.28.560046>

<https://doi.org/10.1182/blood-2022-160219>

Referee #2 (Remarks to the Author):

We thank the authors for thoroughly addressing all the reviewers comments. The new figures and added data significantly improved the manuscript, which we believe will have a big impact in the field of cancer immunotherapy.

Referee #3 (Remarks to the Author):

All the key points I had raised were addressed. My only remaining concern relates to the title.

I think the authors should reconsider the title. I mean, the combination "functional, terminally exhausted CD8 + T cells" is simply a wired mixture of contradictory information. Why does it need to be overloaded with terms that are difficult for a broader audience to understand? The authors could simply use a descriptive approach and write "functional superior tumor-targeting T cells" or something similar.

Author Rebuttals to First Revision:

Additional comments from the reviewers:

We are grateful to the reviewers for their insightful comments and suggestions that helped improve our study.

Referee #1 (Remarks to the Author):

Feng et al. have invested significant efforts in revising their exciting study on the function of Fc-IL4 as an enhancer of anti-tumor CAR T cell efficacy. I would like to commend them for these efforts and their important research on this subject.

In their revision of Extended Data Figure 2d-g, it is intriguing that the percentages of CD45.1 OT1 cells is significantly higher than that of CD90.1 PME (6.9% vs 1.2% in the representative dot plot). ~~Do the authors have a hypothesis as to why this is the case?~~ Additionally, it would be helpful to add the data for the activated CD90.2+ PMEL to panels f and g.

It is indeed interesting that the counts of CD45.1⁺ OT1 T cells are higher than CD90.1⁺ PMEL T cells in the PBS group on the day of TIL analysis. Initially, we co-injected the naive CD45.1⁺ OT1 and naive CD90.1⁺ PMEL T cells at a ratio of 1:1 prior to tumor inoculation. These two TCR-transgenic T cells may have different proliferative capacity in vivo. Naive OT-1 T cells may outcompete naive PMEL T cells for homeostatic cytokines and other stimulatory factors, leading to better survival before the tumor inoculation. Consistently, we did observe that OT-1 T cells (recognizing OVA peptide) typically expanded more than PMEL T cells (recognizing gp100 antigen) in vitro culture. Without Fc-IL-4, the level of tumor-infiltration of PMEL T cells was also typically low.

The endogenous CD8⁺ T cells of the recipient mice were also CD90.2 positive. We depleted

the endogenous CD8⁺ T cells using irradiation, but they gradually recovered on the day of TIL analysis. Among all the CD90.2⁺ PMEL T cells, we cannot distinguish the remaining endogenous CD8⁺ T cells or the transferred activated CD90.2⁺ PMEL T cells. Therefore, we prefer not to add the data of activated CD90.2⁺ PMEL T cells, which can be rather confusing.

A very minor comment is that regarding the new exciting data in Extended Data Figure 12, it would be helpful to present the pSTAT6 and STAT6 plots next to each other (i.e. panels a and b (not a and d)). The increase in pSTAT6 following Fc-IL-4 is even more impressive given that there appears to be a compensatory decrease in total STAT6 levels.

We apologize for the confusion. The result shown in Extended Data Figure 12d is used to confirm that STAT6 is knocked out in the OT-1 T cells. It is NOT the comparison of STAT6 expression with or without Fc-IL-4 treatment. We have re-organized these figures in the revised manuscript to avoid such confusion.

The new data on glucose uptake is more convincing to this reviewer than the 2-NBDG studies which pose significant problems due to the difference in affinity of glucose and 2-NBDG for GLUT1. In the opinion of this reviewer, I would include the glucose uptake (extended Figure 9d) in the main figure and not 2-NBDG.

Thanks for the suggestion. We have moved the 2-NBDG data to Extended Figure 7c. The new data on glucose uptake is also provided in Extended Figure 7d due to the page limit of main text.

One point is that it will be important for the authors to add a point to their discussion regarding the recent study by S. Kenderian (Stewart et al.) pointing to a negative role of IL-4 in CAR T cell function (“...when CART cells were treated with IL-4, they developed signs of exhaustion, but when CART cells were treated with an IL-4 monoclonal antibody, they showed improved antitumor efficacy and reduced signs of exhaustion in preclinical models. Therefore, our study identified both a novel role for IL-4 on CART cells and the improvement of CART cell therapy through IL-4 neutralization.”). This study was presented at both ASH and AACR and the DOI for their bioRxiv manuscript is copied below.

This could be of significant interest in light of your new data showing that prior to transfer (and after Fc-IL4 treatment), your cells exhibited a complete bias to a Th1 phenotype (93% IFN γ secretion, new Extended Figure 1f). Interestingly, the Kenderian study also finds that the function of IL4 is independent of Th2 polarization.

<https://doi.org/10.1101/2023.09.28.560046>

<https://doi.org/10.1182/blood-2022-160219>

Thanks for the suggestions. We have noticed this interesting finding reported by Dr. S. Kenderian and colleagues. Their findings seem contradictory to ours. However, taking a close look at the experiments, we realized that many experimental settings were different.

First, in the Kenderian paper, the CAR-T cells were based on CD28 co-stimulation, while we used 41BB-costimulated CAR-T cells in this manuscript. It has been reported that the intrinsic CAR structures are critical in determining CAR-T cell differentiation and function. CD28-costimulated CAR-T cells are more susceptible to be exhausted as compared to 41BB-costimulated CAR-T cells (Long et al. Nat Med 21, 581–590 (2015)). CD28-based CAR is essentially hardwired for dysfunction unless exerting pharmacological inhibitor (e.g., dasatinib, Weber et al. Science 372, eaba1786 (2021).) or kinetic control (e.g., insertion into the TRAC locus, Zhou et al. Nat. Immunol. 24, 1499-1510 (2023)) over its hyperactive tonic CAR signaling. Therefore, the role of IL-4 signaling may vary depending on the co-stimulatory domain in CAR structure, which needs further investigation.

Second, the T cells used in the two studies were at different differentiation stages. Kenderian et al. used T cells at the early activation stage of CAR- T cells. They found that adding IL-4 impaired their cytotoxicity at a low E/T ratio, modestly reduced cell counts ($p = 0.0655$), and likely restrained the cytokine secretion capacity (no statistical analysis was given). In the study reported in the current manuscript, the T cells experienced chronic restimulation and became terminally exhausted (PD-1+TIM-3+) prior to the treatment with Fc-IL-4, a scenario better mimicking tumor-infiltrating T cells. We conclude that Fc-IL-4 could significantly improve the survival of terminally exhausted T cells and their effector function. Thus, the role of IL-4 signaling may also vary depending on the differentiation stages.

Finally, there are several technical details that may worth mentioning. As a key experiment reported in the Kenderian paper, the gene ontology enrichment analysis and ingenuity pathway analysis was based on the comparison between in vitro-induced CAR-T cells co-cultured with CD19+ Nalm6 cells and unstimulated CAR-T cells, which may not fully recapitulate T cell differentiation in vivo. Among several differentiated pathways identified, including IFN γ , IL-2 pathways, IL-4 pathway was not even the dominated one. In addition, we noticed that neutralizing IL-4 showed rather minor improvement compared to CAR-T cells alone ($p = 0.055$) as they reported.

We have added a paragraph of discussion regarding the finding reported in the Kenderian paper:

“Although Th2 function in pre-infused CAR-T cells with 4-1BB co-stimulatory domain was found essential for ultra-long-term remission in ALL patients⁵, the IL-4 signalling pathway was recently found to drive exhaustion of CAR-T cells that rely on CD28 domain for co-stimulation⁴⁴, suggesting that the impact of type 2 cytokine on CAR-T cell function may depend on the specific structure of CAR design of responding CAR-T cells. Nevertheless, revisiting the role of different components of type 2 immunity in anti-tumour therapy and exploring their synergies with type 1 immunity could provide new insights for designing next-generation immunotherapy.”

Referee #2 (Remarks to the Author):

We thank the authors for thoroughly addressing all the reviewers comments. The new figures and added data significantly improved the manuscript, which we believe will have a big impact in the field of cancer immunotherapy.

We thank the reviewer for the favorable remarks.

Referee #3 (Remarks to the Author):

All the key points I had raised were addressed. My only remaining concern relates to the title.

I think the authors should reconsider the title. I mean, the combination "functional, terminally exhausted CD8 + T cells" is simply a wired mixture of contradictory information. Why does it need to be overloaded with terms that are difficult for a broader audience to understand? The authors could simply use a descriptive approach and write "functional superior tumor-targeting T cells" or something similar.

We totally agree and thank the reviewer for the suggested titles. Many terminologies currently used in the field of "T cell exhaustion" can be rather confusing (we hope the leaders of the field can refine these terms together). To avoid such ambiguity, we changed the title to "A type 2 cytokine Fc-IL-4 revitalises exhausted CD8⁺ T cells against cancer".